UNIVERSIDADE FEDERAL DO RIO GRANDE DO SUL

INSTITUTO DE CIÊNCIAS BÁSICAS DA SAÚDE

PROGRAMA DE PÓS-GRADUAÇÃO EM CIÊNCIAS BIOLÓGICAS:

FISIOLOGIA

Felipe Kawa Odorcyk

Diferenças no substrato metabólico utilizado e na função mitocondrial induzem prognósticos distintos à hipóxia-isquemia neonatal em diferentes estágios de desenvolvimento em ratos Wistar

Porto Alegre

2020

Felipe Kawa Odorcyk

Diferenças no substrato metabólico utilizado e na função mitocondrial induzem prognósticos distintos à hipóxia-isquemia neonatal em diferentes estágios de desenvolvimento em ratos Wistar

Tese apresentada ao Programa de Pós-Graduação em Ciências Biológicas: Fisiologia do Instituto de Ciências Básicas da Saúde da Universidade Federal do Rio Grande do Sul como requisito parcial para a obtenção do título de doutor em Fisiologia.

Orientador(a): Prof. Dr. Carlos Alexandre Netto

Porto Alegre

2020

Agradecimentos

A conclusão desta Tese não teria sido possível sem o apoio, o esforço, a dedicação e o voto de confiança que recebi por muitas pessoas.

Ao meu Prof. Carlos Alexandre Netto, trabalhar sob sua orientação durante esses anos foi fundamental para minha formação como pesquisador e para o desenvolvimento desse trabalho.

Aos meus colegas de laboratório que sempre estavam disponíveis para ajudar com os experimentos, discussões científicas e projetos. À Luz Elena pela ajuda praticamente todas as etapas dessa tese e pela amizade. Ao Eduardo Sanches pela amizade e pelo auxílio mesmo que muitas vezes à distância.

Às parcerias com os demais grupos de pesquisa que enriqueceram a tese com diferentes abordagens e motodologias de pesquisa. Aos pesquisadores do Instituto do Cérebro da PUCRS Samuel Greggio e Gianina Venturin bem como ao da UFRGS prof. Eduardo Zimmer pela aquisição e análise das imagens de microPET. Ao prof. Luiz Carlos Rios Kucharski e à Debora Santos Rocha nas análises de oxidação de substratos energéticos. À profa. Carla Dalmaz e à Natividad Pereira pelo auxílio com as técnicas de Western Blot. Ao prof. Moacir Wajner e seus orientados Ana Cristina Roginski e Rafael Ribeiro pelas análises bioquímicas que compuseram o capítulo II da presente tese.

Ao PPG Fisiologia por proporcionar excelente formação e construção de conhecimentos aos seus alunos.

Às agências de fomento CAPES e CNPq pelos recursos para a realização do projeto.

Um agradecimento especial a todos os meus amigos e à minha família pelo apoio incondicional mesmo nos momentos mais difíceis.

Apresentação

Esta tese é constituída por:

PARTE I:

1. Introdução: contém o embasamento teórico necessário para a compreensão da proposta de trabalho e objetivos.

2. Hipótese: expõe os principais resultados esperados.

3. Objetivos: definem os propósitos centrais do trabalho, desenvolvidos ao longo dos capítulos 1 e 2.

PARTE II:

Capítulo 1: Artigo publicado no periódico Experimental Neurology – "Differential glucose and beta-hydroxybutyrate metabolism confers an intrinsic neuroprotection to the immature brain in a rat model of neonatal hypoxia ischemia".

Capítulo 2: Artigo submetido ao periódico Molecular Neurobiology – "Differential age-dependent mitochondrial dysfunction, oxidative stress and apoptosis induced by neonatal hypoxia-ischemia in the immature rat brain".

PARTE III:

Discussão Geral: contém a interpretação dos resultados obtidos nos Capítulos 1 e 2, englobando-os em um contexto geral.

Conclusões: apresenta as conclusões gerais da tese.

Referências: lista as referências citadas nas seções Introdução e Discussão.

Lista de figuras

Lista de abreviações

ATP: Adenosina trifosfato
CS: Citrato sintase;
EROs: Espécies reativas de oxigênio
$FADH_2$: Dinucleótido de flavina e adenina reduzido
GABA: Ácido gama-aminobutírico
GLUT: Transportador de glicose
GPx: Glutationa peroxidase
GSH: Glutationa reduzida
HI: Hipóxia isquemia neonatal
KCC2: Transportador de cloreto de potássio 2
LPV: Leucomalácia Periventricular
MCT-1: Transportador de monocarboxilato 1
MDH: Malato desidrogenase;
microPET: Microtomografia por emissão de pósitrons
NADH: Dinucleótido de nicotinamida e adenina reduzido
NKCC1: Cotransportador Na-K-Cl 1
NMDA: N-metil D-Aspartato
P: Dia pós-natal
SNC: Sistema nervoso central
SOD: Superóxido dismutase
TCA: Ácido tricarboxílico
TDAH: Transtorno de déficit de atenção e hiperatividade
[^{18}F]FDG: [^{18}F]-fluordesoxiglicose

Sumário

RESUMO

A hipóxia-isquemia neonatal (HI) causa severas sequelas e faz parte da etiologia de diversas doenças neurológicas. Já é bem descrito que o mesmo protocolo de HI que causa danos cognitivos e teciduais significativos em animais no dia pós-natal 7 (P7), ou HIP7, não causa danos em animais mais jovens, HIP3. Os fatores que culminam na diferença de resposta à lesão hipóxico-isquêmica ainda não foram estudados. Diferenças no metabolismo encefálico como utilização de corpos cetônicos e glicose, além de mudanças na função mitocondrial observados durante estes estágios parecem estar entre os fatores que mais contribuem para a diferença de severidade na lesão. Essa tese tem como objetivo estudar a influência desses mecanismos no modelo de HI neonatal induzido em diferentes estágios do desenvolvimento em ratos Wistar. No primeiro capítulo comparamos o efeito da lesão em 3 idades: HIP3, HIP7 e HIP11, com seus respectivos sham. Observamos prejuízos no aprendizado e dano tecidual de maneira dependente da idade, em que o grupo HIP11 possuía déficits de aprendizado e grande lesão tecidual, o grupo HIP7 possuía menor prejuízo, enquanto o grupo HIP3 não apresentava nenhum dano detectável. Através do imageamento por [^{18}F]FDG microPET realizados 24 e 72h após a lesão mostrou um crescimento linear da captação de glicose do encéfalo com a idade, além de um hipometabolismo significativo no hemisfério ipsilateral no grupo HIP11, enquanto o mesmo não foi encontrado no grupo HIP3. Observamos também uma acentuada redução da oxidação de β-hidroxibutirato com o desenvolvimento, sugerindo que a maior contribuição de β-hidroxibutirato e menor de glicose podem estar entre os fatores que conferem ao encéfalo imaturo maior resiliência à lesão. Além disso, foram encontradas correlações significativas entre a captação de glicose (determinada por imageamento por [^{18}F]FDG microPET), principalmente 72h após a HI, e os déficits de aprendizado, bem como a lesão tecidual na idade adulta, mostrando que a técnica é eficaz em prever as consequências da lesão na idade adulta. No capítulo II investigamos diferentes respostas à HI na função mitocondrial, utilizando os grupos HIP3 e HIP11, com seus respectivos sham. Um aumento na apoptose e perda do potencial de membrana mitocondrial foram observados apenas no grupo HIP11. Além disso, observamos um aumento na atividade do ciclo do ácido tricarboxílico (TCA) e dos complexos da cadeia respiratória mitocondrial com o desenvolvimento, na ausência de lesão. A HI induziu uma redução na atividade de enzimas do ciclo TCA, bem como dos complexos mitocondriais apenas no grupo HIP11, sugerindo que um aumento de demanda metabólica no encéfalo em fases avançadas do desenvolvimento pode explicar sua maior susceptibilidade à lesão HI. Ainda, uma maior produção de espécies reativas de oxigênio somadas a uma menor atividade de enzimas antioxidantes também parecem contribuir para o maior dano observado no grupo HIP11. Os resultados da presente tese demonstram que as diferenças no metabolismo encefálico durante o desenvolvimento estão entre os principais determinantes da severidade da HI. O maior uso de corpos cetônicos e a redução do metabolismo encefálico parecem ser alvos terapêuticos importantes que merecem ser mais estudados.

Palavras-chave: hipóxia-isquemia neonatal (HI); neurodesenvolvimento; metabolismo encefálico; função mitocondrial.

ABSTRACT

Neonatal hypoxia-ischemia (HI) causes severe sequelae and is part of the etiology of several neurological pathologies. It is known that the same HI protocol that causes significant cognitive and tissue damage in animals on the postnatal day 7 (P7), or HIP7, does not cause damage to younger animals, HIP3. The factors that culminate in the different responses to the HI injury have not yet been studied. Differences in brain metabolism such as the use of ketone bodies and glucose, in addition to changes in mitochondrial function observed during these stages seem to be among the factors that contribute to the difference in injury severity. This thesis aims to study the influence of such mechanisms in a model of neonatal HI induced at different developmental stages in Wistar rats. In the first chapter we compare the effect of the injury in 3 ages: HIP3, HIP7 and HIP11, with their respective sham groups. We observed impairments in learning and tissue damage in an age-dependent manner, in which the HIP11 group had learning deficits and more tissue damage, the HIP7 group showed less impairment, while the HIP3 group presented no detectable damage. [^{18}F] FDG microPET imaging performed 24 and 72h after the injury showed a linear increase in brain glucose uptake during development, in addition to a significant hypometabolism in the ipsilateral hemisphere in the HIP11 group, while it was not found in the HIP3 group. We also observed a marked reduction in the oxidation of β-hydroxybutyrate throughout development, suggesting that the greater β-hydroxybutyrate contribution and lower glucose usage may be among the factors that give the immature brain greater resilience to HI injury. In addition, significant correlations were found between glucose uptake (determined by [^{18}F] FDG microPET imaging), especially 72 hours after the HI, and learning deficits, as well as tissue injury in adulthood, showing that the technique is effective in predicting the consequences of the injury in adulthood. In chapter II we investigated different HI-induced responses in mitochondrial function, using the HIP3 and HIP11groups, with their respective shams. An increase in apoptosis and loss of mitochondrial membrane potential was observed in the HIP11 group only. In addition, we observed an increase in the activity of the tricarboxylic acid (TCA) cycle and in the mitochondrial respiratory complexes with development, in the absence of injury. HI induced a reduction in the activity of TCA cycle enzymes as well as in the mitochondrial complexes in the HIP11 group only, suggesting that an increase in metabolic demand in the brain in advanced stages of development may explain its greater susceptibility to HI injury. Still, a higher production of reactive oxygen species associated with a lower activity of antioxidant enzymes also seem to contribute to the greater damage observed in the HIP11 group. The results of the present thesis demonstrate that the differences in brain metabolism during development are among the main determinants of HI severity. The greater use of ketone bodies and the reduction of brain metabolism seem to be important therapeutic targets that deserve further study.

Keywords: neonatal-hypoxia ischemia (HI); neurodevelopment; brain metabolism; mitochondrial function.

1.Introdução

1.1 Hipóxia-isquemia neonatal

A hipóxia-isquemia neonatal, HI, é uma das principais causas de dano encefálico durante o desenvolvimento de recém-nascidos. Ela pode levar a óbito ou gerar incapacidade neurológica em variados graus que vão desde comprometimentos leves (como alterações do tônus muscular) a danos cognitivos severos, como os observados nos casos graves de paralisia cerebral (Volpe, 2009). Disfunções circulatórias e/ou complicações obstétricas como a hipóxia materna, o descolamento prematuro da placenta e a compressão do cordão umbilical podem interferir na transferência de substratos e levar à asfixia fetal, causando a HI neonatal (Berger and Garnier, 1999; Ferriero, 2001; Volpe, 2009). Complicações sistêmicas da asfixia neonatal frequentemente ocorrem e incluem alterações cardiovasculares, respiratórias, metabólicas e renais, sendo, no entanto, o sistema nervoso central (SNC) a estrutura mais comprometida (Arteni et al., 2003; Pereira et al., 2009; Sanches et al., 2015). A HI está ainda relacionada com a ocorrência de doenças como a epilepsia, o autismo, o transtorno de déficit de atenção e hiperatividade (TDAH), além de transtornos de aprendizagem, acarretando deficiências intelectuais nos indivíduos acometidos (Huang et al., 2009; Volpe, 2009). Os achados neuropatológicos da HI variam de acordo com a maturidade fetal, a natureza e a extensão da lesão e podem resultar em diferentes tipos de lesões (Khwaja and Volpe, 2008; Silbereis et al., 2010; Volpe, 2009) como demonstrado na Figura 1.

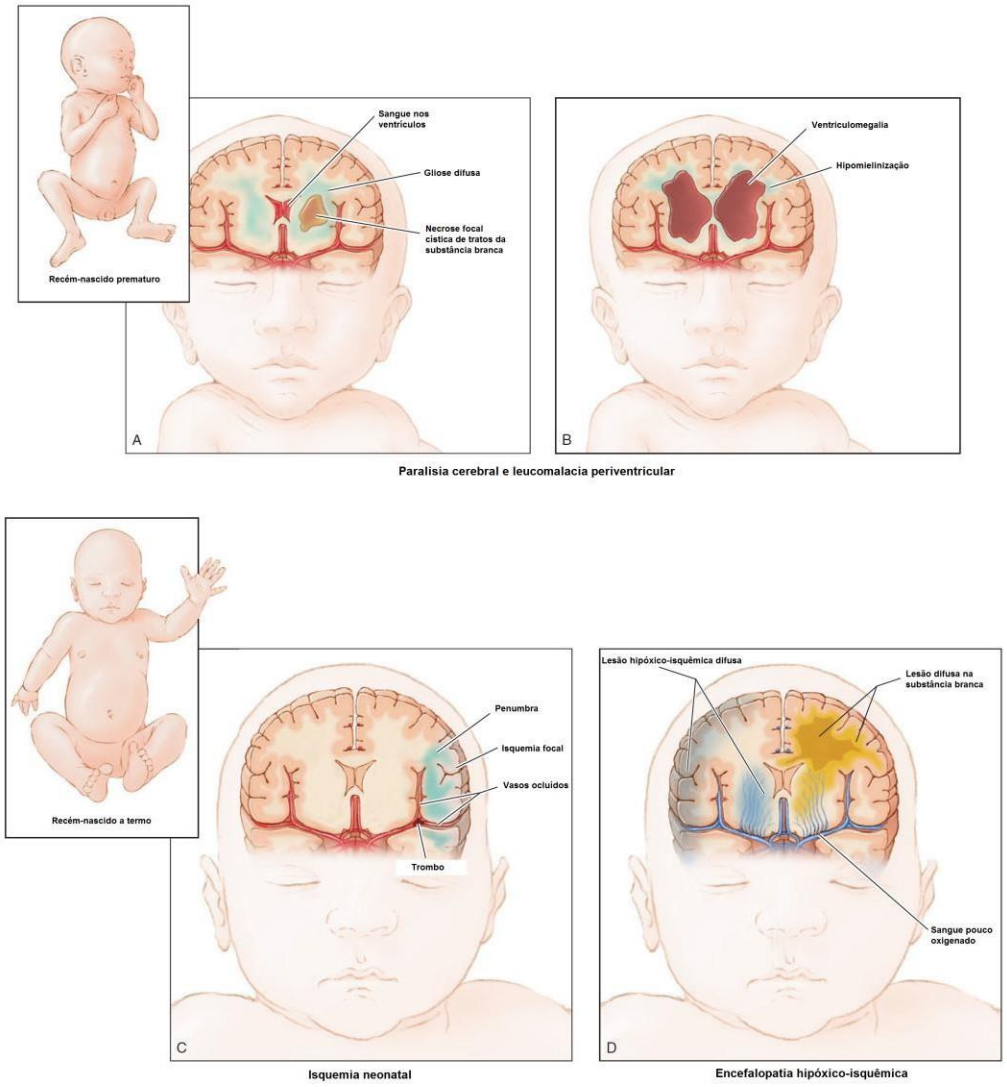

Figura 1. Ilustração de lesões cerebrais que afetam neonatos prematuros de baixo peso e a termo. Principais características das lesões em prematuros de baixo peso incluem: (A) hemorragia intraventricular, frequentemente estendendo-se para o parênquima cerebral. Há também uma elevada incidência de leucomalácia periventricular (LPV), um tipo de lesão à substância branca, que ocasiona necrose cística dos tratos da substância branca também podendo apresentar gliose difusa. (B) Esses eventos deixam sequelas de longo prazo que incluem hipomielinização com conectividade neuronal prejudicada e ventriculomegalia, que representa uma perda significativa de tecido do parênquima cerebral. Esse padrão contrasta com o mais frequente observado em recém-nascidos a termo, que apresentam maior predominância de (C) acidente vascular cerebral neonatal, em que uma região focal cortical é afetada. (D) Observa-se lesão difusa ocasionada pelo episódio hipóxico-isquêmico, bem com lesão na substância branca. Adaptado de Silbereis e colaboradores (Silbereis et al., 2010).

Um dos modelos experimentais mais utilizados de HI neonatal em roedores combina a ligação unilateral de uma das artérias carótidas comuns à posterior exposição dos animais a um período variável de hipóxia, visando mimetizar a encefalopatia encontrada em neonatos humanos após um quadro de asfixia (Rice et al., 1981). Esse

modelo é amplamente utilizado por reproduzir diversos danos observados na clínica como alterações no desenvolvimento e morte de oligodendrócitos; cistos necróticos na substância branca e córtex; dano axonal; ativação microglial; morte neuronal e ventriculomegalia (Silbereis et al., 2010). Para mimetizar a HI em nascidos prematuros utiliza-se o modelo no dia pós-natal 3 (P3) (HIP3) em roedores (Alexander et al., 2014; Sanches et al., 2015; Sizonenko et al., 2005). Essa idade é utilizada porque a maturação de oligodendrócitos, o desenvolvimento do sistema imunitário e a formação da barreira hematoencefálica são equivalentes ao encontrado em fetos entre a 28ª e a 32ª semana de gestação (Semple et al., 2013). O modelo que simula a HI em nascidos a termo, no entanto, é realizada em ratos no P7 (HIP7), pois nessa idade há o pico de crescimento encefálico e gliogênese, aumento da densidade axonal e dendrítica, maior maturação de oligodendrócitos e a consolidação do sistema imunitário, que são equivalentes ao encontrado em humanos entre a 36ª e 40ª semana de gestação (Semple et al., 2013). No entanto, alguns pesquisadores têm proposto que a idade de indução do modelo em ratos que melhor reproduz a lesão HI em nascidos a termo seria no P10-11 e não no P7 como utilizado na maior parte dos estudos (Patel et al., 2015, 2014).

A soma da isquemia unilateral com a hipóxia sistêmica causa danos localizados predominantemente no hemisfério ipsilateral à carótida ocluída, sendo o hemisfério contralateral afetado em menor grau ou mesmo não afetado morfologicamente (Jansen & Low, 1996; Rice et al., 1981). O modelo de HI perinatal causa lesões no córtex cerebral, substância branca periventricular e subcortical e no estriado (núcleos da base); no entanto, a estrutura mais afetada é o hipocampo (Arteni et al., 2010; Pereira et al., 2007). Dados anteriores de nosso grupo evidenciam que lesões em tais estruturas após a HIP7 causam danos bioquímicos, tais como aumento da formação de espécies reativas de oxigênio e diminuição das defesas antioxidantes (Dafre et al., 2003). Essa lesão causa danos

histológicos em regiões responsáveis por controlar processos cognitivos como formação, consolidação e evocação das memórias espacial, aversiva e de trabalho (Arteni et al., 2010; Pereira et al., 2007; Sanches et al., 2015).

1.2 Progressão da HI

Em linhas gerais, o dano da HI se inicia imediatamente após o insulto, que é o dano que decorre diretamente da falência energética, conhecido como **lesão primária** (Figura 2), que é caracterizada pela redução no fluxo sanguíneo e suprimento de oxigênio; com isso, compostos fosforilados de alta energia como o ATP e a fosfocreatina são severamente reduzidos, acarretando uma acidose tecidual (Lorek et al., 1994). A falência energética afeta principalmente a atividade da bomba de Na^+/K^+-ATPase, enzima que consome maior parte do ATP encefálico para a manutenção do potencial da membrana neuronal dando início ao processo de excitotoxicidade (Arnaiz & Ordieres, 2014). A perda do potencial de membrana causa despolarização neuronal em massa com grande liberação de neurotransmissores como o glutamato (Erecińska & Silver, 1994). A liberação excessiva de glutamato nas fendas sinápticas e, possivelmente, outros neurotransmissores excitatórios, como a glicina, contribuem para a abertura de receptores de glutamato do tipo N-metil D-Aspartato (NMDA), o que aumenta o influxo de cálcio (Ca^{2+}) (Johnston et al., 2001). O aumento na concentração de Ca^{2+} intracelular ativa cascatas neurotóxicas, além da formação de um gradiente osmótico que favorece a formação de edema e lise celular (Hassell et al., 2015). O Ca^{2+} ativa a óxido nítrico sintase neuronal, que conduz à liberação do radical óxido nítrico (NO), causando disfunção mitocondrial, dano oxidativo e morte celular (Hagberg et al., 2009; Vannucci, 2004). O excesso de Ca^{2+} no citoplasma também desencadeia a ativação de fosfolipases citosólicas, que atuam no aumento da liberação de eicosanóides e ocasionam um processo inflamatório (Hassell et al., 2015).

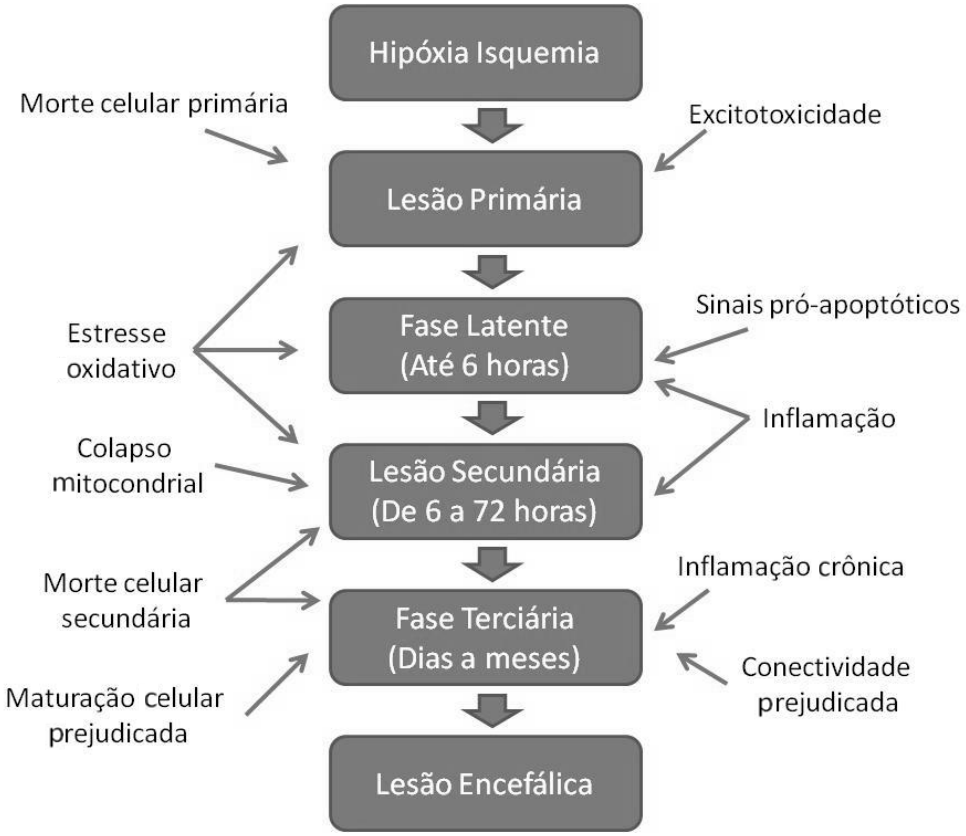

Figura 2. Mecanismos de evolução da lesão neural - nas fases primária, latente, secundária e terciária que contribuem para o dano de longo prazo (Adaptado de Davidson et al., 2015).

Após a retomada da circulação inicia-se o período de reperfusão, no qual o fluxo sanguíneo é retomado e com ele a disponibilidade de oxigênio e metabólitos energéticos permitindo uma recuperação celular parcial, na chamada **fase latente** (Davidson et al., 2015a). A duração da fase latente é inversamente relacionada à gravidade do insulto, ou seja, quanto mais severo o comprometimento energético durante a HI, menor será a fase latente, consequentemente o déficit energético secundário e a morte neuronal serão mais extensos (Iwata et al., 2007). Acredita-se que a cascata neurotóxica seja amplamente inibida durante a fase latente, quando há inibição endógena do metabolismo oxidativo e aumento da oxigenação tecidual (Hassell et al., 2015).

Apesar do restabelecimento dos níveis de oxigênio e glicose no tecido, o dano celular causado anteriormente provoca a liberação de padrões moleculares associados ao

dano (PMADs) que causam um processo neuroinflamatório que associado ao dano mitocondrial às células sobreviventes vão desencadear um processo conhecido como **lesão secundária** (Burda & Sofroniew, 2014; Davidson et al., 2015a). A neuroinflamação e o estresse oxidativo são os principais mecanismos que induzem a morte celular secundária, processo que causa a maior parte da morte celular após a HI; seu auge ocorre 24 horas após a lesão e mantém-se em níveis elevados até 72 horas (Huang et al., 2009; Liu & Zhang, 2014).

A resposta imunitária aguda no SNC é mediada principalmente por células gliais, como os astrócitos. Esses atuam como sensores intrínsecos na detecção de PMADs, reagindo a insultos de forma rápida e efetiva, principalmente na liberação de citocinas pró-inflamatórias (Zhao et al., 2013). O conjunto de reações das células gliais frente a um insulto é chamado de gliose reativa (Burda & Sofroniew, 2014; Liu & McCullough, 2013). As células microgliais são o componente imunitário do sistema nervoso, com uma importante função, mesmo na ausência de lesões. Estas, ao detectarem PMADs, tornam-se reativas, passando a liberar citocinas e adquirindo função fagocítica (Burda & Sofroniew, 2014; Liu & McCullough, 2013).

Os astrócitos são protagonistas dos eventos relacionados com a progressão da HI. Essas células dão suporte metabólico para os neurônios, fator que é de especial importância em eventos isquêmicos (Burda & Sofroniew, 2014; Saito et al., 2005). Na presença de PMADs, no entanto, passam a participar também na regulação do processo inflamatório liberando mediadores como citocinas(Burda & Sofroniew, 2014; Liu & McCullough, 2013). A liberação de citocinas como TNF-α pelas células gliais pode agravar a reação inflamatória e a consequente mobilização e ativação de células inflamatórias periféricas (McLean & Ferriero, 2004; Mishra & Delivoria-Papadopoulos, 1999). É bem descrito na literatura que eventos que provocam estresse ao sistema nervoso

como a HI, causam uma alteração na atividade do sistema imunitário (Fathali et al., 2013; Jellema et al., 2013; Liu & McCullough, 2013). A ativação da resposta imunitária é um dos fatores que determinam a gravidade da lesão, sendo que, quanto maior for a resposta imunitária, maiores serão as sequelas (Fathali et al., 2013; Jin et al., 2009).

A falência metabólica e os níveis excessivos de Ca^{2+} intracelular provocam dano mitocondrial que consequentemente aumenta o dano causado pelo estresse oxidativo. O estresse oxidativo é causado quando há grande liberação de espécies reativas de oxigênio (EROs) excedendo a capacidade das defesas antioxidantes de combatê-las. Em condições normais, EROs como o ânion superóxido são produzidas pela mitocôndria, no entanto, uma vez produzido ele é convertido em peróxido de hidrogênio, que também é uma ERO, pela enzima superóxido-dismutase (SOD) (Saito et al., 2005; Weis et al., 2011). O peróxido de hidrogênio, por sua vez, tem sua redução catalisada pela enzima glutationa peroxidase (GPx) que utiliza a glutationa reduzida para converter o peróxido de hidrogênio em água e oxidar a glutationa, produtos que não causam dano celular (Saito et al., 2005; Weis et al., 2011). Por essa razão as enzimas SOD e GPx são chamadas de defesas antioxidantes, pois combatem com eficiência as EROs formadas em situações fisiológicas (Saito et al., 2005). Em encefalopatias como a HI, no entanto, há produção excessiva de EROs muitas vezes associada com a redução das defesas antioxidantes provocando peroxidação lipídica, além de dano a proteínas e a ácidos nucléicos (Dafre et al., 2003; Davidson et al., 2015a; Pereira et al., 2009).

Durante a **lesão terciária** tem início a fase de reconstrução tecidual, frequentemente com processos inflamatórios crônicos e morte celular ainda presentes, ainda que em menor grau em relação à fase secundária (Burda & Sofroniew, 2014). As células remanescentes, apesar de funcionais, amadurecem de forma tardia e não são capazes de fazer as conexões normais. O tecido, portanto, tem um desenvolvimento muito

prejudicado que culmina na redução do volume das estruturas encefálicas afetadas e na formação de cicatriz glial pelos astrócitos (Arteni et al., 2003; Burda & Sofroniew, 2014; Davidson et al., 2015a). Todos esses fatores fazem com que a HI cause danos cognitivos e motores permanentes.

1.3 O modelo de HI induzido em diferentes idades possui prognósticos distintos

As diferentes características celulares e moleculares do encéfalo em diferentes fases do desenvolvimento conferem prognósticos distintos à HI. Estudos que comparam os efeitos do mesmo protocolo em HIP3 e HIP7 demonstram resultados surpreendentes. Quando comparados na idade adulta, os animais HIP7 apresentam déficits cognitivos maiores do que os apresentados pelos animais HIP3 na memória aversiva, com menor aprendizado na esquiva inibitória (Sanches et al., 2015) e na memória espacial, reduzindo o tempo de latência no labirinto aquático de Morris (Alexander et al., 2014; Sanches et al., 2015). O aprendizado motor também apresenta o mesmo padrão, com um aprendizado dos animais HIP3 superior ao dos HIP7 (Alexander et al., 2014). A análise histológica reforça ainda mais esse padrão, com ratos HIP7 apresentando volumes reduzidos de diversas estruturas encefálicas como estriado, córtex e hipocampo, além de um aumento no volume dos ventrículos; enquanto pouco ou nenhum efeito é observado nessas estruturas no HIP3 (Alexander et al., 2014; Sanches et al., 2015). Portanto, é notável o fato de que o mesmo protocolo de HI cause consequências tão diferentes em animais com apenas 4 dias de diferença. No entanto, os mecanismos celulares e moleculares que conferem a neuroproteção intrínseca aos HIP3 ainda não foram estudados. Uma vez elucidados, esses mecanismos, além de aumentar a compreensão sobre a neurobiologia da HI, podem auxiliar na identificação de alvos terapêuticos importantes para o tratamento dessa encefalopatia.

Atualmente, o principal tratamento para recém-nascidos acometidos pela HI neonatal é a hipotermia terapêutica (Davidson et al., 2015a; Jacobs et al., 2013). Essa abordagem consiste em reduzir a temperatura encefálica para 32-34ºC durante 48-72h e, quando iniciada até 6h após o nascimento, é capaz de reduzir a mortalidade e o grau de morbidade apresentados por bebês acometidos pela HI (Jacobs et al., 2013). Um dos principais mecanismos de ação desse tratamento é a redução da taxa metabólica e, por consequência, da demanda energética das células do sistema nervoso (Globus et al., 1995; Jacobs et al., 2013). A redução do metabolismo energético aumenta a resiliência celular à privação de substratos energéticos e oxigênio, como no caso da HI, fazendo com que mais ATP possa ser usado para a manutenção do potencial de membrana dos neurônios (Globus et al., 1995; Laptook et al., 2017). A manutenção da polaridade da membrana dos neurônios reduz a liberação de glutamato que, por sua vez, reduz o influxo de Ca^{2+} que causa dano mitocondrial (Davidson et al., 2015a; Globus et al., 1995). Apesar da redução da mortalidade e demais prejuízos causados pela HI, a hipotermia possui importantes limitações. Além da limitada janela terapêutica, que é de apenas 6h após o nascimento, o fato de ser recomendada apenas para recém-nascidos com 36 semanas de gestação ou mais deixa recém-nascidos prematuros sem opção de tratamento (Davidson et al., 2015a; Jacobs et al., 2013). Há, portanto, grande necessidade de se compreender as diferenças na resposta à HI em diferentes períodos de desenvolvimento. Nesse contexto, o metabolismo encefálico parece um fator-chave, tanto pela natureza da lesão, que o afeta diretamente, quanto pelas grandes variações que ele apresenta durante o período neonatal.

1.3 Metabolismo encefálico

O metabolismo encefálico sofre grandes alterações com o desenvolvimento (Figura 3). O encéfalo adulto, em condições normais, usa quase que exclusivamente glicose como fonte energética (McKenna et al., 2012) e, apesar dos níveis circulantes de

glicose não apresentarem grandes variações no período neonatal, o consumo desse substrato pelo encéfalo varia muito (Brekke et al., 2015). O consumo encefálico de glicose em ratos neonatos (P7) é de aproximadamente 50% do consumo adulto; além disso a atividade de todas as enzimas da via glicolítica aumentam muito entre o período neonatal e o adulto (Brekke et al., 2015). O aumento no consumo de glicose no encéfalo está diretamente relacionado com a presença de transportadores de glicose (GLUT), entre os principais estão o GLUT1 que está presente na barreira hematoencefálica e células gliais, e o GLUT3 que é o transportador neuronal (Brekke et al., 2015; Vannucci et al., 1998). A atividade das enzimas da via glicolítica também apresenta variações significativas, tendo sua atividade muito reduzida nos primeiros dias pós-natais quando comparada ao encéfalo adulto (Booth et al., 1980). O menor consumo de glicose nos animais neonatos, no entanto, não ocorre apenas por uma menor demanda metabólica do encéfalo, mas principalmente pelo uso de outras fontes energéticas, como os corpos cetônicos e o lactato, os quais são usados para a produção de ATP necessária para o tecido cerebral (Brekke et al., 2015; McKenna et al., 2012). Portanto, no encéfalo adulto a glicose supre quase 100% da demanda energética do encéfalo, no rato no P7 ela supre apenas 63% (Vannucci et al., 1994).

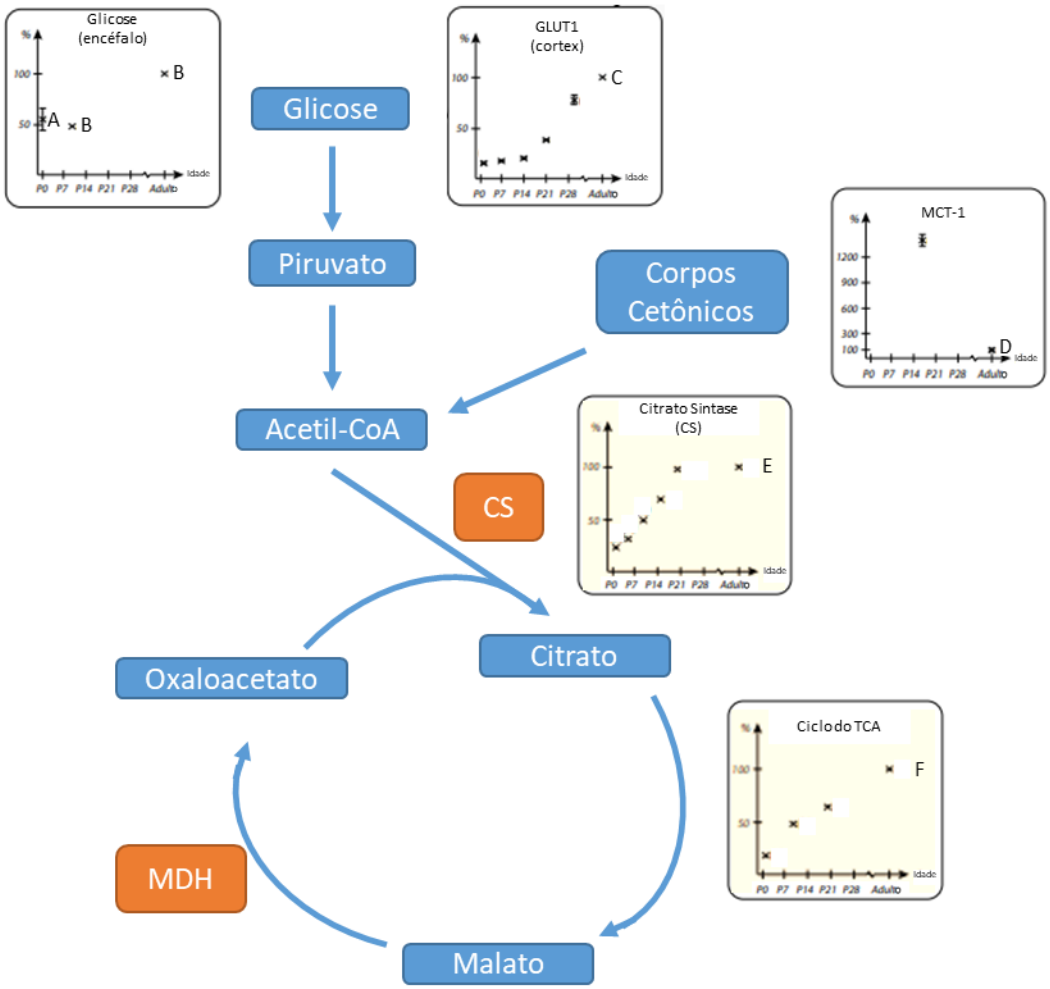

Figura 3. Alterações no metabolismo encefálico durante o desenvolvimento. Gráficos representam média ± erro padrão considerando os valores adultos como 100%. A)(Thurston and McDougal, 1969) B)(Lowry et al., 1964) C) (Vannucci et al., 1994) D)(Leino et al., 1999) E)(Booth et al., 1980) F) (Baquer et al., 1977). Abreviações: TCA: Ácido tricarboxílico; CS: Citrato sintase; MDH: Malato desidrogenase; GLUT1: Transportador de glicose 1; MCT-1: Transportador de monocarboxilato 1. Adaptado de Brekke e colaboradores (Brekke et al., 2015).

Durante a lactação o consumo de leite com alto teor lipídico proporciona uma elevada produção de corpos cetônicos que vão suprir grande parte do metabolismo encefálico de neonatos (Brekke et al., 2015; McKenna et al., 2012). Corpos cetônicos circulantes passam a barreira hematoencefálica através do transportador de monocarboxilato 1 (MCT1), que é mais expresso em animais neonatos do que em adultos (Brekke et al., 2015). As enzimas que metabolizam corpos cetônicos, como a D-β-hidroxibutirato desidrogenase e a aceto-acetil-succinil-CoA transferase, têm suas

atividades muito aumentadas nos primeiros dias após o nascimento quando comparados aos níveis observados em adultos (McKenna et al., 2012). A utilização de diferentes substratos energéticos pode influenciar a severidade da HI, visto que enquanto a hiperglicemia está relacionada com um pior prognóstico em neonatos humanos (Pinchefsky et al., 2019), a administração de β-hidroxibutirato reduz os efeitos deletérios causado por um modelo de HI em ratos (Lee et al., 2018). Embora diversos estudos tenham abordado a utilização de glicose, pouco se sabe sobre a utilização de corpos cetônicos após lesões como a HI.

No modelo de HI neonatal já foi demonstrado que 30 minutos após a hipóxia há um aumento de 26% nos níveis de glicose no hemisfério ipsilateral e de 44% no contralateral, evidenciando uma redução do metabolismo energético (Brekke et al., 2014). Já foi demonstrado também que os níveis de transportadores de glicose são afetados pela HI, com aumento da expressão de GLUT 1 tanto nos hemisférios ipsi e contralaterais à lesão em 24 e 72 horas, principalmente em astrócitos (Vannucci et al., 1998). A expressão de GLUT3 (transportador neuronal) teve um aumento nas regiões perilesionais, mas foi reduzida rapidamente nas áreas mais afetadas como córtex e hipocampo (Vannucci et al., 1998). No modelo de hipóxia-isquemia em ratos adultos, análise com microtomografia por emissão de pósitrons (microPET) com o radiofármaco [^{18}F]fluordesoxiglicose ([^{18}F]FDG) demonstrou uma redução no consumo de glicose 24 horas após a lesão (Marik et al., 2009).

O imageamento molecular pré-clínico refere-se à visualização não invasiva e em tempo real de eventos bioquímicos complexos, como a captação de glicose através do [^{18}F]FDG. Para tal, equipamentos específicos foram adaptados para detectar determinadas características teciduais ou marcadores bioquímicos em animais de pequeno porte, como ratos e camundongos. Algumas destas tecnologias foram adaptadas

a partir daquelas já utilizadas na clínica, como por exemplo microPET. Esta técnica oferece vantagens sobre os estudos *in vitro* e *ex vivo* tradicionais, uma vez que se utiliza anestesia durante os escaneamentos, pode-se elaborar estudos longitudinais com os mesmos animais, reduzindo custos e o número de ratos ou camundongos usados em um dado experimento. Ao contrário das análises que utilizam células, órgãos e amostras teciduais isoladas, os dados obtidos com a utilização da imagem molecular, de maneira não-invasiva e em tempo real, são adquiridos em condições fisiológicas reais e sem alteração do microambiente natural celular (James and Gambhir, 2012; Marik et al., 2009).

As diferenças no metabolismo encefálico durante o desenvolvimento não se limitam ao substrato energético mais utilizado, mas se estendem ao funcionamento mitocondrial. Grandes alterações na atividade do ciclo do ácido tricarboxílico (TCA) e da cadeia respiratória mitocondrial são observadas nessa etapa do desenvolvimento. A atividade da piruvato desidrogenase, por exemplo, entre P0 e P7 é de apenas 10% da observada em ratos adultos (Booth et al., 1980), de maneira semelhante, a citrato sintase (CS) em P7 tem menos de 50% da atividade de animais adultos (Booth et al., 1980). O ciclo do TCA integra diversas vias metabólicas e tem entre suas principais funções a formação de dinucleótido de nicotinamida e adenina reduzido (NADH) e dinucleótido de flavina e adenina reduzido ($FADH_2$) que doarão elétrons, auxiliando na formação do potencial de membrana mitocondrial através dos complexos da cadeia respiratória mitocondrial (McKenna et al., 2012). Os complexos da cadeia respiratória são encontrados na membrana interna da mitocôndria que separa a matriz mitocondrial do espaço intermembranar. Esses complexos são responsáveis pela criação do potencial de membrana mitocondrial e o fazem levando o íon H+ -obtido através da oxidação de NADH e $FADH_2$, por exemplo- para a matriz mitocondrial, criando uma diferença de

potencial entre a matriz e o espaço intermembrana. Essa diferença de potencial é utilizada pela enzima ATP sintase para produzir ATP (McKenna et al., 2012). Esse mecanismo fundamental para o metabolismo energético de nossas células também sofre mudanças com o desenvolvimento, e já foi demonstrado que a atividade tanto no complexo I quanto nos complexos II e III dobram entre P0 e P10 em ratos (Bates et al., 1994).

1.4 Hipótese

A reduzida demanda metabólica do encéfalo imaturo pode estar entre os mecanismos que conferem maior resiliência à HI. Tendo em vista que a redução do metabolismo cerebral é considerada um dos mecanismos primários de neuroproteção da hipotermia terapêutica, é possível que as diferenças metabólicas observadas durante o desenvolvimento apontem para novos alvos terapêuticos para a HI.

2.Objetivos

2.1Geral

Investigar os efeitos da lesão hipóxico-isquêmica induzida em diferentes estágios do desenvolvimento através de parâmetros comportamentais, histológicos e metabólicos.

2.2 Específicos

1) Avaliar, em ratos submetidos à HI em diferentes fases do desenvolvimento (P3, P7 e P11), o grau de comprometimento e severidade da lesão sobre os déficits cognitivos, motores e histológicos através do labirinto aquático de Morris, escada horizontal e análise do volume da lesão na idade adulta.

2) Investigar, em ratos submetidos à HI em diferentes fases do desenvolvimento (P3, P7 e P11), os efeitos da HI induzida no metabolismo encefálico através do [^{18}F]FDG microPET 24 e 72h após a lesão.

3) Avaliar, em ratos submetidos à HI em diferentes fases do desenvolvimento (P3, P7 e P11), o poder preditivo dos parâmetros de imageamento por [^{18}F]FDG microPET nos primeiros dias após a lesão sobre a cognição dos animais na idade adulta.

4) Quantificar, em ratos submetidos à HI em diferentes fases do desenvolvimento (P3, P7 e P11), a oxidação dos substratos energéticos β-hidroxibutirato e glicose 24 e 72h após a lesão.

5) Investigar, em ratos submetidos à HI em diferentes fases do desenvolvimento (P3 e P11), morte celular por apoptose e perda de potencial mitocondrial 24h após a lesão.

6) Avaliar, em ratos submetidos à HI em diferentes fases do desenvolvimento (P3 e P11), os efeitos da idade e lesão na atividade das enzimas MDH e CS do ciclo do TCA 24h após a lesão.

7) Verificar, em ratos submetidos à HI em diferentes fases do desenvolvimento (P3 e P11), os efeitos da idade e lesão na atividade dos complexos da cadeia respiratória através de respirometria de alta resolução 24h após a lesão.

8) Investigar, em ratos submetidos à HI em diferentes fases do desenvolvimento (P3 e P11), a atividade de enzimas antioxidantes e parâmetros de dano por estresse oxidativo 24h após a lesão.

3. Capítulo I

Differential glucose and beta-hydroxybutyrate metabolism confers an intrinsic neuroprotection to the immature brain in a rat model of neonatal hypoxia ischemia.

Odorcyk FK, Duran-Carabali LE, Rocha DS, Sanches EF, Martini AP, Venturin GT, Greggio S, da Costa JC, Kucharski LC, Zimmer ER, Netto CA.

Exp Neurol. 2020 Aug;330:113317. doi: 10.1016/j.expneurol.2020.113317. Epub 2020 Apr 15.

PMID: 32304750

Differential glucose and beta-hydroxybutyrate metabolism confers an intrinsic neuroprotection to the immature brain in a rat model of neonatal hypoxia ischemia.

Odorcyk FK[1]*, Duran-Carabali LE[1], Rocha DS[1], Sanches EF[4], Martini AP[2], Venturin GT[3], Greggio S[3], da Costa JC[3], Kucharski LC[1], Zimmer ER[4,5,6], Netto CA[1,2,4,7].

[1]Graduate Program in Phisiology, Universidade Federal do Rio Grande do Sul (UFRGS), Porto Alegre, RS, Brazil.

[2] Graduate Program in Neuroscience, Universidade Federal do Rio Grande do Sul (UFRGS), Porto Alegre, RS, Brazil.

[3]Preclinical Research Center, Brain Institute (BraIns) of Rio Grande do Sul, Pontifical Catholic University of Rio Grande do Sul (PUCRS), Porto Alegre, Brazil

[4] Graduate Program in Biochemistry, Universidade Federal do Rio Grande do Sul (UFRGS), Porto Alegre, RS, Brazil.

5 Graduate Program in Pharmacology and therapeutics, Universidade Federal do Rio Grande do Sul (UFRGS), Porto Alegre, RS, Brazil.

[6] Department of Pharmacology, Universidade Federal do Rio Grande do Sul (UFRGS), Porto Alegre, RS, Brazil.

[7] Department of Biochemistry, Universidade Federal do Rio Grande do Sul (UFRGS), Porto Alegre, RS, Brazil.

*Corresponding author at: Felipe Kawa Odorcyk, Post-graduation Program of Physiology, Instituto de Ciências Básicas da Saúde (ICBS), Universidade Federal do Rio Grande do Sul (UFRGS). Rua Ramiro Barcelos 2600, anexo. CEP 90035-003, Porto Alegre, RS, Brazil.

Phone: 0055-51 33085568.

E-mail: felipe.odorcyk@gmail.com

Abstract

Neonatal hypoxia ischemia (HI) is the main cause of newborn mortality and morbidity. Preclinical studies have shown that the immature rat brain is more resilient to HI injury, suggesting innate mechanisms of neuroprotection. During neonatal period brain metabolism experience changes that might greatly affect the outcome of HI injury. Therefore, the aim of the present study was to investigate how changes in brain metabolism interfere with HI outcome in different stages of CNS development. For this purpose, animals were divided into 6 groups: HIP3, HIP7 and HIP11 (HI performed at postnatal days 3, 7 and 11, respectively), and their respective shams. *In vivo* [^{18}F]FDG micro positron emission tomography (microPET) imaging was performed 24 and 72h after HI, as well as *ex-vivo* assessments of glucose and beta-hydroxybutyrate (BHB) oxidation. At adulthood behavioral tests and histology were performed. Behavioral and histological analysis showed greater impairments in HIP11 animals, while HIP3 rats were not affected. Changes in [^{18}F]FDG metabolism were found only in the lesion area of HIP11, where a substantial hypometabolism was detected. Furthermore, [^{18}F]FDG hypometabolism predicted impaired cognition and worst histological outcomes at adulthood. Finally, substrate oxidation assessments showed that glucose oxidation remained unaltered and higher level of BHB oxidation found in P3 animals, suggesting a more resilient metabolism. Overall, present results show [^{18}F]FDG microPET predicts long-term injury outcome and suggests that higher BHB utilization is one of the mechanisms that confer the intrinsic neuroprotection to the immature brain and should be explored as a therapeutic target for treatment of HI.

Keywords: Neonatal hypoxia ischemia, brain metabolism, [^{18}F]FDG microPET, beta-hydroxybutyrate, brain development.

1.Introduction

Neonatal hypoxia ischemia (HI) is one of the main cause of mortality and morbidity in newborns (Perlman JM., 2004; Volpe, 2009). The surviving infants develop various degrees of neurologic deficits that range from slight cognitive impairments to severe cases of cerebral palsy (Volpe, 2009). This pathology affects both preterm and term newborns. Although the nature of the injury is similar (e.g. hypoxia and ischemia), the consequences and therapeutic interventions may present substantial differences according to the stage of brain maturation (Jacobs et al., 2013).

The Rice-Vannucci rat model is one of the most widely used to mimic HI in pre-clinical settings. It combines the unilateral permanent occlusion of the common carotid artery with a period of hypoxic exposure. The age of induction of the HI model may vary according to the degree of brain development and, in order to model HI in very preterm infants (ranging from 28 to 32 weeks of gestation) the injury procedure is performed at post-natal day 3 (PND3) in rats (Alexander et al., 2014; Sanches et al., 2015; Sizonenko et al., 2005). In order to model the injury in late preterm newborns (32-36 weeks of gestation) the procedure is performed at PND7, and for modeling HI occurred in term infants (> 36 weeks of gestation) the procedure is performed at PND10 or 11 (Semple et al., 2013). Nevertheless, it is important to point out that which rat PND resembles exactly which phase of brain development in humans is still an issue of debate (Patel et al., 2015, 2014).

Previous studies have compared the differences of the same HI model induced at PND3 (HIP3) and at PND7 (HIP7) (Alexander et al., 2014; Sanches et al., 2015). They showed that the same insult, that caused impairments in spatial and aversive memory, in motor learning as well as significant reductions in striatum, cortex and hippocampus when HI was performed at P7, barely caused any detectable deficits when performed at

P3 (Alexander et al., 2014; Sanches et al., 2015). The fact that HIP7 animals present lesions that are more severe than the same insult in HIP3 animals suggests the existence of an "intrinsic protection" of the brain in earlier stages of development. However, the mechanisms underlying this protection of the immature brain are not fully understood. Brain metabolism is likely to be among the features that may underlie the greater resilience of the immature brain to injury. It is well known that the immature brain uses around half of the glucose that the mature brain does in relation to its size, whereas it uses much higher levels of ketone bodies than the mature brain (Brekke et al., 2015). These differences seem to play a major role in HI outcome, while hyperglycemia is linked to detrimental outcome in clinical (Pinchefsky et al., 2019) and experimental HI studies (Park et al., 2001), administration of exogenous beta-hydroxybutyrate improves neuropathological score as well as reduces HI-induced cell death in rats (Lee et al., 2018). However, the capacity of brain cells to utilize either glucose or ketone bodies is also poorly understood in context of neonatal HI.

Brain metabolism has a predictive value in HI in humans (Zou et al., 2018). In fact, the severity of brain damage is crucial for determining the therapeutic approaches, since treatments such as hypothermia do not present the same beneficial effects in all injury severities (Chiang et al., 2017; Jacobs et al., 2013). In this context, [^{18}F]FDG microPET has showed strong correlations with HI outcome in the clinical setting, being a useful tool to aid clinicians in choosing the best therapeutic approach for each case (Shi et al., 2012; Thorngren-Jerneck et al., 2001). Nevertheless, it is not known if these clinical findings are translated into the experimental settings, since the predictive value of [^{18}F]FDG microPET scan neuroimaging in the first days after the induction of the HI model in rats has never been studied. The assessment of the replicability of clinical findings in the pre-clinical setting, this "back-translation" enables the usage of advanced

methods of analysis, only possible in animal models with high translational value (Parent et al., 2017).

Therefore, the present study aims to investigate the different responses triggered by HI insult in brain metabolism, such as *in vivo* glucose metabolism and whether the utilization of glucose as well as ketone bodies are mechanisms underlying the immature brain "intrinsic protection" to HI injury. The better understanding of such mechanisms may assist in the search for therapeutic strategies to reduce the mortality and detrimental effects of infants suffering from HI.

2. Methodology

2.1 Animals

Adult female Wistar rats and their male pups were used in this study. Mating was planned so that all groups would have the appropriate age so that the HI procedure would be performed in the same day, meaning that there was at least one litter of each age used in this study in each HI induction procedure. Such litters were composed of an adult female and 10 male rat pups, in order to avoid the litter effect, each litter contained pups of at least 3 different mothers, with a maximum of 4 pups of the same mother in each litter. All litters were standardized at PND1. All experimental procedures were performed in accordance with the recommendations of the Council for International Organizations of Medical Sciences (CIOMS - Publication 85-23, 1985) and the Brazilian Society of Science in Laboratory Animals - Law nº 11.794. Ethical approval was obtained by the review board of the Universidade Federal do Rio Grande do Sul protocol # 31632. Rats were housed in standard conditions in cages measuring 16 x 41 x 34 cm (height x width x length), provided with wood shaving bedding.

2.2 Neonatal Hypoxia-Ischemia

PND3, PND7 and PND11 male pups were randomly assigned for receiving either Sham or HI procedure. HI animals were anesthetized (isoflurane 4-5% for induction and 1.5-2% for maintenance) and underwent permanent right common carotid artery occlusion, as previously described (Sanches et al., 2013). Animals were kept in warming pads (37ºC) for 10 minutes to recover from anesthesia and were returned to the dam. Two hours after surgery, pups were placed in a hypoxia chamber with fraction inspired of oxygen (FIO_2: 0.08) at 37°C for 90 minutes. Sham animals underwent carotid artery isolation without occlusion and were kept under atmospheric conditions (FIO_2: 0.21). At the end of hypoxic period, all pups returned to their dams.

2.3 Experimental design

Animals were divided into 6 groups, sham (Sh) and hypoxia ischemia (HI) operated in the PND3 (ShP3 and HIP3 respectively), in the PND7 (ShP7 and HIP7 respectively) and in the PND11 (ShP11 and HIP11 respectively). In surgery days litters of 10 male pups with a mother were randomly divided into Sham or HI groups. For every surgery day, at least one litter of each age was present. In Experiment I, 24 and 72h after the surgery animals were submitted to microPET scan imaging. Animals were weaned at PND23 and behavioral tests were performed from PND60 onwards. After, animals underwent perfusion and brains were used for histological analysis. In Experiment II, animals of the same experimental groups were used for ^{14}C-Hydroxybutiric acid and ^{14}C-glucose incorporation into $^{14}CO_2$ at 24 and 72h after the injury.

2.4.1 [^{18}F]FDG microPET scan

MicroPET scans were conducted at the Preclinical Research Center of the Brain Institute of Rio Grande do Sul (BraIns). Brain microPET images were acquired 24 and 72h post-HI. The animals were anesthetized individually using a mixture of isoflurane

and oxygen (3-4% induction and 2-3% maintenance), and 250 μCi of [^{18}F]FDG was administered intraperitoneally (Dagnino et al., 2019). The animals were returned to the home cage for a 40-minute period of conscious tracer uptake and were placed on a heat plate to maintain the body temperature at 36±1°C. After the uptake period, the rats were placed in headfirst prone position on the heated bed of the equipment (Triumph microPET, LabPET-4, TriFoil Imaging, Northridge, CA, USA). The static acquisition was performed under inhalational anesthesia for 10 minutes with the field of view (FOV: 3.75 cm) centered on the head (Nunes Azevedo et al., 2020; Zanirati et al., 2018).

2.4.2 Image reconstruction and data analysis

An exploratory analysis of glucose metabolism was performed in the whole brain, cortex, striatum, hippocampus and corpus callosum bilaterally. All images were reconstructed using a 3-dimensional maximum likelihood expectation maximization (3D-MLEM) algorithm with 20 iterations (Zanirati et al., 2018). MicroPET images were manually co-registered to a standard magnetic resonance imaging (MRI) histological templates corresponding to animals age. MRI templates were obtained from the Duke Center for In Vivo Microscopy NIBIB P41 EB015897 (Calabrese et al., 2013). Standard uptake values (SUVs) were calculated using the following equation: SUV = (radioactivity)/(dose injected/body weight). Each hemisphere SUV was calculated based on manually delimited VOIs, defined on the rat templates and SUV ratio (SUVr) was calculated using the following equation SUVr = structure SUV/Cerebellum SUV (Nonose et al., 2018; Zimmer et al., 2017).

2.5 ^{14}C-Hydroxybutiric acid and ^{14}C-glucose incorporation into $^{14}CO_2$

The ^{14}C-BHB and ^{14}C-glucose incorporation into $^{14}CO_2$ was performed as previously described (de Assis et al., 2016; Ferreira et al., 2007; Torres et al., 2001).

Briefly, animals were decapitated, the right hemisphere was quickly removed, dissected and sliced, in a process that took less than 2 minutes. The samples were then incubated at 37°C for 60 min in flasks sealed with rubber caps containing 1.0 mL of HBSS (Hanks' Balanced Salt solution, pH 7.4), 0.2 µCi Sodium salt Beta-[1-14C] hydroxybutyric acid (55 mCi/mmol, American Radiolabeled Chemicals, St. Louis, MO, EUA) and 5 mM of L-BHB sodium salt (for the ^{14}C-BHB assay) or 0.1µCi [U-^{14}C] glucose (55 mCi/mmol, Amersham, Little Chalfont, UK), and 5 mM of glucose (for the ^{14}C-glucose assay). The gaseous phase was exchanged with a 5% CO_2 and 95% O_2 mixture. Small glass wells containing strips of 3 MM-Whatman paper were placed above the level of the incubation medium ($^{14}CO_2$ wells). The assay was stopped by injecting 0.25 mL of trichloracetic acid solution 50% (v/v) through the rubber caps, and 0.25 mL of NaOH (2.0 M) solution directly into the $^{14}CO_2$ wells. The flasks were kept for 12 h at room temperature in order to capture $^{14}CO_2$ into 3 MM-Whatman paper. The paper contents were transferred to vials containing a liquid scintillation mixture (toluene – Triton X®-100 (2:1, v/v); 2,5-diphenyloxazole (0.4%, v/v) and 2-p-phenylenebis 5-phenyloxazole (0.01%v/v), and radioactivity was measured using a liquid scintillation counter (LKB-Wallac, Perkin Elmer, WALTham, MA, USA). The levels of BHB and glucose oxidation are expressed as nmol incorporated into CO_2/gram of tissue /hour.

2.6 Behavioral Assessment

Behavioral tasks were performed between PND 60 and 80. Ladder Walking and Morris Water Maze tasks were performed for assessing animal's motor and cognitive deficits, respectively.

2.6.1 Ladder Walking

The motor assessment was performed using the ladder walking apparatus, which consists of two transparent acrylic walls (Diameter: 1 m. High: 20 cm) with metal rungs (Diameter: 3mm) inserted into the walls. The ladder remained 30 cm above the ground and a dark cage was located at the end of the apparatus (Metz and Whishaw, 2002). Animals were trained for two days using a regular distance between the rungs. Along each training session, the rats walked across the ladder three times.

On the third day, the walking of the animals was evaluated using an irregular rungs pattern, i.e. the rungs were spaced in intervals of 1 to 3 cm. The test was video-recorded from an inferior view in order to record the four paws. The paws placement on the metal rungs were rated from 0 to 6, with zero being a total miss and six was scored for a totally correct placement (Metz and Whishaw, 2009). An error was considered when the animal slipped the paw or failed to place it on the rung. The final score corresponded to the mean of the three trials for each paw in the third day.

2.6.1 Morris Water Maze

Spatial memory protocol was performed as previously described (Arteni et al., 2003). Briefly, each rat performed four daily trials, during five consecutive days to find a 10cm circumference hidden platform, which was kept in the same position during the training phase. The interval between trials was 10 minutes and the maximum time to find the platform was of 60 seconds for each animal in each attempt. If the animal was unable to find the platform it was gently placed on the platform for 15 seconds. The reduction in the latency to find the platform during the training days was considered an indication of learning. In the probe test, performed 24h after the lasting training day, the platform was removed and each rat had a single 60-second trial. Latency for crossing the platform area for the first time, average speed and time spent in target quadrant were recorded using

ANY-Maze software. The results of the probe trial were considered an indication of the animal's memory retention in the task.

2.7 Brain Histology

Histological analysis was performed in order to assess tissue injury. In brief, animals were anesthetized (100 mg/kg of thiopental sodium, Thiopentax, Cristália®) and transcardially perfused with 0.9% saline solution and 4% paraformaldehyde solution (PFA 4%). Brains were removed from the skull and placed in 4% PFA. Then, the brains were placed in sucrose solution (30%) for cryoprotection and sliced in a cryostat (Leica) at 30 μm thickness between Bregma -1.6 and – 3.8mm (Paxinos and Watson, 2006). Every tenth section was mounted on a gelatin-coated slide and stained using hematoxylin and eosin (Sigma-Aldrich. St Louis. MO.USA). Volumes of hemisphere, cortex, striatum, corpus callosum and hippocampus were assessed using NIH-ImageJ software and calculated using Cavalieri's method, using the equation : $\Sigma \text{ area x (interslice interval)}$. Data are expressed as volume ratio of the ipsilateral hemisphere compared to the contralateral side of carotid occlusion (Odorcyk et al., 2016).

2.8 Statistics

Statistical analysis was performed using SPSS-21 for Windows. Sample sizes were calculated based on previous studies using similar methodologies (Sanches et al., 2015) considering alpha=0.05 and a power of 80%. Two-way ANOVA considering the factors I) Age (P3, P7 or P11) and II) Lesion (Sham and HI), followed by Duncan post-hoc was used in order to identify differences among the groups. In the water maze learning curve a repeated measures two-way ANOVA was performed. Data are expressed as means ± standard error. Significance was accepted whenever $P < 0.05$.

3 Results

3.1 HI did not induce significant motor impairments.

In order to assess HI-induced motor impairments the ladder walking test was performed. There were no differences neither in the number of total errors, nor in the number of errors for each individual paw (data not shown). The comparison of the foot fault score showed no effect of the lesion in any of the assessed parameters. However, an effect of the age was present with asmall decrease was observed in P11 groups and the in the left forelimb ($F(5,90)=3.89$, $p=0.024$, n=14-18 per group) and in the right hindlimb ($F(5,90)=6.11$, $p=0.003$, n=14-18 per group), with no differences among groups in the score of the other paws (Figure 1A-D). The fact that there were no differences in the number of errors between HI groups and their respective Sham groups indicates that the HI insult did not induce significant motor damage, regardless of the age in which the injury occurs.

3.2 HI induced age-dependent cognitive deficits

The Morris water maze task was performed to assess HI-induced learning and memory impairments. During the training sessions, latency to find the platform was considered an indicative of learning. Repeated measures two-way ANOVA showed significant effect of the age and lesion ($F(5,90)=5.69$, $p=0.005$ and $F(5,90)=15.09$, $p<0.001$ respectively, n=14-18 per group), but no interaction ($p=0.146$), meaning that the HI animals had learning impairments when compared to the Sham animals and that the P11 animals also presented such impairment when compared to the other ages. In order to have an overall average for learning, the area under curve for the training days was assessed. A similar pattern was observed with differences in age and lesion ($F(5,90)=5.69$, $p=0.006$ and $F(5,90)=15.09$, $p=0.001$ respectively, n=14-18 per group) and no significant interaction ($p=0.156$). Duncan *pos-hoc* showed no difference between ShP3 and HIP3 groups, however, there was a significant learning deficit in HIP7 group compared to ShP7.

Furthermore, the HIP11 group was not only different from the ShP11, but was also different from other HI groups (Figure 2B). These results clearly show that the learning deficits are worse in animals in which HI is induced at later stages of development. The probe trial, performed 24h after the last training session is used for assessing deficits in memory retention. There were no differences in the swimming speed (data not shown) which implies no motor deficits. The worse performance of P11 group was also present in the latency to reach the platform zone in the probe trial, where only the effect of the age was found significant ($F(5,90)=4.78$, $p=0.011$, n=14-18 per group), while the lesion ($p=0.189$) and the interaction ($p=0.36$) were not (Figure 2C). No differences were observed in the time spent in the platform quadrant ($F(5,90)=1.65$, $p=0.154$, n=14-18 per group) (Figure 2D). Overall, present results suggest that HI induces mainly learning deficits, and that such deficits increase when the lesion is induced at later stages of development.

3.3 HI induced age-dependent tissue injury

After performing behavioral tests, in order to assess HI-induced damage in motor and cognitive parameters, the volumes of main brain structures were analyzed in order to evaluate tissue injury at adulthood. The volumes of the ipsi (right) and contralateral (left) hemisphere, cortex, striatum, corpus callosum and hippocampus were analyzed and are presented as ipsi/contralateral volume ratio. The volume of all structures presented an interaction between age and lesion. Brain hemispheres ($F(5,40)=11.04$, $p<0.001$, n=6-9 per group), corpus callosum ($F(5,40)=11.70$, $p<0.001$, n=6-9 per group) and hippocampus ($F(5,40)=21.22$, $p<0.001$, n=6-9 per group) presented the same pattern, with reductions in HIP7 and HIP11 when compared to their respective shams, with no differences between HIP3 and ShP3. In addition, the comparison among HI groups showed that the most affected group was the HIP11, which presented a greater volume loss when compared to

the other HI groups, whereas the HIP7 group also presented a reduction when compared to the HIP3 group. The cortex ($F(5,40)=8.32$, $p=0.001$, n=6-9 per group) and striatum ($F(5,40)=9.66$, $p<0.001$, n=6-9 per group) presented a similar pattern, with HIP7 and HIP11 being different from their shams, while the HIP3 had no decrease. In these structures, however, although the HIP3 group presented less reduction in relation to other HI groups, the HIP7 and HIP11 groups were not different from each other. Altogether, these results show, in agreement with the behavioral data, that HI-induced tissue damage is more severe when induced in animals in more advanced stages of development.

3.4 HI induced age-dependent hypometabolism detected by microPET

After establishing the age dependent behavioral deficits and HI-induced tissue damage, the aim of this study was to assess how the injury would impact glucose brain metabolism in the first post-lesion days, namely 24 and 72h after HI. The analysis of the standard uptake value (SUV) of the Sham groups already provides relevant information regarding the metabolic changes that the developing brain undergoes at this stage. A linear regression was performed with the SUV in the whole brain of the Sham groups showing that the glucose uptake increases linearly ($r^2=0.497$, $p<0.0001$, $y=0.038x+0.604$, n=8-10 per group) (Figure 4). This analysis revealed a linear daily increase and that between the P4 and P14 the brain glucose uptake doubles.

The effect of HI in glucose metabolism was also assessed in different brain regions 24 and 72h after injury, all structures presented a significant interaction between age and injury in the Two-way ANOVA test (Figure 5). In the hippocampus at 24h there was a reduction in the HIP11 when compared to ShP11, showing that in this region a HI-induced hypometabolism can be found at 24h ($F(5,57)=3.68$, $p=0.032$, n=9-13 per group). At 72h, a similar pattern was observed with HIP11 being the only group that is different from its Sham, furthermore, HIP11 was also reduced when compared to the other HI groups

(F(5,58)=15.46, p<0.001, n=9-13 per group). The same pattern was observed in other structures, with HIP11 group presenting a reduction not only in relation to its Sham, but also from the other HI groups. This pattern was observed in the striatum (24h: F(5,57)=7.20, p=0.002, and 72h: F(5,58)=3.61, p=0.034, n=9-13 per group) and cortex (24h: F(5,57)=8.74 and 72h: F(5,58)=12.55, p<0.001, n=9-13 per group) both in 24 and 72h.

The hypometabolism in HIP11 can also be observed in Figure 6, that shows the percentage of hypometabolism in relation to age matched Sham group. No hypometabolic areas are seen in HIP3 animals in either 24 or 72h. In the HIP7 areas of hypometabolism can be seen only 72h after HI, whereas in HIP11 they can be seen in both 24 and 72h, with a greater area in comparison to the other HI groups. In agreement with behavioral and histological findings, present results also show that HI is more severe when induced in later stages of development.

3.5 [^{18}F]FDG microPET metabolism in the first day post-injury correlates with cognitive and histological parameters in adulthood.

Parameters that are able to predict the injury outcome are often valuable for plaining the best therapeutic strategy (Negro et al., 2018). In order to assess if the [^{18}F]FDG microPET imaging performed 24 and 72h after HI was able to predict the cognitive deficits and size of tissue injury, bivariate correlations were performed. For assessing cognitive deficits, the main outcome was the area under curve during the water maze training phase. This parameter was compared to ipsi/contralateral ratio of histological analysis performed in adulthood and of microPET scan imaging in 3 regions of interest: Cortex, striatum, and hippocampus (Table 1).

As expected, [^{18}F]FDG microPET imaging correlated more strongly with histological than with cognitive parameters. Interestingly, the cortex is the structure that showed the strongest correlation with an r^2 of 0.355, while the striatum showed the weakest with an r^2 of 0.245 in 72h (Table 2). Again, the 72h period presented better predictive power compared to 24h. Overall, present results show that [^{18}F]FDG microPET during the first post-injury days correlate with both cognitive deficits and histological damage, and that 72h period presents better correlations to both parameters than 24h.

When a split by age is performed, meaning doing one correlation with ShP3 and HIP3, a separate one with ShP7 and HIP7 and the same thing with the P11groups, a different pattern emerges. In the comparison with the area under the water maze learning curve (Table 3) there are no significant correlations in the P3 groups, while in the P7 groups they were found only in histological analysis. In the P11 groups, on the other hand, there were correlations in both histology and [^{18}F]FDG microPET at 24h, but not at 72h. When comparing histological data with [^{18}F]FDG microPET (Table 4) a complex pattern emerges, with some significant correlations found in the P3 animals, while none are found in P7. Nevertheless, P11 animals showed significant correlations in all structures at both 24h and 72h. Overall, such results show that [^{18}F]FDG microPET shows its highest predictive value in P11 animals, likely because of their greater lesion.

3.6 HI affects glucose and BHB oxidation

After observing the differences in glucose uptake using microPET scan, questions regarding the actual oxidation of such substrate and others for brain metabolism after HI remained to be answered. The first important observation was obtained assessing the Sham groups only at P4, P8 and P12. Interestingly, the ^{14}C-glucose incorporation into $^{14}CO_2$ did not present significant differences across different ages (Figure 7), whereas ^{14}C-BHB incorporation had a linear reduction of 4 fold in the same period (r^2=0.716,

p<0.001, y=-77.214x+1044.4, n=6-7 per group). These results suggest that although the uptake of glucose increases within development, the tissue capacity of oxidizing glucose remains constant. In contrast, the capacity for BHB oxidation shows greater differences within the same period in healthy animals.

Assessment using in vivo microPET imaging in the ipsilateral hemisphere showed no significant effects the lesion at 24h, but showed an increase in SUVr value with age ($F(5,56)=24.46$, $p<0.001$, n=8-13 per group), without interaction between the two factors (Figure 8A). Furthermore, at 72h a similar pattern is found, with significant effect only in the age ($F(5,58)=42.45$, $p<0.001$, n=8-13 per group) no effect of the injury ($p=0.457$) or interaction ($p=0.122$). It is possible to observe that the reduction in the P3 groups was maintained, but the difference observed between P7 and P11 groups is likely due to the effect of HI injury in the HIP11 group that reduced the average in the P11 animals in relation to the P7 ones.

In order to understand the effects of HI on substrate oxidation, the incorporation of ^{14}C-Glucose and ^{14}C-BHB were assessed in the right hemisphere at 24 and 72h after HI. ^{14}C-Glucose incorporation into $^{14}CO_2$ assessed 24 h after HI showed an interaction between age and lesion ($F(5,41)=4.16$, $p=0.023$, n=6-10 per group). A reduction in both HIP7 and HIP11 was observed when compared to their respective Shams, whereas the HIP3 group did not (Figure 8C). A similar pattern was observed at 72h, also presenting an interaction between the age and lesion ($F(5,39)=6.38$, $p=0.004$, n=7-8 per group), although only the HIP11 group presented a reduction when compared to it respective Sham difference (Figure 8D). These results show that HI is able to induce a reduction in the brain`s capacity to use glucose as an energy substrate in an age-dependent manner, once again, with animals in which injury was induced in latter stages of development presenting more detrimental effects.

Another important substrate for brain metabolism is BHB, mainly in the early stages of CNS development. Here, the ^{14}C-BHB incorporation into $^{14}CO_2$ assessed 24 hours after HI revealed an effect of age ($F(5,41)=46.47$, $p<0.001$, n=7-8 per group), but not of the lesion ($p=0.073$), with significant differences between all ages, with P3 animals presenting the highest levels (Figure 8E). However, it is worth noticing a great tendency of reduction between the ShP3 and HIP3 animals only. A similar pattern was observed in 72h, with the only significant effect being the age ($F(5,40)=3.98$, $p=0.026$, n=6-11 per group), with the P3 group being different from the P11 group, but presenting no differences in relation to the P7 group. Here, it should also be observed that the HIP3 presents higher levels in relation to its sham, in contrast to the patterns observed at 24h (Figure 8F). These results show that HI alters glucose consumption in HIP7 and even more in the HIP11 groups, whereas in the HIP3 group BHB seems to more affected.

4. Discussion

Present study investigated the different responses to neonatal HI injury induced in different neurodevelopmental stages. The injury showed to be more severe when induced in later stages (causing more cognitive deficits, tissue damage and hypometabolism assessed through microPET imaging in the early post-injury days). Differences in brain metabolism that occur at this age seem to play a pivotal role, namely the more prevalent usage of BHB as a metabolic substrate in earlier stages of development compared to glucose. In addition, microPET imaging data, mainly 72h after the neonatal insult, showed significant correlations with behavioral and histological parameters observed at adulthood, showing to be a potential tool to predict the long-term outcome induced by HI. Overall, present results show that brain metabolism plays a pivotal role in the different outcomes observed in HI induced in different stages of development and suggest that

these factors present promising clinical value, being as predictors of the injury outcome or as therapeutic targets.

No significant motor impairments were observed in any of the experimental groups with the injury protocol used in this study, confirming previous literature (Greggio et al., 2014; Miguel et al., 2015; Odorcyk et al., 2016; Sanches et al., 2019). Nevertheless, HI cognitive deficits were clear, being more severe when the injury was induced in more advanced stages of development (Figure 2). Previous studies have investigated the different behavioral outcomes in animals exposed to the same HI model at P3 and P7 (Alexander et al., 2014; Sanches et al., 2015) found similar results, with P7 animals being more affected than P3. In the present study P11 animals were also included, since they resemble the term infant more closely than the P7 animals (Patel et al., 2015, 2014). Indeed, an interesting pattern emerged from these experiments, with P3 animals presenting almost no damage, while increased damage was observed in P7 animals and P11 animals were the most affected. The same pattern was present in histological analysis of the volume of brain structures, namely the cortex, striatum, corpus callosum and hippocampus (Figure 3). These results are again in accordance to previous studies comparing differences between P3 and P7 animals (Alexander et al., 2014; Sanches et al., 2015).

The degree of HI damage is greatly dependent on brain metabolism and it is well documented that it presents significant changes during development (Brekke et al., 2015). Indeed, in the present study, a linear increase in the glucose uptake in the brain was observed between P4 and P14, assessed by microPET scan imaging *in vivo*, (Figure 4). Such findings are in accordance with previous studies that, using different methodologies, found an increase in glucose utilization in the brain is expected during early development (Brekke et al., 2017). Nevertheless, glucose oxidation assay showed a different pattern,

with no differences among the Sham groups, but with more glucose oxidation in the HIP3 animals (Figures 8C). These differences occur because the main limiting factor for glucose uptake in the brain is the small amount of glucose transporters present in the blood-brain barrier (Brekke et al., 2015; Vannucci et al., 1994), whereas ^{14}C-glucose incorporation into $^{14}CO_2$ assay assesses the capacity of cells to oxidize it *ex vivo*, without the limitation imposed by glucose transporters. Altogether, results presented here suggest that one of the mechanisms that can explain the P3 intrinsic neuroprotection is the resilience of the systems involved in the glucose oxidation system, since it was the only age in which ^{14}C-glucose incorporation into $^{14}CO_2$ was not reduced by HI injury.

During the neonatal period, brain utilization of ketone bodies such as BHB in increased in comparison to the adult brain (Brekke et al., 2017). In our study, the brain capacity of oxidizing BHB is at least 4 times greater in the P4 brain when compared to the P12 (Figure 7A). This increased capacity of utilizing BHB, associated to the unchanged glucose usage as energetic source is likely to be involved in the P3 brain intrinsic protection to HI insult. Present results also show a relevant pattern in the BHB oxidation capacity in which P3 animals show increased capacity of BHB oxidation in relation to the other ages, which are probably underlying the resilience of the more immature brain to HI injury. Interestingly, the protective effects of BHB have been previously demonstrated in a study that administered exogenous BHB after HI and showed a reduction of lesion size and cell death (Lee et al., 2018). It has also been demonstrated that the positive effects of dexamethasone treatment are likely dependent on an increase in BHB levels in the blood (Dardzinski et al., 2000). Interestingly, the ketogenic diet is an efficient and safe therapeutic approach for pediatric refractory epilepsy (Cai et al., 2017; Neal et al., 2009), suggesting that BHB administration, as well as ketogenic diet, have high translational value. Overall, present results show that the

higher utilization of BHB is involved in the reduced lesion observed in animals in earlier stages of development, making it a promising therapeutic target that ought to be further investigated.

Furthermore, microPET [^{18}F]FDG has provided important insights in the HI physiopathology. To the best of our knowledge, this is the first study that has used this method to assess the neonatal brain after HI injury in rodents. Here, we show that HIP11 group presented a significant glucose hypometabolism, whereas no significant differences were observed in the HIP7 or HIP3 groups (Figure 5). The hypometabolism mentioned here should be interpreted with caution, since cell death, oxidative stress and inflammation are occurring at this period, which leads to edema and liquification of the brain tissue. This means that the reduction of glucose uptake should not be understood as a simple reduction of cellular metabolism, but as a marker of brain damage. In agreement with findings obtained in clinical studies (Shi et al., 2012; Thorngren-Jerneck et al., 2001), here, stronger correlations were observed between adult cognitive deficits and microPET [^{18}F]FDG 72h post-injury compared to those based on adult histology when all groups were included (Table 1). Although it is likely that an analysis of volume of brain structures performed in the same time points as the microPET [^{18}F]FDG imaging would reveal more powerful correlations, we aimed to assess its ability to predict the resulting histological lesion in the adult, therefore, histological analysis was performed only at adulthood. Indeed, all structures assessed, namely the cortex, striatum and hippocampus presented significant correlations. However, the striatum parameters presented the weakest whereas the cortex presented the strongest predictive value. When the correlations are splitted by age, as shown in tables 3 and 4, it is possible to see that P11 animals present the correlations with higher predictive value. This is likely due to the more severe injury presented by animals of this age that translates in higher cognitive

deficits, tissue damage and hypometabolism. Previous studies have correlated [^{18}F]FDG microPET to behavioral assessments in a model of epilepsy induced by pilocarpine injection, showing significant correlations between behavioral parameters, such as social interactions and anxiety tests and imaging (Di Liberto et al., 2018; van Dijk et al., 2018; Zanirati et al., 2018). A recent study from our research group showed correlations between histological and behavioral tasks of PET scan analysis performed in adulthood in a model of HI induced at P7 (Nunes Azevedo et al., 2020). Nevertheless, the comparison between the predictive values of the present study and the previously mentioned ones is limited by the experimental model, different behavioral tasks used, as well as different statistical analysis and more importantly, because both behavioral tasks and microPET [^{18}F]FDG were performed during adulthood (usually with few days of difference between the imaging acquisition and behavioral tasks).

Although results are interesting and confirm the working hypothesis, there are a few limitations in the present study. The use of male animals only leaves possible sex-differences unexplored and it is known that response to HI injury and to several treatments are sex-specific (Netto et al., 2017). Limitations intrinsic to the animal model are also present; here it is shown that the immature rat brain is less susceptible to HI injury, while in humans it is known that prematurity worsens the prognosis of affected newborns (Volpe, 2009). Therefore, present results ought to be interpreted with caution.

Overall, present study has shown that P3 brain has an intrinsic neuroprotection, showing less or no effects of HI-induced injury in behavioral and histological parameters. This phenomenon can be explained, at least in part, by a more resilient capacity of oxidizing glucose and mainly by a greater capacity of using BHB as an alternative metabolic substrate. MicroPET scan analysis in the first post-injury days presented significant correlations to behavioral deficits and tissue injury observed in adulthood,

suggesting that it should be helpful in clinical settings. Present results suggest that brain metabolism and mainly BHB seem to be promising therapeutic strategies for the treatment of neonatal hypoxia ischemia, such parameters are involved in the greater resistance of neonatal brain to metabolic challenges.

5. Acknowledgements

This study was supported by research grants from the Conselho Nacional de Desenvolvimento Científico e Tecnologico (CNPq, Brazil; Chamada Universal MCTI/CNPq Nº 01/2016, grant number 405470/2016-9) and PUCRS. E. R. Zimmer, C A Netto, and J.C. DaCosta are CNPq researchers.

6. References

Alexander, M., Garbus, H., Smith, A.L., Rosenkrantz, T.S., Fitch, R.H., 2014. Behavioral and histological outcomes following neonatal HI injury in a preterm (P3) and term (P7) rodent model. Behav. Brain Res. 259, 85–96. https://doi.org/10.1016/j.bbr.2013.10.038

Arteni, N.S., Salgueiro, J., Torres, I., Achaval, M., Netto, C.A., 2003. Neonatal cerebral hypoxia-ischemia causes lateralized memory impairments in the adult rat. Brain Res. 973, 171–178. https://doi.org/10.1016/S0006-8993(03)02436-3

Brekke, E., Berger, H.R., Widerøe, M., Sonnewald, U., Morken, T.S., 2017. Glucose and Intermediary Metabolism and Astrocyte–Neuron Interactions Following Neonatal Hypoxia–Ischemia in Rat. Neurochem. Res. 42, 115–132. https://doi.org/10.1007/s11064-016-2149-9

Brekke, E., Morken, T.S., Sonnewald, U., 2015. Glucose metabolism and astrocyte-neuron interactions in the neonatal brain. Neurochem. Int. 82, 33–41. https://doi.org/10.1016/j.neuint.2015.02.002

Cai, Q.Y., Zhou, Z.J., Luo, R., Gan, J., Li, S.P., Mu, D.Z., Wan, C.M., 2017. Safety and tolerability of the ketogenic diet used for the treatment of refractory childhood epilepsy: a systematic review of published prospective studies. World J. Pediatr. https://doi.org/10.1007/s12519-017-0053-2

Calabrese, E., Badea, A., Watson, C., Johnson, G.A., 2013. A quantitative magnetic resonance histology atlas of postnatal rat brain development with regional estimates of growth and variability. Neuroimage. https://doi.org/10.1016/j.neuroimage.2013.01.017

Chiang, M.C., Jong, Y.J., Lin, C.H., 2017. Therapeutic hypothermia for neonates with hypoxic ischemic encephalopathy. Pediatr. Neonatol. https://doi.org/10.1016/j.pedneo.2016.11.001

Dagnino, A.P.A., Da Silva, R.B.M., Chagastelles, P.C., Pereira, T.C.B., Venturin, G.T., Greggio, S., Da Costa, J.C., Bogo, M.R., Campos, M.M., 2019. Nociceptin/orphanin FQ receptor modulates painful and fatigue symptoms in a mouse model of fibromyalgia. Pain 160, 1383–1401. https://doi.org/10.1097/j.pain.0000000000001513

Dardzinski, B.J., Smith, S.L., Towfighi, J., Williams, G.D., Vannucci, R.C., Smith, M.B., 2000. Increased plasma beta-hydroxybutyrate, preserved cerebral energy metabolism, and amelioration of brain damage during neonatal hypoxia ischemia with dexamethasone pretreatment. Pediatr. Res. https://doi.org/10.1203/00006450-200008000-00021

de Assis, A.M., da Silva, J.S., Rech, A., Longoni, A., Nonose, Y., Repond, C., de Bittencourt Pasquali, M.A., Moreira, J.C.F., Souza, D.O., Pellerin, L., 2016. Cerebral ketone body oxidation is facilitated by a high fat diet enriched with advanced glycation end products in normal and diabetic rats. Front. Neurosci. https://doi.org/10.3389/fnins.2016.00509

Di Liberto, V., van Dijk, R.M., Brendel, M., Waldron, A.M., Möller, C., Koska, I., Seiffert, I., Gualtieri, F., Gildehaus, F.J., von Ungern-Sternberg, B., Lindner, M., Ziegler, S., Palme, R., Hellweg, R., Gass, P., Bartenstein, P., Potschka, H., 2018. Imaging correlates of behavioral impairments: An experimental PET study in the rat pilocarpine epilepsy model. Neurobiol. Dis. https://doi.org/10.1016/j.nbd.2018.06.010

Ferreira, G.C., Tonin, A., Schuck, P.F., Viegas, C.M., Ceolato, P.C., Latini, A., Perry, M.L.S., Wyse, A.T.S., Dutra-Filho, C.S., Wannmacher, C.M.D., Vargas, C.R., Wajner, M., 2007. Evidence for a synergistic action of glutaric and 3-hydroxyglutaric acids disturbing rat brain energy metabolism. Int. J. Dev. Neurosci. https://doi.org/10.1016/j.ijdevneu.2007.05.009

Greggio, S., De Paula, S., Azevedo, P.N., Venturin, G.T., Dacosta, J.C., 2014. Intra-arterial transplantation of human umbilical cord blood mononuclear cells in neonatal hypoxic-ischemic rats. Life Sci. https://doi.org/10.1016/j.lfs.2013.10.017

Jacobs, S.E., Berg, M., Hunt, R., Tarnow-Mordi, W.O., Inder, T.E., Davis, P.G., 2013. Cooling for newborns with hypoxic ischaemic encephalopathy. Cochrane Database Syst. Rev. https://doi.org/10.1002/14651858.CD003311.pub3

Lee, B.S., Woo, D.C., Woo, C.W., Kim, K.S., 2018. Exogenous β-Hydroxybutyrate Treatment and Neuroprotection in a Suckling Rat Model of Hypoxic-Ischemic Encephalopathy. Dev. Neurosci. https://doi.org/10.1159/000486411

Metz, G.A., Whishaw, I.Q., 2009. The ladder rung walking task: A scoring system and its practical application. J. Vis. Exp. https://doi.org/10.3791/1204

Metz, G.A., Whishaw, I.Q., 2002. Cortical and subcortical lesions impair skilled walking in the ladder rung walking test: A new task to evaluate fore- and hindlimb stepping, placing, and co-ordination. J. Neurosci. Methods. https://doi.org/10.1016/S0165-0270(02)00012-2

Miguel, P.M., Schuch, C.P., Rojas, J.J., Carletti, J.V., Deckmann, I., Martinato, L.H.M., Pires, A.V., Bizarro, L., Pereira, L.O., 2015. Neonatal hypoxia-ischemia induces attention-deficit hyperactivity disorder-like behavior in rats. Behav. Neurosci. 129, 309–320.

Neal, E.G., Chaffe, H., Schwartz, R.H., Lawson, M.S., Edwards, N., Fitzsimmons, G., Whitney, A., Cross, J.H., 2009. A randomized trial of classical and medium-chain triglyceride ketogenic diets in the treatment of childhood epilepsy. Epilepsia. https://doi.org/10.1111/j.1528-1167.2008.01870.x

Negro, S., Benders, M.J.N.L., Tataranno, M.L., Coviello, C., De Vries, L.S., Van Bel, F., Groenendaal, F., Longini, M., Proietti, F., Belvisi, E., Buonocore, G., Perrone, S., 2018. Early prediction of hypoxic-ischemic brain injury by a new panel of biomarkers in a population of term newborns. Oxid. Med. Cell. Longev. https://doi.org/10.1155/2018/7608108

Netto, C.A., Sanches, E., Odorcyk, F.K., Duran-Carabali, L.E., Weis, S.N., 2017. Sex-dependent consequences of neonatal brain hypoxia-ischemia in the rat. J. Neurosci. Res. https://doi.org/10.1002/jnr.23828

Nonose, Y., Gewehr, P.E., Almeida, R.F., da Silva, J.S., Bellaver, B., Martins, L.A.M., Zimmer, E.R., Greggio, S., Venturin, G.T., Da Costa, J.C., Quincozes-Santos, A., Pellerin, L., de Souza, D.O., de Assis, A.M., 2018. Cortical Bilateral Adaptations in Rats Submitted to Focal Cerebral Ischemia: Emphasis on Glial Metabolism. Mol. Neurobiol. https://doi.org/10.1007/s12035-017-0458-x

Nunes Azevedo, P., Zanirati, G., Teribele Venturin, G., Garcia Schu, G., Elena Durán–Carabali, L., Kawa Odorcyk, F., Vinicius Soares, A., de Oliveira Laguna, G., Alexandre Netto, C., Rigon Zimmer, E., Costa da Costa, J., Greggio, S., 2020. Long-term changes in metabolic brain network drive memory impairments in rats following neonatal hypoxia-ischemia. Neurobiol. Learn. Mem. https://doi.org/10.1016/j.nlm.2020.107207

Odorcyk, F.K., Sanches, E.F., Nicola, F.C., Moraes, J., Pettenuzzo, L.F., Kolling, J., Siebert, C., Longoni, A., Konrath, E.L., Wyse, A., Netto, C.A., 2016. Administration of Huperzia quadrifariata Extract, a Cholinesterase Inhibitory Alkaloid Mixture, has Neuroprotective Effects in a Rat Model of Cerebral Hypoxia–Ischemia. Neurochem. Res. 42, 552–562. https://doi.org/10.1007/s11064-016-2107-6

Parent, M.J., Zimmer, E.R., Shin, M., Kang, M.S., Fonov, V.S., Mathieu, A., Aliaga, A., Kostikov, A., do Carmo, S., Dea, D., Poirier, J., Soucy, J.P., Gauthier, S., Cuello, A.C., Rosa-Neto, P., 2017. Multimodal imaging in rat model recapitulates Alzheimer's disease biomarkers abnormalities. J. Neurosci. https://doi.org/10.1523/JNEUROSCI.1346-17.2017

Park, W.S., Chang, Y.S., Lee, M., 2001. Effects of hyperglycemia or hypoglycemia on brain cell membrane function and energy metabolism during the immediate reoxygenation-reperfusion period after acute transient global hypoxia-ischemia in the newborn piglet. Brain Res. https://doi.org/10.1016/S0006-8993(01)02295-8

Patel, S.D., Pierce, L., Ciardiello, A., Hutton, A., Paskewitz, S., Aronowitz, E., Voss, H.U., Moore, H., Vannucci, S.J., 2015. Therapeutic hypothermia and hypoxia-ischemia in the term-equivalent neonatal rat: characterization of a translational preclinical model. Pediatr. Res. 78, 264–71. https://doi.org/10.1038/pr.2015.100

Patel, S.D., Pierce, L., Ciardiello, A.J., Vannucci, S.J., 2014. Neonatal encephalopathy: pre-clinical studies in neuroprotection. Biochem. Soc. Trans. 42, 564–8. https://doi.org/10.1042/BST20130247

Paxinos, G., Watson, C., 2006. The Rat Brain in Stereotaxic Coordinates Sixth Edition by. Acad. Press 170, 547612. https://doi.org/10.1016/0143-4179(83)90049-5

Perlman JM., 2004. Brain injury in the term infant. Semin. Perinatol. 28, 415–424. https://doi.org/10.1053/j.semperi.2004.10.003

Pinchefsky, E.F., Hahn, C.D., Kamino, D., Chau, V., Brant, R., Moore, A.M., Tam, E.W.Y., 2019. Hyperglycemia and Glucose Variability Are Associated with Worse Brain Function and Seizures in Neonatal Encephalopathy: A Prospective Cohort Study. J. Pediatr.

https://doi.org/10.1016/j.jpeds.2019.02.027

Sanches, E.F., Arteni, N., Nicola, F., Aristimunha, D., Netto, C.A., 2015. Sexual dimorphism and brain lateralization impact behavioral and histological outcomes following hypoxia-ischemia in P3 and P7 rats. Neuroscience 290, 581–593. https://doi.org/10.1016/j.neuroscience.2014.12.074

Sanches, E.F., Arteni, N.S., Nicola, F., Boisserand, L., Willborn, S., Netto, C.A., 2013. Early hypoxia-ischemia causes hemisphere and sex-dependent cognitive impairment and histological damage. Neuroscience 237, 208–215. https://doi.org/10.1016/j.neuroscience.2013.01.066

Sanches, E.F., van de Looij, Y., Toulotte, A., Sizonenko, S.V., Lei, H., 2019. Mild Neonatal Brain Hypoxia-Ischemia in Very Immature Rats Causes Long-Term Behavioral and Cerebellar Abnormalities at Adulthood. Front. Physiol. https://doi.org/10.3389/fphys.2019.00634

Semple, B.D., Blomgren, K., Gimlin, K., Ferriero, D.M., Noble-Haeusslein, L.J., 2013. Brain development in rodents and humans: Identifying benchmarks of maturation and vulnerability to injury across species. Prog. Neurobiol. 106–107, 1–16. https://doi.org/10.1016/j.pneurobio.2013.04.001

Shi, Y., Zhao, J.N., Liu, L., Hu, Z.X., Tang, S.F., Chen, L., Jin, R. Bin, 2012. Changes of positron emission tomography in newborn infants at different gestational ages, and neonatal hypoxic-ischemic encephalopathy. Pediatr. Neurol. https://doi.org/10.1016/j.pediatrneurol.2011.11.005

Sizonenko, S. V., Kiss, J.Z., Inder, T., Gluckman, P.D., Williams, C.E., 2005. Distinctive neuropathologic alterations in the deep layers of the parietal cortex after moderate ischemic-hypoxic injury in the P3 immature rat brain. Pediatr. Res. 57, 865–872. https://doi.org/10.1203/01.PDR.0000157673.36848.67

Thorngren-Jerneck, K., Ohlsson, T., Sandell, A., Erlandsson, K., Strand, S.E., Ryding, E., Svenningsen, N.W., 2001. Cerebral glucose metabolism measured by positron emission tomography in term newborn infants with hypoxic ischemic encephalopathy. Pediatr. Res. https://doi.org/10.1203/00006450-200104000-00010

Torres, I.L.S., Gamaro, G.D., Silveira-Cucco, S.N., Michalowski, M.B., Corrêa, J.B., Perry, M.L.S., Dalmaz, C., 2001. Effect of acute and repeated restraint stress on glucose oxidation to CO2 in hippocampal and cerebral cortex slices. Brazilian J. Med. Biol. Res. https://doi.org/10.1590/S0100-879X2001000100013

van Dijk, R.M., Di Liberto, V., Brendel, M., Waldron, A.M., Möller, C., Gildehaus, F.J., von Ungern-Sternberg, B., Lindner, M., Ziegler, S., Hellweg, R., Gass, P., Bartenstein, P., Potschka, H., 2018. Imaging biomarkers of behavioral impairments: A pilot micro–positron emission tomographic study in a rat electrical post–status epilepticus model. Epilepsia. https://doi.org/10.1111/epi.14586

Vannucci, S.J., Seaman, L.B., Brucklacher, R.M., Vannucci, R.C., 1994. Glucose transport in developing rat brain: Glucose transporter proteins, rate constants and cerebral glucose utilization. Mol. Cell. Biochem. https://doi.org/10.1007/BF00926756

Volpe, J.J., 2009. Brain injury in premature infants: a complex amalgam of destructive and developmental disturbances. Lancet Neurol. https://doi.org/10.1016/S1474-4422(08)70294-1

Zanirati, G., Azevedo, P.N., Venturin, G.T., Greggio, S., Alcará, A.M., Zimmer, E.R., Feltes, P.K., DaCosta, J.C., 2018. Depression comorbidity in epileptic rats is related to brain glucose hypometabolism and hypersynchronicity in the metabolic network architecture. Epilepsia. https://doi.org/10.1111/epi.14057

Zimmer, E.R., Parent, M.J., Souza, D.G., Leuzy, A., Lecrux, C., Kim, H.I., Gauthier, S., Pellerin, L., Hamel, E., Rosa-Neto, P., 2017. [18F]FDG PET signal is driven by astroglial glutamate transport. Nat. Neurosci. https://doi.org/10.1038/nn.4492

Zou, R., Xiong, T., Zhang, L., Li, S., Zhao, F., Tong, Y., Qu, Y., Mu, D., 2018. Proton magnetic resonance spectroscopy biomarkers in neonates with hypoxic-ischemic encephalopathy: A systematic review and meta-analysis. Front. Neurol. https://doi.org/10.3389/fneur.2018.00732

Figures

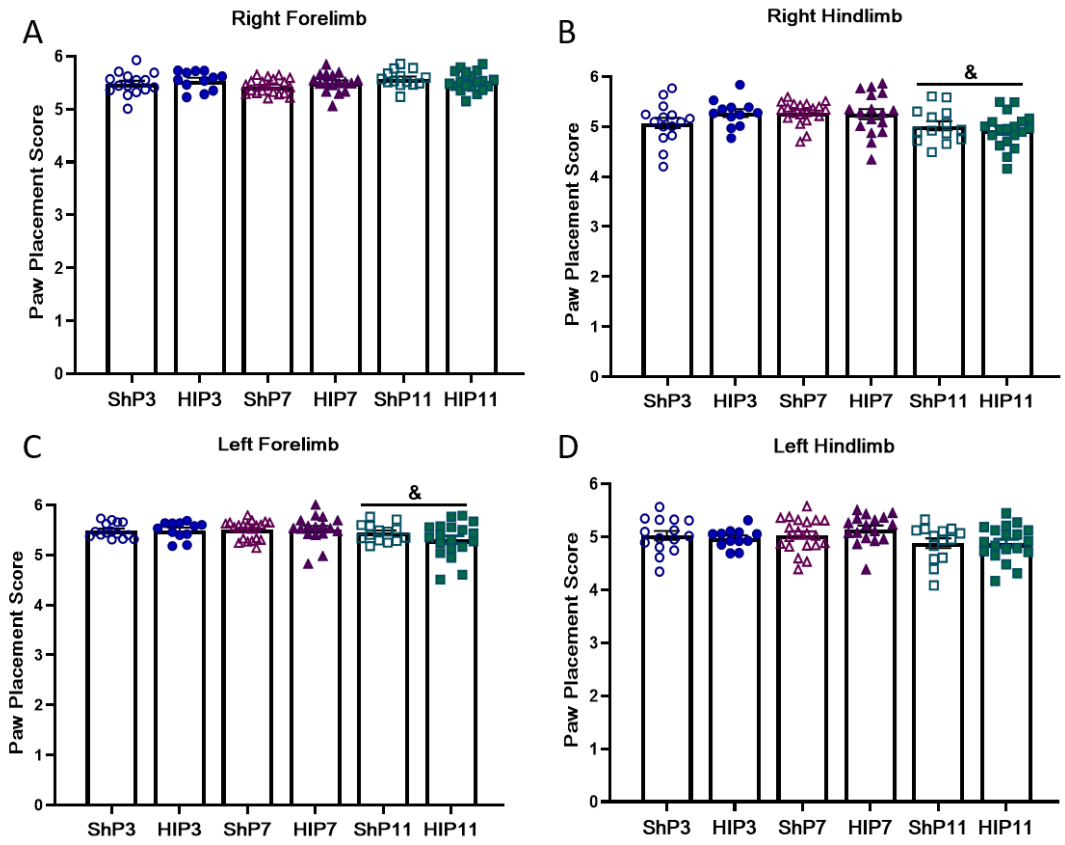

Figure 1- Ladder walking test motor coordination assessment. Data expressed as average of Paw Placement Score ± SE. Two-way ANOVA followed by Duncan's *post-hoc*. N=14-18 per group. & Age effect.

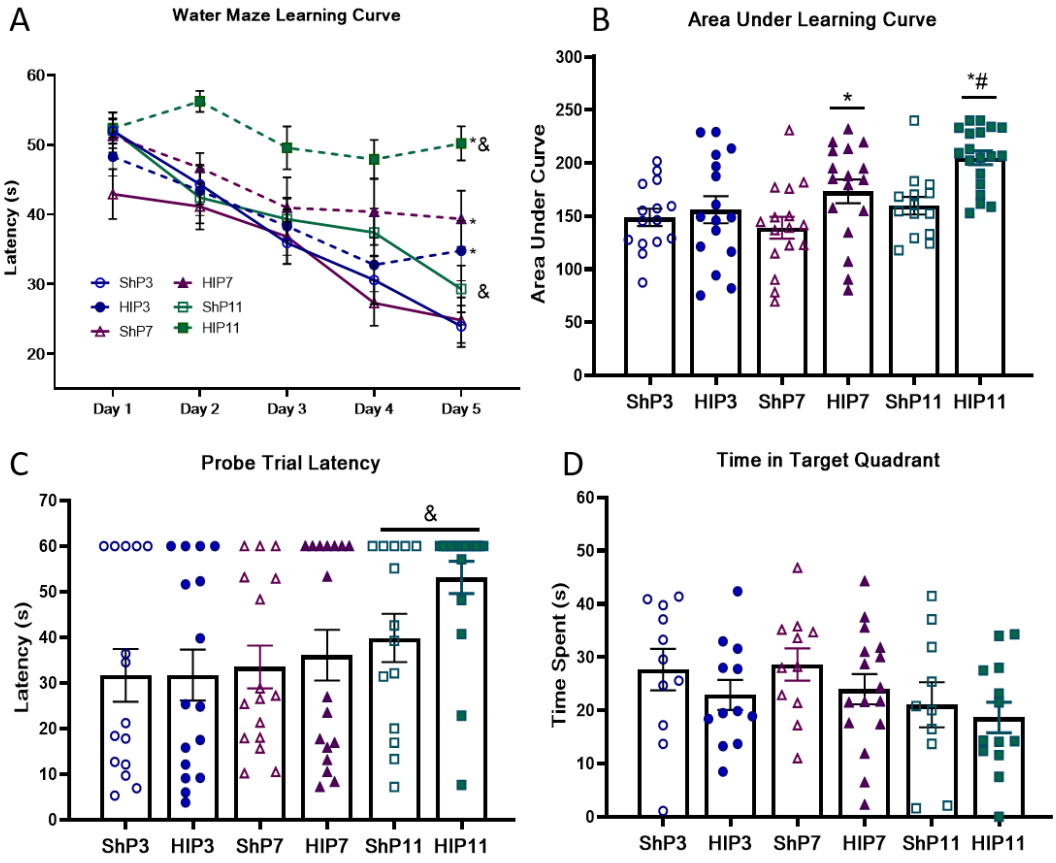

Figure 2- Morris Water Maze cognitive analysis. Learning curve during the training days (A) and Area under the learning curve (B) during the five days of training. Probe trial latency to reach the platform location and (C) time spent in the target quadrant (D). Data are expressed as average ± SE. Two-way ANOVA followed by Duncan's *post-hoc*. N=14-18 per group. * HI vs. respective Sham; # Difference to other HI groups; & Age effect.

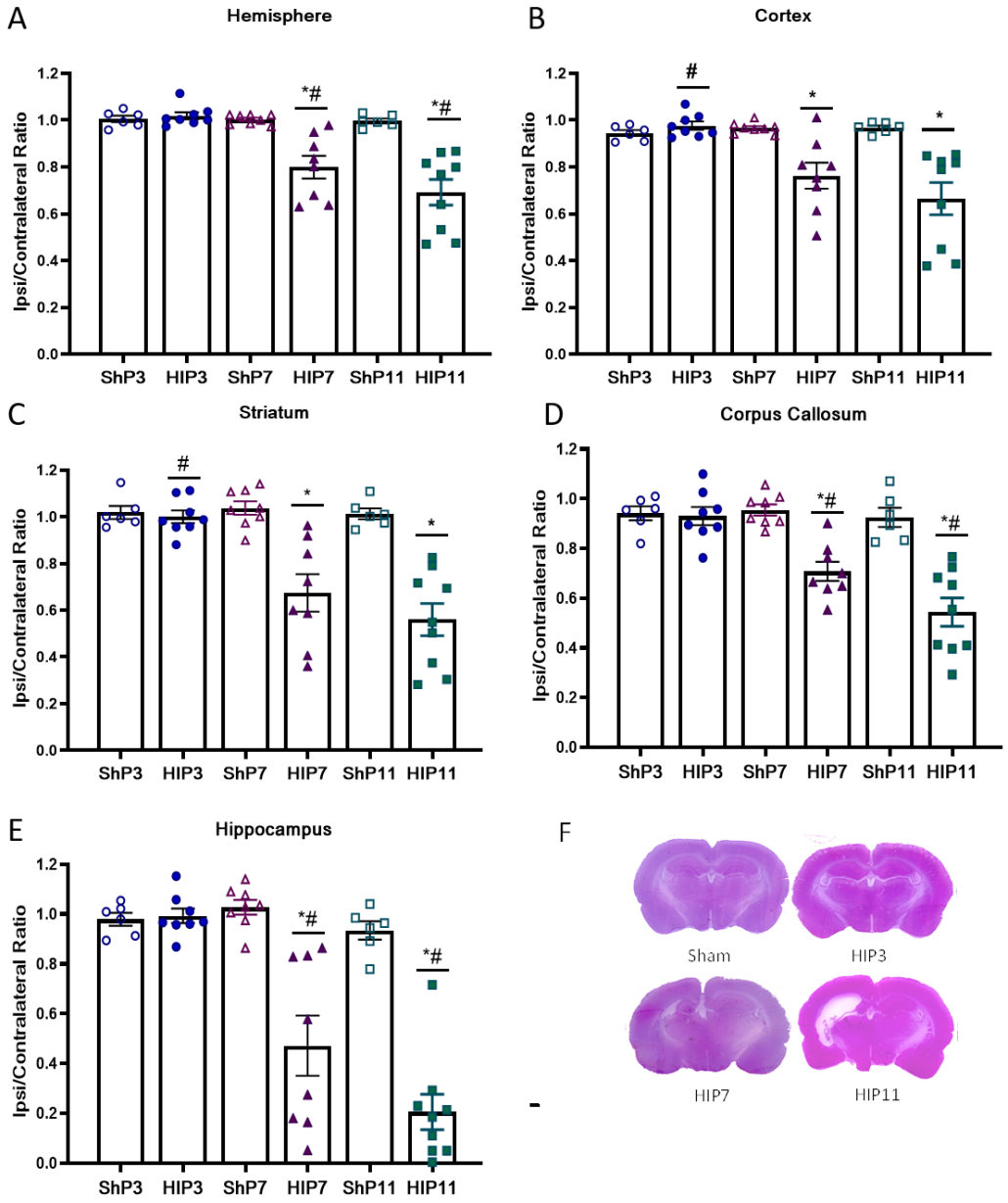

Figure 3- HI-induced brain damage in different brain structures. Ipsi/contralateral volume ratio of hemispheres (A), cortices (B), striatum (C), corpus callosum (D) and hippocampi (E), as well as representative images of the HE staining (F). Data are expressed as average ± SE. Two-way ANOVA followed by Duncan's *post-hoc*. N=6-9 per group. * HI vs. respective Sham; # Difference to other HI groups.

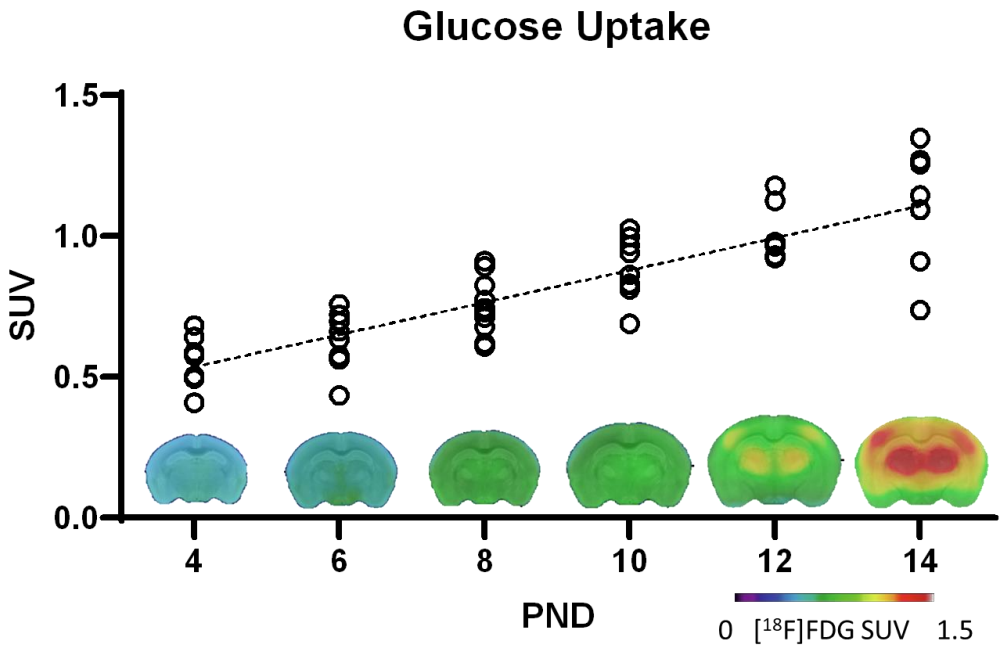

Figure 4 - Brain glucose uptake increase during neurodevelopment. Glucose Standard Uptake Value ratio (SUVr) assessed by microPET scan imaging after [^{18}F]FDG injection in each post-natal day (PND) in non-injured rats. Linear regression (r^2=0.497, p<0.0001, y=0.038x+0.604, n=8-10 per group). At the graph's bottom, representative images showing SUV average for each PND (4, 6, 8, 10, 12 and 14).

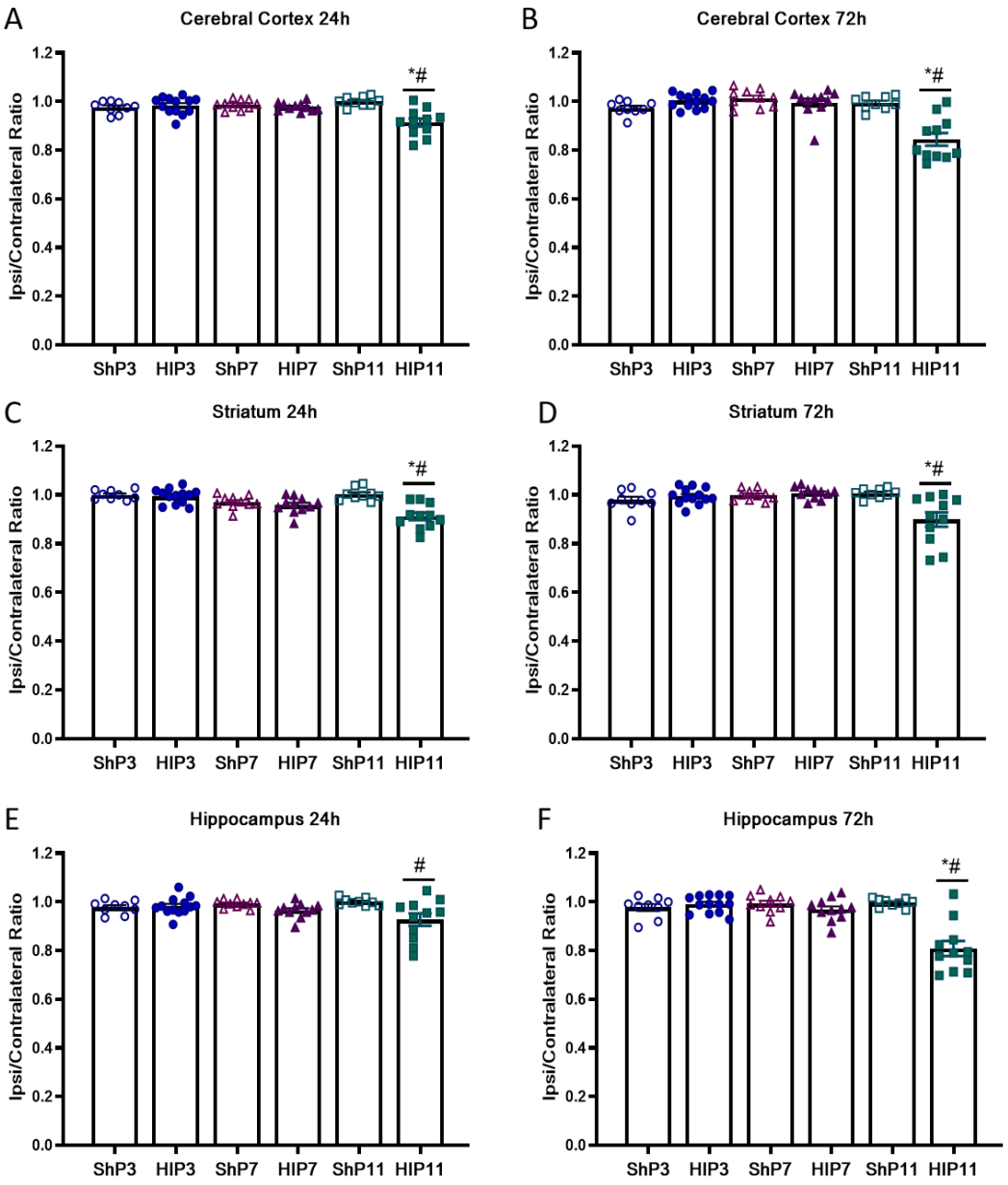

Figure 5- HI-induced hypometabolism in different brain structures. Ipsi/contralateral SUV ratio 24 and 72h post-HI on cortex (A, B), striatum (C, D), and hippocampus (E, F). Data expressed as average ± SE. Two-way ANOVA followed by Duncan's *post-hoc*. N=9-13 per group. * HI vs. respective Sham; # Difference to other HI groups.

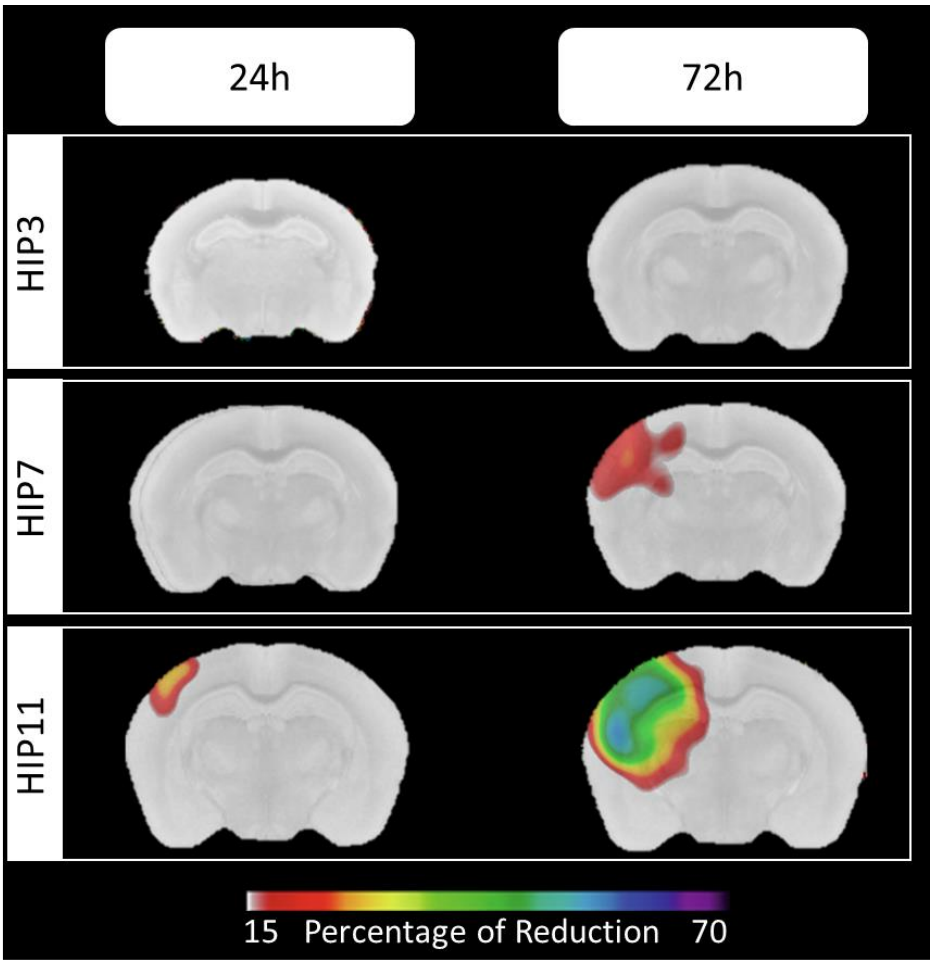

Figure 6- Hypometabolism decrease percentage following HI. Images showing areas with 15% or more of hypometabolism after HI induced at the three different ages and assessed 24 and 72 hours after injury compared to their respective Sham group. An increase in the hypometabolic area can be seen when HI is induced in latter stages of development. It is also possible to notice that this area grows from 24 to 72h after the initial insult.

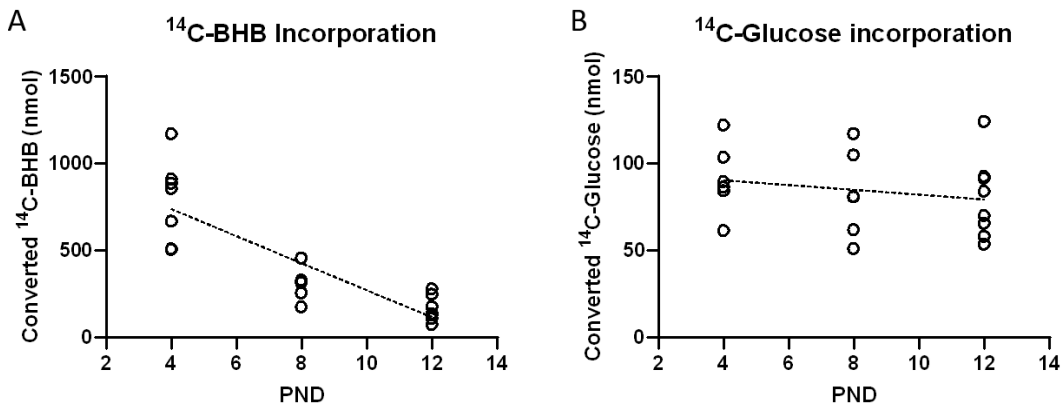

Figure 7- Beta-hydroxybutyrate (BHB) oxidation capacity in the total brain tissue. With the increase in age, while with glucose it remains unchanged. ^{14}C-BHB incorporation into $^{14}CO_2$ reduces linearly within the assessed post-natal days (PND) (A) (r^2=0.716, p<0.001, y=-77.214x+1044.4). Whereas ^{14}C-Glucose incorporation into $^{14}CO_2$ remained unchanged. N=6-7 per group.

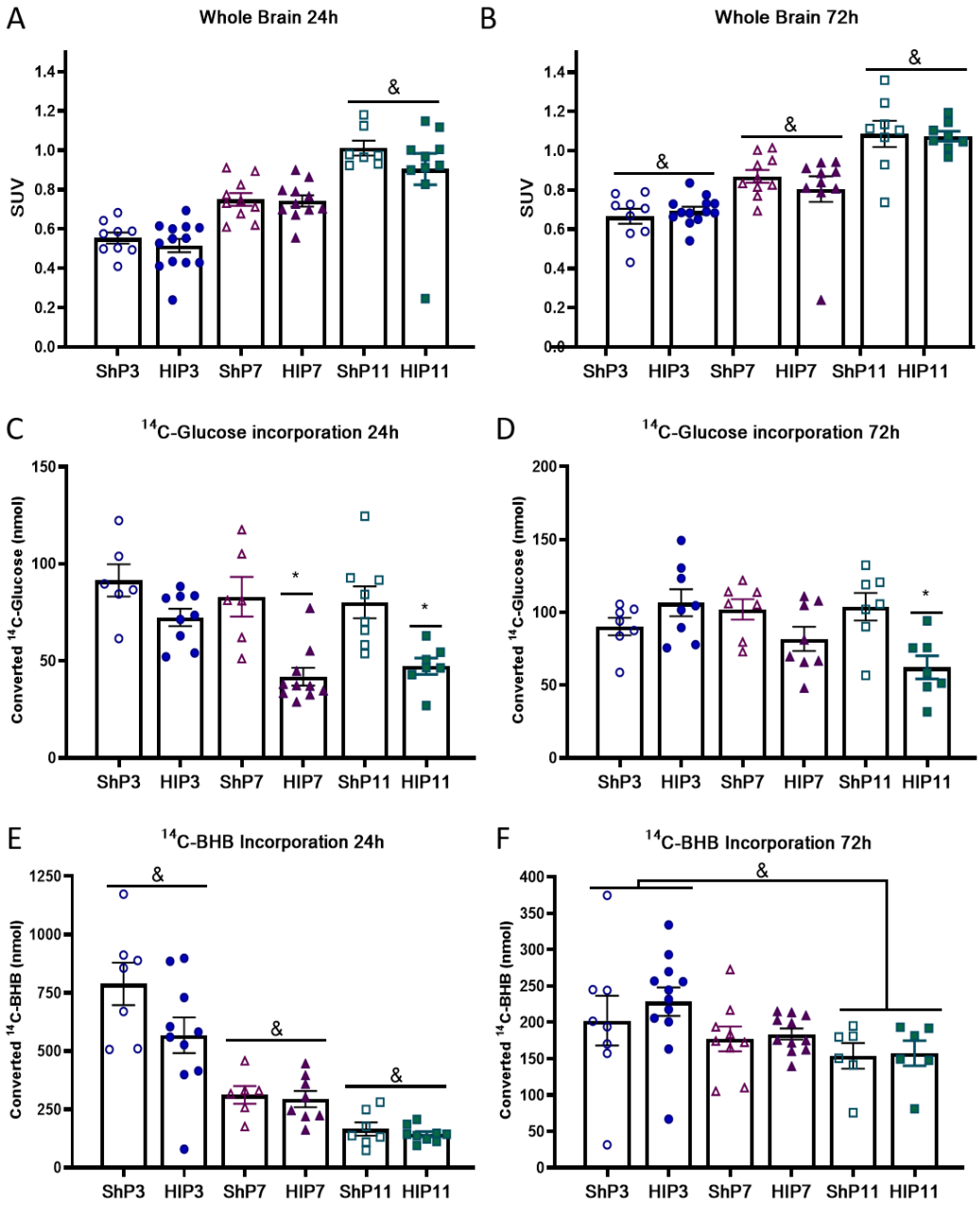

Figure 8- HI-induced age-dependent metabolic substrate utilization changes in both *in vivo* and *ex vivo* in the ipsilateral hemisphere. *In vivo* assessment of glucose uptake 24 (A) and 72h (B) after HI by microPET scan imaging after [^{18}F]FDG injection (N=8-13 per group). *Ex vivo* evaluation of ^{14}C-Glucose incorporation into $^{14}CO_2$ (C and D) and of ^{14}C-BHB incorporation into $^{14}CO_2$ (E and F) (N=6-11 per group). Data are expressed as

average ± SE. Two-way ANOVA followed by Duncan's *post-hoc*. * HI vs. respective Sham; # Difference to the other groups; & Age effect.

4. Capítulo II

Differential age-dependent mitochondrial dysfunction, oxidative stress and apoptosis induced by neonatal hypoxia-ischemia in the immature rat brain

Odorcyk FK, Ribeiro RT, Roginski AC, Duran-Carabali LE, Couto-Pereira NS, Dalmaz C, Wajner M, Netto CA.

Artigo submetido à revista Molecular Neurobiology.

Differential age-dependent mitochondrial dysfunction, oxidative stress and apoptosis induced by neonatal hypoxia-ischemia in the immature rat brain

Odorcyk FK[1]*, Ribeiro RT[3], Roginski AC[3], Duran-Carabali LE[1], Couto-Pereira NS[3], Dalmaz C[3], Wajner M[3], Netto CA[1,2,3].

[1]Graduate Program in Phisiology, Universidade Federal do Rio Grande do Sul (UFRGS), Porto Alegre, RS, Brazil.

[2] Graduate Program in Neuroscience, Universidade Federal do Rio Grande do Sul (UFRGS), Porto Alegre, RS, Brazil.

[3]Department of Biochemistry, Universidade Federal do Rio Grande do Sul (UFRGS), Porto Alegre, RS, Brazil.

*Corresponding author at: Felipe Kawa Odorcyk, Post-graduation Program of Physiology, Instituto de Ciências Básicas da Saúde (ICBS), Universidade Federal do Rio Grande do Sul (UFRGS). Rua Ramiro Barcelos 2600, anexo. CEP 90035-003, Porto Alegre, RS, Brazil.

Phone: 0055-51 33085568.

E-mail: felipe.odorcyk@gmail.com

Abstract

Neonatal hypoxia-ischemia (HI) is among the main causes of mortality and morbidity in newborns. Experimental studies show that the immature rat brain is less susceptible to HI injury, suggesting that changes that occur during the first days of life drastically alter its susceptibility. Among the main developmental changes observed is the mitochondrial function, namely the tricarboxylic acid (TCA) cycle and respiratory complexes (RC) activities. Therefore, in the present study we investigated the influence of neonatal HI on mitochondrial functions, redox homeostasis and cell damage at different postnatal ages in hippocampus of neonate rats. For this purpose, animals were divided into four groups: sham postnatal day 3 (ShP3), HIP3, ShP11 and HIP11. We initially observed increased apoptosis in the HIP11 group only, indicating a higher susceptibility of these animals to brain injury. Mitochondrial damage, as determined by flow cytometry showing mitochondrial swelling and loss of mitochondrial membrane potential, was also demonstrated only in the HIP11 group. This was consistent with the decreased mitochondrial oxygen consumption, reduced TCA cycle enzymes and RC activities and induction of oxidative stress in this group of animals. Considering that HIP3 and the sham animals showed no alteration of mitochondrial functions, redox homeostasis and showed no apoptosis, our data suggest an age-dependent vulnerability of the hippocampus to HI. The present results highlight age-dependent metabolic differences in the brain of neonate rats submitted to HI indicating that different treatments might be needed for HI newborns with different gestational ages.

Key-words: neonatal hypoxia-ischemia (HI); brain metabolism; brain development, mitochondrial function; oxidative stress.

1. Introduction

Neonatal hypoxia-ischemia (HI) is among the major causes of neonatal death and morbidity, affecting up to 1.5% of neonates (Laptook et al., 2017). Recent medical advances improved the survival rates of affected newborns, although they often develop life-long disabilities such as cognitive disabilities, epilepsy and cerebral palsy (Volpe, 2009). HI affects both pre-term and at term neonates and, despite the similarity in the nature of the insult, developmental stage differences seem to underlie their differential response to both injury and treatment strategies (Jacobs et al., 2013).

Pre-clinical rodent models of brain injuries have substantially contributed to the understanding of mechanisms and development of new treatments. The Rice-Vannucci model is one of the most used in HI research, combining the unilateral permanent occlusion of the common carotid artery with a period of hypoxic exposure (Rice et al., 1981). This allows the same injury protocol to be inflicted to animals at different stages of brain development. When performed in post-natal day 3 (PND3), it mimics the injury of very preterm human infants (ranging from 28 to 32 weeks of gestation). Whereas, when performed at PND11 it mimics the injury in term infants (> 36 weeks of gestation) (Patel et al., 2015; Sanches et al., 2015; Semple et al., 2013; Sizonenko et al., 2005).

Brain metabolism is a key determinant of the severity of the HI insult in both clinical (Shi et al., 2012; Thorngren-jerneck et al., 2001) and experimental (Odorcyk et al., 2020) studies. The decrease in cerebral blood flow reduces the availability of oxygen and energy substrates such as glucose, decreasing the activity of the tricarboxylic acid (TCA) cycle and oxidative phosphorylation, which culminates in the lack of ATP for brain cells (Brekke et al., 2017). Although several cells die because of the metabolic stress alone, the majority of cell death occurs several hours or days later in a process known as the secondary injury phase (Davidson et al., 2015b; Liu & Zhang, 2014). The secondary

damage occurs because of the long-lasting mitochondrial dysfunction observed after HI that leads to increased production of reactive oxygen species often coupled with a reduction of the activity of antioxidant enzymes (Liu & McCullough, 2013; Odorcyk et al., 2017). Oxidative stress associated with a neuroinflammatory process induces cell death by apoptosis that reaches its peak at 24h after the insult but can remain elevated up to 72h (Liu & Zhang, 2014).

Previous experimental reports have shown that the brain developmental stage is critical to determine the severity of HI injury, being more severe in animals in more advanced stages of development (Alexander et al., 2014; Sanches et al., 2015). A recent study showed that while animals with PND11 injury presented significant brain tissue loss and cognitive deficits, animals injured at PND3 showed almost no detectable damage when exposed to the same HI protocol in rats (Odorcyk et al., 2020). Although the mechanisms that provide the immature brain this "intrinsic protection" are not fully understood, the brain energy metabolism seems to play a pivotal role. During development, brain metabolism passes through dramatic changes, ranging from substantial usage of ketone bodies in the more immature brain to glucose, which is the main energy substrate in the adult brain (Brekke et al., 2015). In fact, the higher utilization of ketone bodies such as beta-hydroxybutyrate is suggested to be one of the mechanisms of the "intrinsic protection" of the immature brain (Odorcyk et al., 2020).

Nevertheless, the metabolic substrate is not the only parameter that goes through changes during development. Indeed, the TCA cycle and its enzymes present a considerable increase of activity between PND5 and PND20 (Baquer et al., 1977; Booth et al., 1980). Interestingly, despite being greatly affected by HI and presenting significant changes during development, it is unknown how HI affects the mitochondrial function in animals at different developmental stages. Understanding such mechanisms may aid in

the development of new therapeutic interventions for the treatment of neonatal hypoxia-ischemia.

2. Methodology

2.1 Animals

Adult female Wistar rats and their male pups were used in this study. The litters were composed 10 male rat pups with an adult female; in order to avoid any litter effect, each litter contained pups of at least 3 different mothers, with a maximum of 4 pups of the same mother in each litter. All litters were standardized at PND1. All experimental procedures followed the recommendations of the Council for International Organizations of Medical Sciences (CIOMS - Publication 85-23, 1985) and the Brazilian Society of Science in Laboratory Animals - Law nº 11.794. All techniques were previously approved by the review board of the Universidade Federal do Rio Grande do Sul protocol # 31632. Rats were housed in standard conditions in cages measuring 16 x 41 x 34 cm (height x width x length), provided with wood shaving bedding.

2.2 Neonatal Hypoxia-Ischemia

PND3 and PND11 male pups were randomly assigned for receiving either Sham or HI procedure. HI animals were anesthetized with isoflurane (4-5% for induction and 1.5-2% for maintenance) and underwent permanent right common carotid artery occlusion, as previously described (Odorcyk et al., 2020). Animals were maintained at 37ºC for 10 minutes until fully recovery from anesthesia and were returned to the dam. 2h after surgery, pups were placed in a hypoxic chamber with fraction of inspired oxygen (FiO_2: 0.08) at 37°C for 1.5h. Sham animals underwent anesthesia, carotid artery isolation without occlusion and were kept under atmospheric conditions (FiO_2: 0.21). At the end of the hypoxic period, all pups returned to their dams.

2.3 Experimental design

Animals were divided into 4 groups, sham (Sh) and hypoxia-ischemia (HI) operated at PND3 (ShP3 and HIP3 respectively) and at PND11 (ShP11 and HIP11 respectively). In surgery days, litters of 10 male pups with a mother were divided into Sham or HI groups. All assessments were performed 24 h after surgery.

2.4 Western Blot

Brains were quickly dissected out and the right hippocampus (ipsilateral to the carotid occlusion) was collected and stored at -80 ºC. Western blot analysis was performed as previously described (Durán-Carabali et al., 2019). Briefly, hippocampi were homogenized and the protein concentration was measured. An equal concentration (40 µg of total protein/lane) was loaded into gels (NuPAGE® 4–12% Bis-Tris). Following electrophoresis, proteins were then transferred to nitrocellulose membranes. The blots were blocked for 2 hours and incubated overnight at 4°C with one of the primary antibodies: anti-caspase-3 (1:1000, Cell Signaling), anti cleaved Caspase-3 (1:1000, Cell Signaling), anti-COX-IV (1:100, Cell Signaling), anti-GAPDH (1:1000, Merck). Membranes were washed with T-TBS and incubated with peroxidase-conjugated secondary antibody (anti-rabbit or anti-mouse concentration of 1:1000) for 2 hours. The detection was made with the enhanced chemiluminescence plus GE-LAS 4000 digital image reader (GE Healthcare Life Sciences). Data were quantified as the ratio between the interest protein´s optical density and GAPDH in the same blot. Results are expressed as a percentage of the control group (ShP3), or cleaved Caspase-3/Caspase-3 ratio.

2.5 Flow cytometry

Samples of the right hippocampus, ipsilateral to the carotid occlusion, were collected 24 h after the HI insult. In short, samples were minced and underwent a gentle

mechanical dissociation with a pestle in HBSS, filtered through a cell strainer (with 70µm pores), and then centrifuged for 5 min at 500 g. The supernatant was removed and the pellet resuspended with Hank's Balanced Salt Solution (HBSS) containing 200nM of the fluorochromes: MitoTracker Red (MTR), a marker of mitochondrial potential and MitoTracker Green (MTG) a marker of mitochondrial mass, for 30 minutes at room temperature (Lima et al., 2018). The samples were analyzed with BD FACSCalibur™ flow cytometer. Negative controls (containing unstained cells, cells stained with MTG only, and cells stained with MTR only) were included to set up the equipment voltages and determine the gating strategy. The population of cells that presented lower potential (MTR fluorescence intensity) in relation to its mass (MTG fluorescence intensity) were considered cells with mitochondrial swelling.

2.6 Tricarboxylic acid cycle enzymes activities

For the measurements of the TCA cycle enzymes activities, citrate synthase (CS) and malate dehydrogenase (MDH), crude hippocampus homogenates were used. The right hippocampus was homogenized (1:10 w/v) in SETH buffer containing 250 mM sucrose, 2.0 mM EDTA, 10 mM Trizma base, and 50 IU/mL heparin), pH 7.4, and the homogenate centrifuged at 800 g for 10 min at 4 °C to discard nuclei and cell debris.

CS activity was assayed according to Srere (Srere, 1969), by spectrometrically monitoring the 5,5-dithio-bis (2-nitrobenzoic acid (DTNB) reduction at 37 °C at 412 nm and expressed as µmol.min^{-1}.mg protein^{-1}. MDH activity was measured according to Kitto (Kitto, 1969), by following the NADH fluorescence at 37 °C at 340 (excitation) and 450 (emission) nm. The absorbance and fluorescence changes were recorded on a SpectraMax M5 plate reader (Molecular Devices, Sunnyvale, CA, USA). The results are expressed as µmol NADH oxidized min^{-1}·mg protein^{-1}.

2.7 Respiratory chain complexes activities

The right hippocampus was homogenized (1:20 w/v) in SETH buffer pH 7.4 and prepared as described above in the section 2.6. The supernatant was aliquoted and submitted to three subsequent freeze-thawing procedures before it was used to determine of the activities of the respiratory chain complexes.

Succinate:cytochrome c oxidoreductase activity (complex II-III) was determined by the reduction of cytochrome c (50μM) at 550 nm (Fischer et al., 1985). The reaction media also contained 40 mM potassium phosphate buffer, pH 7.4, 16 mM sodium succinate, 4 mM sodium azide, 7μM rotenone, and tissue supernatant (approximately 30 μg of protein).

Cytochrome c oxidase (COX; complex IV) activity was evaluated by following cytochrome c oxidation (75 μM) at 25 °C at 550 nm (Rustin et al., 1994). The reaction medium also contained tissue supernatant (approximately 1.5 μg of protein), 10 mM potassium phosphate buffer, pH 7.0, and 0.6 mM dodecylmaltoside.

The absorbance changes were recorded on a SpectraMax M5 plate reader (Molecular Devices, Sunnyvale, CA, USA). These respiratory chain activities were calculated and expressed as $\mu mol \cdot min^{-1} \cdot mg\ protein^{-1}$.

2.8 Mitochondrial oxygen consumption

The rate of oxygen consumption was measured using an OROBOROS Oxygraph-2k (Innsbruck, Austria) in a thermostatically controlled (37 °C) and magnetically stirred incubation chamber (Gnaiger, 2009), with modifications (Cecatto et al., 2016). The assay

was performed with right hippocampus crude homogenates (2 mg tissue/mL) and incubated in MIR 05 buffer containing 0.5 mM EGTA, 3 mM $MgCl_2$, 60 mM K-lactobionate, 20 mM taurine, 10 mM KH_2PO_4, 20 mM HEPES, 110 mM sucrose, 1 g/L BSA, pH 7.1.

Oxygen consumption was measured through substrate-uncoupler inhibitor titration (SUIT) protocol (Makrecka-Kuka et al., 2015). Complex I (C-I) and C-II-linked respiration were obtained by pyruvate (5 mM), malate (0.5 mM), and glutamate (10 mM) (PMG) and succinate (10 mM) supplementation, respectively. Oxidative phosphorylation (OXPHOS) capacity (state 3 respiration) was determined by ADP (500 μM), whereas oligomycin (1 μg mL^{-1}) was used to obtain the resting respiration (state 4). Next, 0.75 μM carbonilcianeto m-clorofenil-hidrazona (CCCP) (three pulses of 0.25 μM) was supplemented to induce the uncoupled respiration, and 2 μM rotenone (complex I inhibitor) was used to obtain the uncoupled respiration stimulated by succinate. Finally, 2.5 μM antimycin A (complex III inhibitor) was used to inhibits the transfer of electrons from heme b_H to oxidized Q, and with this to block all remaining mitochondrial respiration. The real-time oxygen fluxes were calculated using DatLab5 (Oroboros Instruments) and expressed as pmol O2 flux·s^{-1}·mg $protein^{-1}$.

2.9 Redox homeostasis parameters

For the evaluation of the redox homeostasis parameters, the hippocampus was homogenized in 10 volumes (1:10, w/v) of 20 mM sodium phosphate buffer, pH 7.4, containing 140 mM KCl. Homogenates were centrifuged at 750×g for 10 min at 4 °C and the supernatants were utilized for the determination of the parameters.

2.9.1 Malondialdehyde (MDA) levels

Lipid peroxidation was estimated by measuring the concentrations of MDA according to the method described by Yagi (Yagi, 1998), with some modifications (Ribeiro et al., 2018). One hundred microliters of hippocampus supernatant was treated with 200 μL of 10% trichloroacetic acid (TCA) and 300 μL of 0.67% thiobarbituric acid in 7.1% sodium sulfate and incubated for 1 h in a boiling water bath. The tubes containing the mixture were allowed to cool on running tap water for 5 min. The resulting pink-stained complex were extracted with 400 μL of butanol. Fluorescence of organic phase was read at 515 and 553 nm as excitation and emission wavelengths, respectively. A calibration curve was performed using 1,1,3,3-tetramethoxypropane and MDA levels were calculated as nanomole MDA ·mg protein-1.

2.9.2 2′,7′-Dichlorofluorescin (DCFH) oxidation

DCFH oxidation was determined according to LeBel (LeBel and Bondy, 1990), with slight modifications (Ribeiro et al., 2018), in order to examine reactive oxygen species generation. Hippocampus supernatant was incubated with 2′,7′-dichlorofluorescein diacetate (DCF-DA), prepared in 20 mM sodium phosphate buffer, pH 7.4, containing 140 mM KCl, during 1 hour at 37 °C. After incubation, DCF fluorescence was measured using wavelengths of 480 nm (excitation) and 535 nm (emission). The calibration curve was performed with standard DCF. The production of reactive species was calculated as as micromole DCF·mg protein^{-1}.

2.9.3 Reduced glutathione (GSH) concentrations

The GSH concentrations were determined according to Browne and Armstrong (Browne and Armstrong, 1998) with some modifications. One hundred microliters of hippocampus supernatants were treated with 2% metaphosphoric acid (1:1) and centrifuged for 10 min at 7000 g for deproteination. An aliquot of supernatant (30 μL)

was added to a medium containing 185 µL of 100 mM sodium phosphate buffer, pH 8.0, with 5 mM EDTA and 15 µL of ophthaldialdehyde (1 mg/mL in methanol), and incubated in a dark room for 15 min at room temperature. The fluorescence was measured using excitation and emission wavelengths of 350 and 420 nm, respectively . A calibration curve was prepared using a GSH standard solution and the results were expressed as nmol GSH·mg protein^{-1}.

2.9.4 Antioxidant enzymes activities

For the determination of the antioxidant enzyme activities, the samples were prepared in the same manner as for the evaluation of other redox homeostasis parameters. The absorbance changes for all enzymes were recorded on a SpectraMax M5 plate reader (Molecular Devices, Sunnyvale, CA, USA). The specific activities were expressed as U·mg protein^{-1}.

Glutathione peroxidase (GPx) activity was evaluated using tert-butyl hydroperoxide as substrate and monitoring NADPH oxidation at 25 °C at 340 nm (Wendel, 1981). The reaction medium contained tissue supernatants, 100 mM potassium phosphate buffer, pH 7.0, with 1 mM EDTA, 0.4 mM sodium azide, 2 mM GSH, 0.1 U/mL glutathione reductase (GR), 0.1 mM NADPH and 0.5 mM tert-butyl hydroperoxide. One GPx unit (U) is defined as 1 µmol of NADPH consumed per min.

Superoxide dismutase (SOD) activity was measured based on pyrogallol autoxidation. This process is highly dependent on superoxide, the substrate of SOD, and is thereby inhibited by this enzyme. Thus, SOD activity can be measured indirectly following pyrogallol absorbance at 25 °C at 420 nm(Marklund and Marklund, 1974). The reaction medium contained tissue supernatant, 50 mM Tris buffer, pH 8.2, with 1 mM

EDTA, 80 U/mL CAT and 0.8 mM pyrogallol. A calibration curve was performed using purified SOD.

2.10 Protein determination

Protein content was measured by the method of Lowry et al. (Lowry et al., 1951) method, using bovine serum albumin as a standard.

2.11 Statistics

Statistical analysis was performed using SPSS-21 for Windows. Sample sizes were calculated based on previous studies using similar methodologies (Sanches et al., 2015) considering alpha=0.05 and a power of 80%. Two-way ANOVA considering the factors I) Age (P3 or P11) and II) Lesion (Sham and HI), followed by Tukey *post-hoc* test was used in order to identify differences among the groups. Data are expressed as means ± standard deviation. Significance was accepted whenever $P < 0.05$.

3. Results

3.1 HI induced age-dependent apoptosis

Assessment of the cleaved Caspase-3/Caspase-3 ratio 24 hours post-injury in the ipsilateral hippocampus showed no interaction between age and lesion ($F(3,21)=3.88$, $p=0.062$, n=6-7 per group), although both factors reach statistical significance when assessed separately (Age: $F(3,21)=6.51$, $p=0.019$; Injury: $F(3,21)=21.14$, $p<0.001$). No differences were observed between ShP3 and HIP3, in contrast, the HIP11 group showed increased apoptosis when compared to both ShP11 and HIP3 ($F(3,21)=10.34$, $p=0.42$, n=6-7 per group) (Figure 1A). As expected, these results show increased cell death levels

by apoptosis in the HIP11 in relation to HIP3 animals, showing that rats at more advanced stages of development are more vulnerable to HI insult.

3.2 No difference in COX-IV levels were observed among experimental groups

Levels of COX-IV were also assessed by Western blot in the ipsilateral hippocampus 24h after HI; this protein is used as a mitochondrial loading control. No differences were observed in any of the factors (Age: $F(3,23)=0.52$, $p=0.477$; Injury: $F(3,23)=0.15$, $p=0.700$) (Figure 1B). These results suggest that there are no major differences in the total amount of mitochondria, meaning that differences observed in the following results are not likely due to any difference in mitochondrial number or mass.

3.3 Increased mitochondrial swelling and loss of mitochondrial potential in an age-dependent way

The relation of mitochondrial mass and potential was performed by flow cytometry 24h after HI (Figure 2A). The amount of cells presenting mitochondrial swelling was increased in ShP11 group when compared to the Shp3 group, indicating that age alone influences this parameter. Nevertheless, while the HIP3 did not present differences from its sham, the HIP11 group presented an increase, showing that HI induces mitochondrial swelling in the P11 group only ($F(3,29)=11.04$, $p=0.002$, n=7-9 animals per group) (Figure 2B). The potential/mass ratio was also run in order to assess changes in mitochondrial membrane potential. While no differences were observed in the HIP3 group when compared to its sham, the HIP11 group presented a reduction when compared to its sham and in relation to HIP3 group ($F(3,29)=5.33$, $p=0.028$, n=7-9 animals per group) (Figure 2C). These results show that the P11 brain mitochondria are

more susceptible to HI injury when compared to those of P3 brain, as demonstrated by higher rates of mitochondrial swelling and loss of mitochondrial membrane potential.

3.4 TCA cycle enzymes were affected in an age-dependent manner

CS and MDH activities were assessed in the hippocampus 24h after the injury. As expected, CS activity presented an interaction between age and lesion. An increase with age was evidenced by higher values in the ShP11 in relation to ShP3 (Figure 3A). Furthermore, while the HIP3 group did not present significant differences to its sham group, there was a reduction in the HIP11 group when compared to its sham ($F(3,19)=10.74$, $p=0.004$, n = 5-7 per group). These results suggest a greater vulnerability of the P11 brain as compared to the P3 brain.

MDH activity also showed an interaction between age and lesion. There were no differences between the Sham groups, suggesting that this enzyme activity does not change during this stage of development. However, as was the case with CS, the effect of the injury was observed in the HIP11 only, presenting reduced activity in relation to both ShP11 and HIP3 groups ($F(3,21)=13.52$, $p=0.001$, n = 5-7 per group)(Figure 3B). Altogether, presented results suggest that the TCA cycle shows an age-dependent vulnerability to the HI insult, being reduced in the HIP11 group only.

3.5 Activities of mitochondrial complexes were affected in an age-dependent manner

The activities of mitochondrial electron transport chain complexes were assessed in the ipsilateral hippocampus 24h after HI. The activity of complex II-III showed an increase with development, with ShP11 presenting higher levels in relation to ShP3. As regards to the effect of HI, it was again observed that HIP11 presented differences as

compared to its sham ($F(3,18)=15.08$, $p=0.001$, n = 5-6 per group) (Figure 3C). On the other hand, Complex IV activity showed a different pattern, with no significant interaction between age and lesion, but with both factors being significant when assessed separately (Age: $F(3,20)=112.54$, $p<0.001$; Injury: $F(3,20)=13.41$, $p=0.002$). P11 animals showed lower activity when compared to P3, indicating a decrease in the activity with aging. Interestingly, the injury reduced the activity in the HIP3 group only, with no differences between HIP11 and its sham (Figure 3D). These results suggest that mitochondrial complexes were altered in an age-dependent manner, with complex II-III being more affected in HIP11 and complex IV more affected in HIP3.

3.6 HI induced age-dependent impairment of mitochondrial respiration

Mitochondrial respiratory parameters were measured by quantification of oxygen consumption in the ipsilateral hippocampus 24h after HI. State 3 respiration (ADP-stimulated) linked to complexes I and II showed no differences between the sham groups of both ages. However, while HIP3 presented no differences when compared to its sham, a reduction in the HIP11 group was observed when compared to both ShP11 and HIP3, suggesting a greater mitochondrial vulnerability of P11 animals ($F(3,13)=37.12$, $p<0.001$, n=3-5 per group) (Figure 4A). A separate assessment of state 3 respiration to complex I demonstrated an increase in the ShP11 group when compared to ShP3, while the effect of HI was verified as a reduction in the HIP11 in relation to ShP11, with no such differences in the P3 groups ($F(3,13)=64.88$, $p<0.001$, n=3-5 per group) (Figure 4B). In contrast to the age differences observed in state 3 respiration linked to complex I, the ADP-stimulated oxygen consumption by complex II presented no differences between ShP3 and ShP11. Nevertheless, the HI-induced reduction in the HIP11 group was still present, which was different from its ShP11 and HIP3 ($F(3,15)=16.42$, $p=0.002$, n=4-5 per group)(Figure 4C).

In contrast, the effects of age between the Sham groups were verified in the uncoupled respiration (CCCP-stimulated), with ShP11 presenting higher rates of oxygen consumption in relation to ShP3. Moreover, HI-induced reduction of uncoupled respiration in the HIP11 group when compared to the ShP11 group ($F(3,13)=16.82$, $p=0.001$, n=3-5 per group)(Figure 4D). Overall, these results suggest a greater reserve capacity (difference between state 4 and uncoupled respiration) in the ShP11, as compared to ShP3, that was lost in the HIP11 group. The same pattern emerged when assessing the complex I-induced uncoupled respiration, with an increase of ShP11 as related to ShP3, and a reduction of HIP11 when compared to its sham ($F(3,13)=15.84$, $p=0.002$, n=3-5 per group) (Figure 4E). On the other hand, no differences between the sham groups when uncoupled respiration was induced by C-II-linked substrates, but an HI-induced reduction in the HIP11 group in comparison to ShP11 and HIP3 groups ($F(3,11)=16.42$, $p=0.002$, n=3-5 per group) (Figure 4F). Finally, state 4 respiration (oligomycin-stimulated) also showed an increase in the ShP11 group when compared to the ShP3, as well as an HI effect in the HIP11 group only, presenting reduced levels in relation to ShP11 ($F(3,14)=14.09$, $p=0.002$, n=4-5 per group)(Figure 4G). Overall, these results show a great increase in oxygen consumption with development in complex I, while this was not observed in complex II. Furthermore, HI impaired mitochondrial respiration in both assessed mitochondrial complexes, revealing that P11 mitochondrial function is more vulnerable to HI injury.

3.7 HI induces age-specific responses to oxidative stress biomarkers

Oxidative stress biomarkers were also assessed 24h after HI in the ipsilateral hippocampus. There was no difference in production of reactive oxygen species, assessed by the DCFH technique, between the ShP3 and ShP11, although an increase in both HIP3 and HIP11 groups was evidenced in comparison to their respective shams ((F(3,28)= 6.58,

p<0,016, n= 8 per group)(Figure 5A). In order to evaluate lipid peroxidation the MDA assay was performed, that did not show an interaction between age and lesion, although both factors presented significant differences when assessed separately (Age: $F(3,30)=141.43$, $p<0.001$; Injury: $F(3,30)=109.58$, $p<0.001$, n= 8 per group). TBA-RS levels increased with age, since the ShP11 showed higher levels in relation to ShP3. Also, HI induced an increase in TBA-RS in both HIP3 and HIP11 in relation to their respective sham group (Figure 5B).

Antioxidant defenses were also investigated. The activity of superoxide dismutase (SOD), for instance, did not present differences between the sham groups, but showed an increase in both HI groups when compared to their respective shams, with a higher increase in the HIP11 group **(**$F(3,28)=4.50$, $p=0.43$, n= 8 per group) (Figure 5C). Glutathione peroxidase (GPx) activity revealed a distinct pattern, with both factors presenting significant differences, but without interaction (Age: $F(3,26)=17.09$, $p<0.001$; Injury: $F(3,26)=16.70$, $p<0.001$, n=7-8 per group). A decrease in the ShP11 in relation to the ShP3 group was observed, suggesting a reduction in its activity throughout this period of development. Furthermore, a significant increase in relation to its sham was observed in the HIP11 group only, (Figure 5D). The levels of reduced glutathione (GSH) were also assessed, showing no interaction between factors and no differences between the ages, but a decrease in both HIP3 and HIP11 when compared to their respective shams ($F(3,32)=33.53$, $p<0,001$, n= 8-10 per group) (Figure 5E), also suggesting a HI-induced increase in reactive oxygen species. Altogether, presented results show that HI induces changes in oxidative stress biomarkers in both ages increasing the release of ROS often combined with an increase in the activity of the antioxidant enzymes. In most assays, the injury effects in the HIP11 group were increased when compared to the HIP3 group, suggesting a higher susceptibility of P11 animals to the injury.

4. Discussion

The present study investigated age-dependent responses of brain metabolism after neonatal HI. Greater levels of cell death indicate that the P11 brain is more susceptible to the insult. The greater susceptibility of P11 animals was also manifested in HI-induced increase of mitochondrial swelling, loss of mitochondrial potential, reduction in the activity of TCA cycle enzymes, as well as in mitochondrial complexes activity. High-resolution respirometry showed that mitochondrial respiration presented higher levels in P11 animals, when compared to P3-uninjured rats. Mitochondrial complex I substrate supported respiring mitochondria showed more changes along development when compared to complex II substrate supported respiring mitochondria, although both were affected by HI in P11 animals only. Oxidative stress parameters showed that HI induced greater increase in reactive oxygen species production and lipid peroxidation in P11 animals. Overall, the present results show that the higher susceptibility of P11 animals to HI injury is due to higher mitochondrial vulnerability, presenting a reduction in TCA cycle and mitochondrial respiration, which increased ROS production and lipid peroxidation. These findings bring new insights into the mechanisms of HI in different developmental stages and show promising targets for the development of new therapeutic tools for this pathology.

Cell death by apoptosis assessed 24h after HI presented a significant increase in the HIP11. The higher resiliency of the immature P3 brain has been previously shown in rats submitted to the HI model, where animals in more advanced stages of development showed greater behavioral deficits and histological damage (Alexander et al., 2014; Odorcyk et al., 2020; Sanches et al., 2015). A recent study showed that the intrinsic neuroprotection of the immature brain is due, at least in part, to differences in brain metabolism, namely by its higher capacity of ketone bodies oxidation (Odorcyk et al.,

2020). The focus of the present study was to assess whether mitochondrial function was determinant for HI severity when induced in different developmental stages. The assessment of mitochondrial biomarker COX-IV did not reveal any differences between groups. This result suggests that mitochondrial density remained unchanged regardless of age or presence of HI. Although it has been reported that a great increase in activity and levels of proteins occurs in the mitochondria between birth and adulthood (Gregson and Williams, 1969; Hagberg et al., 2014), these alterations do not seem to affect COX-IV levels in the developmental period assessed here.

Mitochondrial damage was assessed by flow cytometry performed with MitoTracker staining. Increase in mitochondrial swelling and loss of mitochondrial membrane potential were induced by HI in P11 animals. These phenomena are classic mitochondrial reactions to hypoxic and/or ischemic events (Garcia et al., 1978; J. Li et al., 2014; Lima et al., 2018). These processes are triggered by increased concentration of intracellular Ca^{2+} caused by mass neuronal depolarization that occurs by the lack of ATP availability to the Na^{+}-K^{+} ATPase pump (Sanderson et al., 2013). This process will induce mitochondrial failure affecting ATP production and increasing damage by oxidative stress (Davidson et al., 2015b). These processes associated to neuroinflammatory processes are going to induce cell death by apoptosis (Benjelloun et al., 2003; S. Li et al., 2014). Once the higher resiliency of the immature mitochondrial to HI damage was established, we aimed to investigate differences in metabolism and mitochondrial function.

The activity of CS showed a great effect of age, with an increase in ShP11 when compared to ShP3, in agreement with previous studies (Booth et al., 1980; Brekke et al., 2015). Interestingly, the response to injury was quite different between both ages, with a great reduction of CS and MDH enzymatic activity observed in the HIP11 group only, while no alterations were observed in the HIP3 group. Furthermore, the activity of

mitochondrial complex II-III presented a similar pattern, increasing with age and presenting HI-induced reduction in P11 animals only. The increase of complex II-III is in agreement with previous studies that showed a steady increase from P0 that reaches its peak at P21 (de-Souza-Ferreira et al., 2019). Despite of the different pattern presented by cytochrome c oxidase, the results of GS, MDH and complex II-III suggest that the increase in metabolic rate observed during development makes the P11 brain more vulnerable to the hypoxic ischemic insult, while the lower metabolic rate of the P3 brain makes it more resilient. Indeed, one of the main protective mechanisms of therapeutic hypothermia, only used in late preterm/term neonates, is the reduction of metabolic rate (Globus et al., 1995; Jacobs et al., 2013), which makes the metabolic rate of these infants more similar to the P3 animals as shown in the present study. The use of therapeutic hypothermia in infants younger than 36 weeks is still an issue in debate, one of the main reasons for this debate is the increase in the rate of adverse events such as coagulopathy (Herrera et al., 2018; Rao et al., 2017). Nevertheless, considering that pre-terms with less gestational weeks present reduced metabolic rate, it is possible that the protective effects of hypothermia would also be reduced; however, more studies are needed to understand the effects of hypothermia in different stages of development.

Respirometry experiments were performed in order to understand the effects of age and response to HI injury in mitochondrial respiratory complexes. A separate assessment of complexes I and II showed that the first presented increase in its activity with development, while the second did not. However, both presented an HI-induced reduction in the P11 group only. Interestingly, when comparing state 3 respiration (more similar to physiological levels), with uncoupled respiration (maximum respiration), these differences increase. The potential of the mitochondria to increase its activity under stressful conditions is known as reserve capacity (Dranka et al., 2010; Nannelli et al.,

2018). Here, it is shown that the ShP11 group possess the highest reserve capacity and that the complex I substrate supported mitochondrial respiration is the one responsible for such phenomenon. Surprisingly, these mitochondrial properties seen as protective, did not avoid the HI-induced mitochondrial damage observed in HIP11 group. In fact, during insults such as HI, when ATP consumption is increased by excitotoxic events, in this context, the increased reserve capacity possibly depletes all energetic reserves quicker, thus increasing mitochondrial damage.

Mitochondrial damage is linked to increased production of ROS. Here, it was shown that HI insult increased ROS production in both ages, but more evident in the HIP11 group, possibly leading to the higher levels of lipid peroxidation and cell death, GSH levels were reduced in both HI groups, and the activities of both antioxidant enzymes GPx and SOD were lower in the ShP11 suggesting that P11 animals have lower defenses against oxidative stress. Nevertheless, the HIP11 group was able to increase the activity of both enzymes when compared to its sham, while HIP3 animals did not. Despite the increase in relation to its sham, HIP11 levels were still either not different (in the case of GPx), or lower (in the case of SOD) when compared to HIP3 group. This increase in activity observed in HIP11 group is should be attributed to the reduced basal activity observed in the ShP11, that increases to HIP3-like levels after the injury. It is expected that along with the increase in oxygen usage observed during development, an increase in superoxide and hydrogen peroxide production also occurs (de-Souza-Ferreira et al., 2019). Nevertheless, these augmented levels of ROS production are not necessarily accompanied by the antioxidant defenses, making the mature brain more susceptible to oxidative stress, Mavelli and coworkers have shown that while SOD presented an increase with age, GPx remained constant (Mavelli et al., 1982), in addition, it has also been reported a decrease in the activity of the antioxidant thioredoxin system during

development (de-Souza-Ferreira et al., 2019). The increase in the activity of antioxidant enzymes after HI model in rats has also been previously described, but without comparisons between different ages (Odorcyk et al., 2017; Weis et al., 2011). The lower activity of antioxidant enzymes such as SOD, combined to the increased production of ROS makes the P11 brain more susceptible to oxidative stress.

The present study have limitations. The exclusive use of male animals does not allow assessments of possible sex-differences and it is known that response to HI injury and to several treatments are sex-specific (Netto et al., 2017). Another important limitation intrinsic to the animal model is that although we showed that the immature rat brain is less susceptible to HI injury this is not translated to the clinic in humans; it is known that prematurity worsens the prognosis of affected newborns (Volpe, 2009). In addition, Western blot analysis used GAPDH enzyme as a control, it is possible that levels of this enzyme change during development, therefore, western blot results should be interpreted with caution.

Concluding, here presented results show that higher mitochondrial vulnerability, as verified by decreased activities of TCA cycle, of complex II-III, state 3 and uncoupled respiration, as well as loss in mitochondrial membrane potential, possibly associated with the higher metabolic rate makes the P11 brain mitochondria more susceptible to HI damage. The mitochondrial dysfunction that possibly could underlie the increase of ROS production coupled with less efficiency of antioxidant defenses makes the P11 brain more prone to apoptosis. Therefore, these factors combined probably lead to an increased cellular death and a more severe lesion. Overall, the present findings show that mitochondrial changes that occur during this stage of development are pivotal to the final outcome of HI injury, being promising therapeutic targets for the design of new treatments for this pathology.

Figures

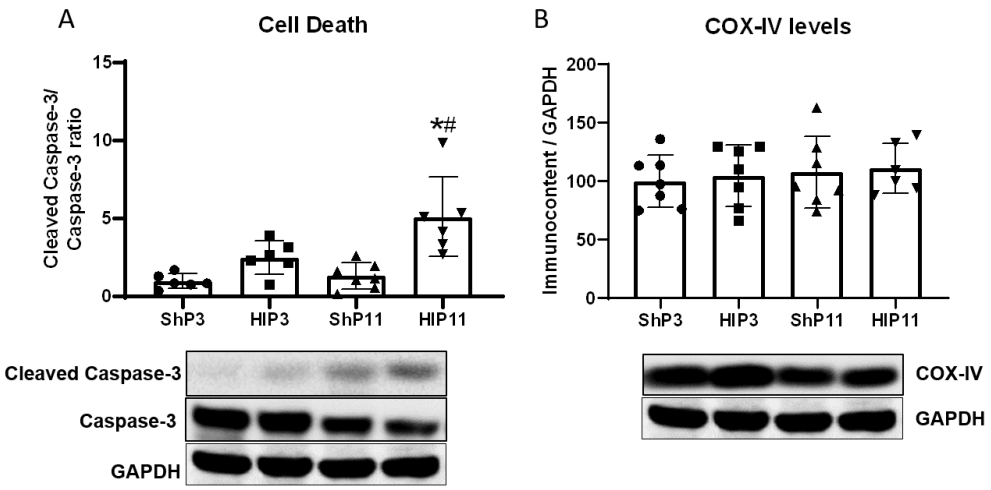

Figure 1. Immunocontent of apoptotic and mitochondrial markers in the ipsilateral hippocampus 24h after HI. Cleaved Caspase-3/ Caspase-3 ratio suggesting increased levels of cell death in the HIP11 group (A). No differences were observed in the expression of the mitochondrial marker COX-IV (B). Data are expressed as mean ± SD, significance was accepted whenever $p<0.05$. *Difference from its respective Sham. # Difference from the respective P3 group.

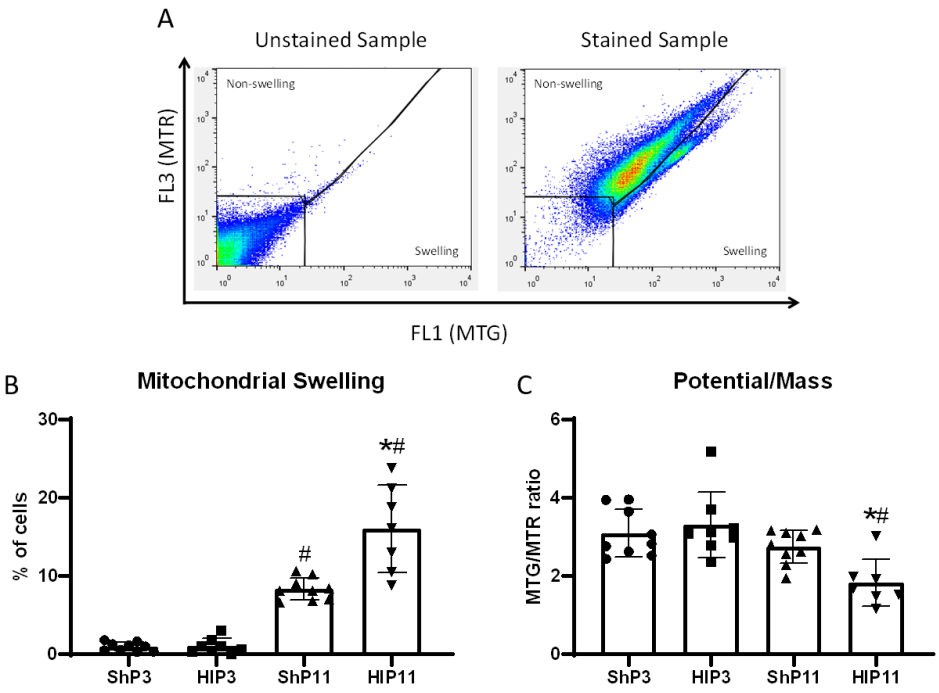

Figure 2. HI induced age-dependent mitochondrial damage. Flow cytometry with MitoTracker staining analysis (A) in the ipsilateral hippocampus 24h after HI. An increase in mitochondrial swelling was observed in the HIP11 group (B). The ratio between MitoTracker green (MTG), a mitochondrial membrane potential marker, and MitoTracker red (MTR), mitochondrial mass marker, was decreased in the HIP11. Data are expressed as mean ± SD, significance was accepted whenever $p<0.05$. *Difference from its respective Sham. # Difference from the respective P3 group.

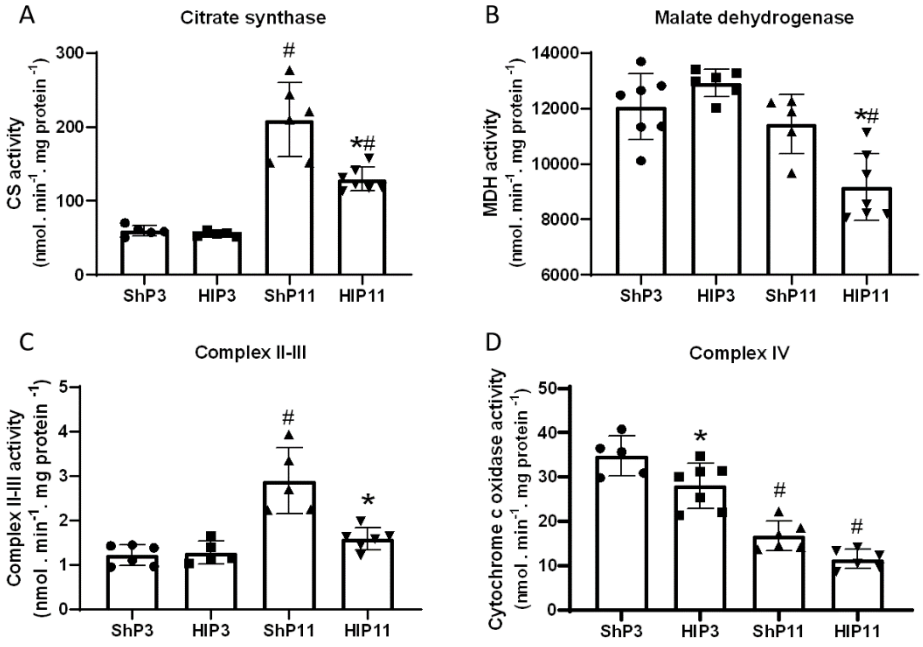

Figure 3. HI induced age-dependent dysfunction of tricarboxylic acid (TCA) cycle enzymes and mitochondrial respiratory complexes activities. Activity of TCA cycle enzymes citrate synthase (A) and malate dehydrogenase (B), as well as of mitochondrial respiratory complexes II-III and IV was assessed in the ipsilateral hippocampus 24 h after HI. Data are expressed as mean ± SD, significance was accepted whenever $p<0.05$. *Difference from its respective Sham. # Difference from the respective P3 group.

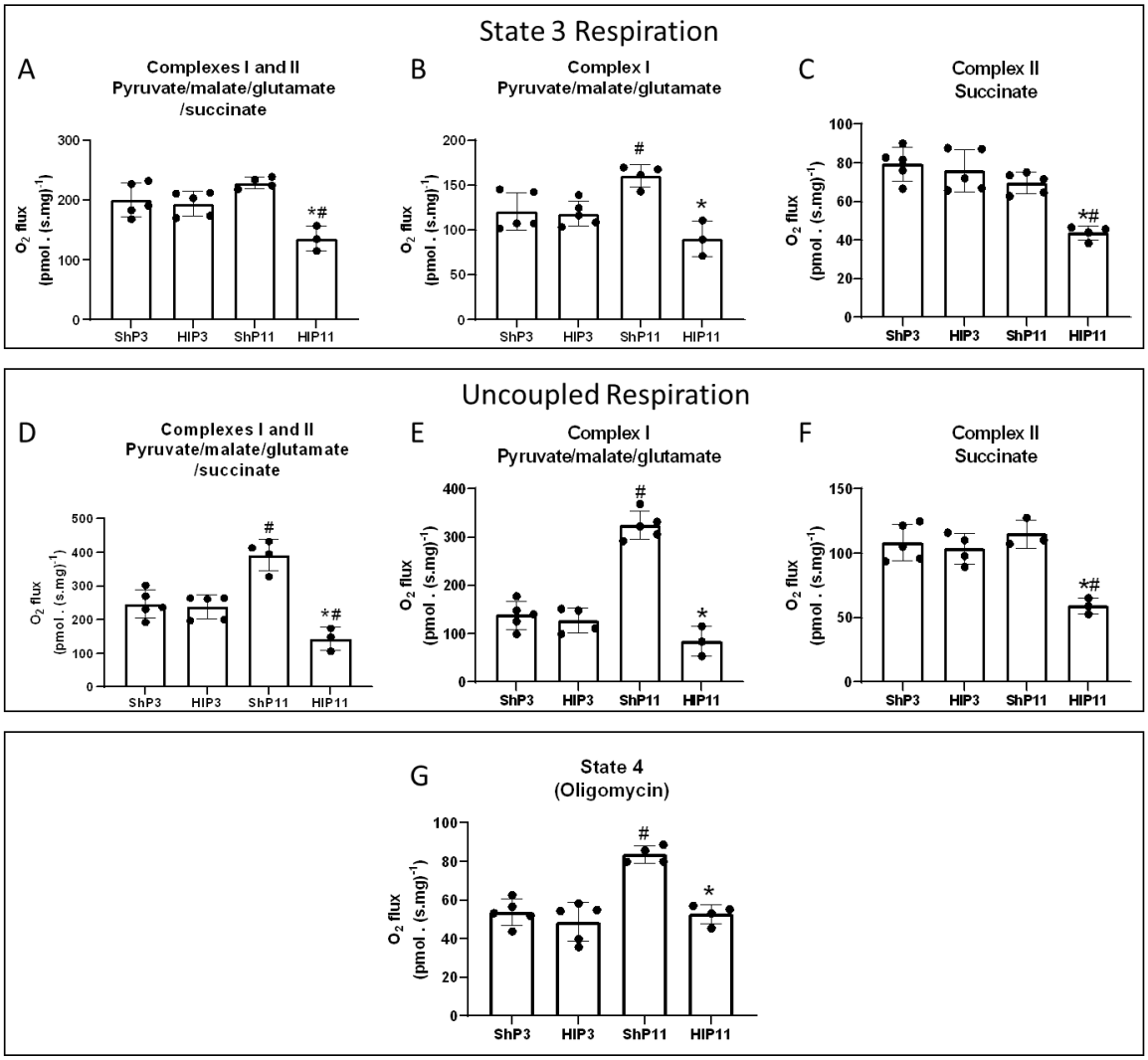

Figure 4. HI induced age-dependent impairment of mitochondrial respiration. High resolution respirometry was used to assess state 3 respiration (ADP-stimulated, A, B and C), uncoupled respiration, CCCP-stimulated (D, E and F) and state 4 respiration (oligomycin-stimulated, G) using complexes I and II (A and D), complex I only (B and E) and complex II respiring substrates (C and F). Data are expressed as mean ± SD, significance was accepted whenever $p<0.05$. *Difference from its respective Sham. # Difference from the respective P3 group.

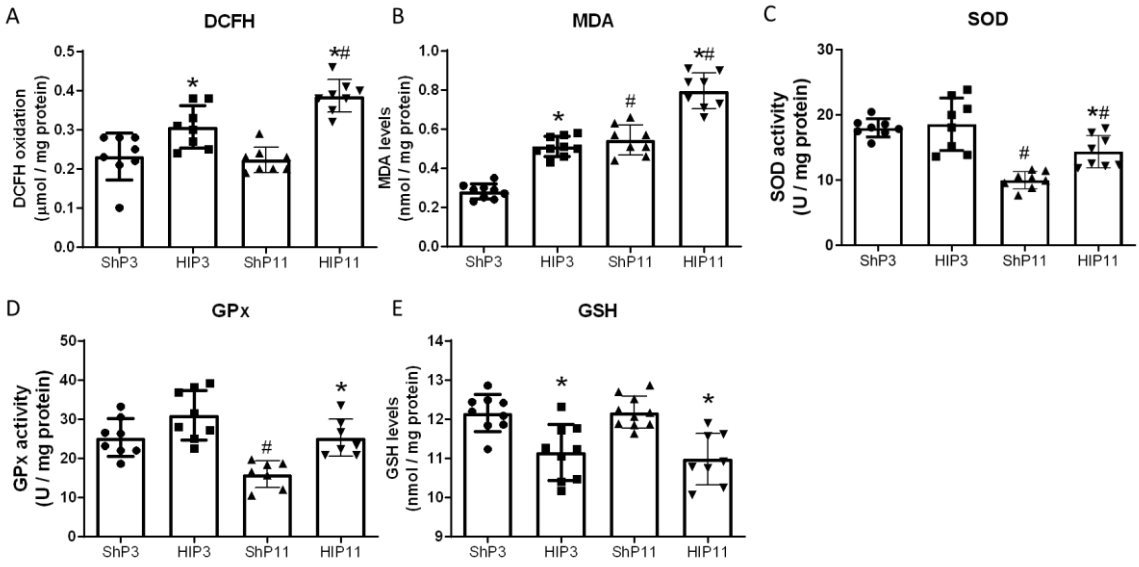

Figure 5. HI induced age-specific oxidative stress biomarker responses. Reactive oxygen species formation was assessed by 2′,7′-dichlorofluorescin (DCFH) oxidation (A). Lipid peroxidation was evaluated by malondialdehyde (MDA) (B). Antioxidant enzyme defenses superoxide dismutase (C), glutathione peroxidase (GPx) (D) and reduced glutathione (GSH) were also assessed. Data are expressed as mean ± SD, significance was accepted whenever $p<0.05$. *Difference from its respective Sham. # Difference from the respective P3 group.

References

Alexander, M., Garbus, H., Smith, A.L., Rosenkrantz, T.S., Fitch, R.H., 2014. Behavioral and histological outcomes following neonatal HI injury in a preterm (P3) and term (P7) rodent model. Behav. Brain Res. 259, 85–96. https://doi.org/10.1016/j.bbr.2013.10.038

Baquer, N.Z., Hothersall, J.S., McLean, P., Greenbaum, A.L., 1977. Aspects of Carbohydrate Metabolism in Developing Brain. Dev. Med. Child Neurol. https://doi.org/10.1111/j.1469-8749.1977.tb08027.x

Benjelloun, N., Joly, L.M., Palmier, B., Plotkine, M., Charriaut-Marlangue, C., 2003. Apoptotic mitochondrial pathway in neurones and astrocytes after neonatal hypoxia-ischaemia in the rat brain. Neuropathol. Appl. Neurobiol. 29, 350–360. https://doi.org/10.1046/j.1365-2990.2003.00467.x

Booth, R.F.G., Patel, T.B., Clark, J.B., 1980. The Development of Enzymes of Energy Metabolism in the Brain of a Precocial (Guinea Pig) and Non-Precocial (Rat) Species. J. Neurochem. https://doi.org/10.1111/j.1471-4159.1980.tb04616.x

Brekke, E., Berger, H.R., Widerøe, M., Sonnewald, U., Morken, T.S., 2017. Glucose and Intermediary Metabolism and Astrocyte–Neuron Interactions Following Neonatal Hypoxia–Ischemia in Rat. Neurochem. Res. 42, 115–132. https://doi.org/10.1007/s11064-016-2149-9

Brekke, E., Morken, T.S., Sonnewald, U., 2015. Glucose metabolism and astrocyte-neuron interactions in the neonatal brain. Neurochem. Int. 82, 33–41. https://doi.org/10.1016/j.neuint.2015.02.002

Browne, R.W., Armstrong, D., 1998. Reduced glutathione and glutathione disulfide. Methods Mol. Biol. https://doi.org/10.1385/0-89603-472-0:347

Cecatto, C., Godoy, K. dos S., da Silva, J.C., Amaral, A.U., Wajner, M., 2016. Disturbance of mitochondrial functions provoked by the major long-chain 3-hydroxylated fatty acids accumulating in MTP and LCHAD deficiencies in skeletal muscle. Toxicol. Vitr. 36, 1–9. https://doi.org/10.1016/j.tiv.2016.06.007

Davidson, J.O., Wassink, G., van den Heuij, L.G., Bennet, L., Gunn, A.J., 2015. Therapeutic hypothermia for neonatal hypoxic-ischemic encephalopathy - Where to from here? Front. Neurol. 6. https://doi.org/10.3389/fneur.2015.00198

de-Souza-Ferreira, E., Rios-Neto, I.M., Martins, E.L., Galina, A., 2019. Mitochondria-coupled glucose phosphorylation develops after birth to modulate H2O2 release and calcium handling in rat brain. J. Neurochem. https://doi.org/10.1111/jnc.14705

Dranka, B.P., Hill, B.G., Darley-Usmar, V.M., 2010. Mitochondrial reserve capacity in endothelial cells: The impact of nitric oxide and reactive oxygen species. Free Radic. Biol. Med. https://doi.org/10.1016/j.freeradbiomed.2010.01.015

Durán-Carabali, L.E., Sanches, E.F., Reichert, L., Netto, C.A., 2019. Enriched experience during pregnancy and lactation protects against motor impairments induced by neonatal hypoxia-ischemia. Behav. Brain Res. https://doi.org/10.1016/j.bbr.2019.03.048

Fischer, J.C., Ruitenbeek, W., Berden, J.A., Trijbels, J.M.F., Veerkamp, J.H., Stadhouders, A.M., Sengers, R.C.A., Janssen, A.J.M., 1985. Differential investigation of the capacity of succinate oxidation in human skeletal muscle. Clin. Chim. Acta. https://doi.org/10.1016/0009-8981(85)90135-4

Garcia, J.H., Lossinsky, A.S., Kauffman, F.C., Conger, K.A., 1978. Neuronal ischemic injury: Light microscopy, ultrastructure and biochemistry. Acta Neuropathol. https://doi.org/10.1007/BF00685002

Globus, M.Y.-., Alonso, O., Dietrich, W.D., Busto, R., Ginsberg, M.D., 1995. Glutamate Release and Free Radical Production Following Brain Injury: Effects of Posttraumatic Hypothermia. J. Neurochem. https://doi.org/10.1046/j.1471-4159.1995.65041704.x

Gnaiger, E., 2009. Capacity of oxidative phosphorylation in human skeletal muscle. New perspectives of mitochondrial physiology. Int. J. Biochem. Cell Biol. 41, 1837–1845. https://doi.org/10.1016/j.biocel.2009.03.013

Gregson, N.A., Williams, P.L., 1969. A COMPARATIVE STUDY OF BRAIN AND LIVER MITOCHONDRIA FROM NEW-BORN AND ADULT RATS. J. Neurochem. https://doi.org/10.1111/j.1471-4159.1969.tb06861.x

Hagberg, H., Mallard, C., Rousset, C.I., Thornton, C., 2014. Mitochondria: Hub of injury responses in the developing brain. Lancet Neurol. https://doi.org/10.1016/S1474-4422(13)70261-8

Herrera, T.I., Edwards, L., Malcolm, W.F., Smith, P.B., Fisher, K.A., Pizoli, C., Gustafson, K.E., Goldstein, R.F., Cotten, C.M., Goldberg, R.N., Bidegain, M., 2018. Outcomes of preterm infants treated with hypothermia for hypoxic-ischemic encephalopathy. Early Hum. Dev. https://doi.org/10.1016/j.earlhumdev.2018.08.003

Jacobs, S.E., Berg, M., Hunt, R., Tarnow-Mordi, W.O., Inder, T.E., Davis, P.G., 2013. Cooling for newborns with hypoxic ischaemic encephalopathy. Cochrane Database Syst. Rev. https://doi.org/10.1002/14651858.CD003311.pub3

Kitto, G., 1969. [19] Intra- and extramitochondrial malate dehydrogenases from chicken and tuna heart. Methods Enzymol. https://doi.org/10.1016/0076-6879(69)13023-2

Laptook, A.R., Shankaran, S., Tyson, J.E., Munoz, B., Bell, E.F., Goldberg, R.N., Parikh, N.A., Ambalavanan, N., Pedroza, C., Pappas, A., Das, A., Chaudhary, A.S., Ehrenkranz, R.A., Hensman, A.M., Van Meurs, K.P., Chalak, L.F., Hamrick, S.E.G., Sokol, G.M., Walsh, M.C., Poindexter, B.B., Faix, R.G., Watterberg, K.L., Frantz, I.D., Guillet, R., Devaskar, U., Truog, W.E., Chock, V.Y., Wyckoff, M.H., McGowan, E.C., Carlton, D.P., Harmon, H.M., Brumbaugh, J.E., Cotten, C.M., Sánchez, P.J., Hibbs, A.M., Higgins, R.D., 2017. Effect of therapeutic hypothermia initiated after 6 hours of age on death or disability among newborns with hypoxic-ischemic encephalopathy a randomized clinical trial. JAMA - J. Am. Med. Assoc. https://doi.org/10.1001/jama.2017.14972

LeBel, C.P., Bondy, S.C., 1990. Sensitive and rapid quantitation of oxygen reactive species formation in rat synaptosomes. Neurochem. Int. 17, 435–440. https://doi.org/10.1016/0197-0186(90)90025-O

Li, J., Yu, W., Li, X.T., Qi, S.H., Li, B., 2014. The effects of propofol on mitochondrial dysfunction following focal cerebral ischemia-reperfusion in rats. Neuropharmacology. https://doi.org/10.1016/j.neuropharm.2013.08.029

Li, S., Liu, W., Zhang, Y., Zhao, D., Wang, T., Li, Y., 2014. The role of TNF-α, IL-6, IL-10, and GDNF in neuronal apoptosis in neonatal rat with hypoxic-ischemic encephalopathy. Eur. Rev. Med. Pharmacol. Sci. 18, 905–909.

Lima, K.G., Krause, G.C., da Silva, E.F.G., Xavier, L.L., Martins, L.A.M., Alice, L.M., da Luz, L.B., Gassen, R.B., Filippi-Chiela, E.C., Haute, G.V., Garcia, M.C.R., Funchal, G.A., Pedrazza, L., Reghelin, C.K., de Oliveira, J.R., 2018. Octyl gallate reduces ATP levels and Ki67 expression leading HepG2 cells to cell cycle arrest and mitochondria-mediated apoptosis. Toxicol. Vitr. https://doi.org/10.1016/j.tiv.2017.12.017

Liu, F., McCullough, L.D., 2013. Inflammatory responses in hypoxic ischemic encephalopathy. Acta Pharmacol. Sin. 34, 1121–30. https://doi.org/10.1038/aps.2013.89

Liu, W., Zhang, Y., 2014. in Neuronal Apoptosis in Neonatal Rat With Hypoxic-Ischemic Encephalopathy 905–909.

Lowry, O.H., Rosenbrough, N.J., Farr, A.L., Randall, R.J., 1951. Protein measurement with the folin. J. Biol. Chem. https://doi.org/10.1016/0304-3894(92)87011-4

Makrecka-Kuka, M., Krumschnabel, G., Gnaiger, E., 2015. High-resolution respirometry for simultaneous measurement of oxygen and hydrogen peroxide fluxes in permeabilized cells, tissue homogenate and isolated mitochondria. Biomolecules. https://doi.org/10.3390/biom5031319

Marklund, S., Marklund, G., 1974. Involvement of the superoxide anion radical in the autoxidation of pyrogallol and a convenient assay for superoxide dismutase. Eur. J. Biochem. 47, 469–474. https://doi.org/10.1111/j.1432-1033.1974.tb03714.x

Mavelli, I., Rigo, A., Federico, R., Ciriolo, M.R., Rotilio, G., 1982. Superoxide dismutase, glutathione peroxidase and catalase in developing rat brain. Biochem. J. https://doi.org/10.1042/bj2040535

Nannelli, G., Terzuoli, E., Giorgio, V., Donnini, S., Lupetti, P., Giachetti, A., Bernardi, P., Ziche, M., 2018. ALDH2 activity reduces mitochondrial oxygen reserve capacity in endothelial cells and induces senescence properties. Oxid. Med. Cell. Longev. https://doi.org/10.1155/2018/9765027

Netto, C.A., Sanches, E., Odorcyk, F.K., Duran-Carabali, L.E., Weis, S.N., 2017. Sex-dependent consequences of neonatal brain hypoxia-ischemia in the rat. J. Neurosci. Res. https://doi.org/10.1002/jnr.23828

Odorcyk, F.K., Duran-Carabali, L.E., Rocha, D.S., Sanches, E.F., Martini, A.P., Venturin, G.T., Greggio, S., da Costa, J.C., Kucharski, L.C., Zimmer, E.R., Netto, C.A., 2020. Differential glucose and beta-hydroxybutyrate metabolism confers an intrinsic neuroprotection to the immature brain in a rat model of neonatal hypoxia ischemia. Exp. Neurol. https://doi.org/10.1016/j.expneurol.2020.113317

Odorcyk, F.K., Kolling, J., Sanches, E.F., Wyse, A.T.S., Netto, C.A., 2017. Experimental neonatal hypoxia ischemia causes long lasting changes of oxidative stress parameters in the hippocampus and the spleen. J. Perinat. Med. 1–7. https://doi.org/10.1515/jpm-2017-0070

Patel, S.D., Pierce, L., Ciardiello, A., Hutton, A., Paskewitz, S., Aronowitz, E., Voss, H.U., Moore, H., Vannucci, S.J., 2015. Therapeutic hypothermia and hypoxia-ischemia in the term-equivalent neonatal rat: characterization of a translational preclinical model. Pediatr. Res. 78, 264–71. https://doi.org/10.1038/pr.2015.100

Rao, R., Trivedi, S., Vesoulis, Z., Liao, S.M., Smyser, C.D., Mathur, A.M., 2017. Safety and Short-Term Outcomes of Therapeutic Hypothermia in Preterm Neonates 34-35 Weeks Gestational Age with Hypoxic-Ischemic Encephalopathy. J. Pediatr. https://doi.org/10.1016/j.jpeds.2016.11.019

Ribeiro, R.T., Zanatta, Â., Amaral, A.U., Leipnitz, G., de Oliveira, F.H., Seminotti, B., Wajner, M., 2018. Experimental Evidence that In Vivo Intracerebral Administration of L-2-Hydroxyglutaric Acid to Neonatal Rats Provokes Disruption of Redox Status and Histopathological Abnormalities in the Brain. Neurotox. Res. https://doi.org/10.1007/s12640-018-9874-6

Rice, J.E., Vannucci, R.C., Brierley, J.B., 1981. The influence of immaturity on hypoxic-ischemic brain damage in the rat. Ann. Neurol. 9, 131–141. https://doi.org/10.1002/ana.410090206

Rustin, P., Chretien, D., Bourgeron, T., Gérard, B., Rötig, A., Saudubray, J.M., Munnich, A., 1994. Biochemical and molecular investigations in respiratory chain deficiencies. Clin. Chim. Acta. https://doi.org/10.1016/0009-8981(94)90055-8

Sanches, E.F., Arteni, N., Nicola, F., Aristimunha, D., Netto, C.A., 2015. Sexual dimorphism and brain lateralization impact behavioral and histological outcomes following hypoxia-ischemia in P3 and P7 rats. Neuroscience 290, 581–593. https://doi.org/10.1016/j.neuroscience.2014.12.074

Sanderson, T.H., Reynolds, C.A., Kumar, R., Przyklenk, K., Hüttemann, M., 2013. Molecular mechanisms of ischemia-reperfusion injury in brain: Pivotal role of the mitochondrial membrane potential in reactive oxygen species generation. Mol. Neurobiol. https://doi.org/10.1007/s12035-012-8344-z

Semple, B.D., Blomgren, K., Gimlin, K., Ferriero, D.M., Noble-Haeusslein, L.J., 2013. Brain development in rodents and humans: Identifying benchmarks of maturation and vulnerability to injury across species. Prog. Neurobiol. 106–107, 1–16. https://doi.org/10.1016/j.pneurobio.2013.04.001

Shi, Y., Zhao, J.N., Liu, L., Hu, Z.X., Tang, S.F., Chen, L., Jin, R. Bin, 2012. Changes of positron emission tomography in newborn infants at different gestational ages, and neonatal hypoxic-ischemic encephalopathy. Pediatr. Neurol. https://doi.org/10.1016/j.pediatrneurol.2011.11.005

Sizonenko, S. V., Kiss, J.Z., Inder, T., Gluckman, P.D., Williams, C.E., 2005. Distinctive neuropathologic alterations in the deep layers of the parietal cortex after moderate ischemic-hypoxic injury in the P3 immature rat brain. Pediatr. Res. 57, 865–872. https://doi.org/10.1203/01.PDR.0000157673.36848.67

Srere, P.A., 1969. [1] Citrate synthase. [EC 4.1.3.7. Citrate oxaloacetate-lyase (CoA-acetylating)]. Methods Enzymol. 13, 3–11. https://doi.org/10.1016/0076-6879(69)13005-0

Thorngren-jerneck, K., Ohlsson, T., Sandell, A., Erlandsson, K., Strand, S., Ryding, E., Svenningsen, N.W., 2001. Cerebral Glucose Metabolism Measured by Positron Emission Tomography in Term Newborn Infants with Hypoxic Ischemic Encephalopathy 49, 495–501.

Volpe, J.J., 2009. Brain injury in premature infants: a complex amalgam of destructive and developmental disturbances. Lancet Neurol. https://doi.org/10.1016/S1474-4422(08)70294-1

Weis, S.N., Schunck, R.V.A., Pettenuzzo, L.F., Krolow, R., Matté, C., Manfredini, V., do Carmo R Peralba, M., Vargas, C.R., Dalmaz, C., Wyse, A.T.S., Netto, C.A., 2011. Early biochemical effects after unilateral hypoxia-ischemia in the immature rat brain. Int. J. Dev. Neurosci. 29, 115–20. https://doi.org/10.1016/j.ijdevneu.2010.12.005

Wendel, A., 1981. Glutathione Peroxidase. Methods Enzymol. https://doi.org/10.1016/S0076-6879(81)77046-0

Yagi, K., 1998. Simple procedure for specific assay of lipid hydroperoxides in serum or plasma. Methods Mol. Biol. https://doi.org/10.1385/0-89603-472-0:107

5. Discussão

A HI é uma das principais causas de óbito e de lesões ao SNC no período perinatal (Verklan, 2009), com incidência de 1,8 a 6 casos/ 1000 nascidos vivos, sendo maior em países em desenvolvimento (Shevell et al., 2001). Essa encefalopatia pode afetar neonatos com diferentes idades gestacionais. Em recém-nascidos a termo a hipotermia terapêutica é o principal tratamento indicado, aumentando a sobrevivência e diminuindo as sequelas causadas pela HI (Davidson et al., 2015a; Jacobs et al., 2013). Esse tratamento, no entanto, não é indicado para neonatos prematuros com menos de 36 semanas de gestação (Davidson et al., 2015a; Jacobs et al., 2013; Rao et al., 2017). Tratamentos que melhorem o prognóstico de prematuros acometidos pela HI são de extrema importância, devido ao aumento significativo na taxa de sobrevivência desses recém-nascidos, por causa do constante avanço científico na medicina neonatal. Estima-se que a cada ano 90% dos 13 milhões de neonatos considerados prematuros extremos, com 24-28 semanas de idade gestacional e peso abaixo de 1,5 kg, sobrevivem até a infância (Abily-Donval et al., 2015; Wilson-Costello et al., 2007). Entretanto, 5% dos sobreviventes desenvolverão paralisia cerebral e entre 40 e 50% apresentarão algum déficit cognitivo e/ou comportamental (Deng, 2010), ambos fortemente associados à HI (Huang et al., 2009; Volpe, 2009).

As peculiaridades observadas no encéfalo de recém-nascidos com diferentes idades gestacionais fazem com que diferentes estratégias terapêuticas para a HI devam ser desenvolvidas (Jacobs et al., 2013). Nesse contexto, estudos pré-clínicos são essenciais para a maior compreensão tanto dos mecanismos envolvidos na lesão quanto das alternativas terapêuticas. O estudo da HI neonatal utiliza de diferentes modelos a fim de caracterizar, da forma mais fiel possível, o estágio de desenvolvimento encefálico e as características patológicas encontradas na clínica (Clancy et al., 2001; Dobbing and Sands, 1979; Silbereis et al., 2010). O modelo da presente tese é o de Rice-Vannucci, que

é o mais utilizado no estudo da HI neonatal e permite mimetizar em ratos a lesão em diferentes estágios de neurodesenvolvimento (Alexander et al., 2014; Sanches et al., 2015).

No capítulo I foi claramente evidenciado através dos resultados cognitivos e de dano tecidual que quanto mais avançado o estágio de desenvolvimento encefálico, maior a susceptibilidade ao dano da HI. O dano histológico no hipocampo, por exemplo, mostra que enquanto nenhuma diferença significativa foi encontrada em animais lesados em P3, uma perda de mais de 50% foi observada em animais P7, enquanto em animais P11 o efeito foi ainda maior, com quase 80% de perda média de tecido neural. A ausência de lesões significativas em P3 já era esperada, visto que estudos prévios já haviam mostrado que o tempo de hipóxia utilizado na presente tese não é capaz de causar lesões severas em animais dessa idade (Alexander et al., 2014; Durán-Carabali et al., 2017; Sanches et al., 2015). Apesar da ausência de lesões nesses animais, a utilização desse tempo de hipóxia foi escolhida por dois critérios: ser o mais utilizado pela literatura e por não causar grande mortalidade em animais P11.

A maior resiliência do encéfalo imaturo à hipóxia já foi demonstrada em trabalhos prévios (Alexander et al., 2014; Rice et al., 1981; Sanches et al., 2015). No entanto, poucos estudos buscaram compreender os mecanismos biológicos que expliquem diferenças tão expressivas na severidade da mesma lesão em animais com idades tão próximas. A hipótese da presente tese é de que as mudanças do metabolismo encefálico possuem papel importante na diferença de prognóstico encontrada em animais expostos à HI em diferentes fases do neurodesenvolvimento.

5.1 O metabolismo encefálico muda drasticamente durante o desenvolvimento

Em mamíferos o período lactacional confere uma dieta particular ao neonato e isso acarreta em diferenças metabólicas importantes entre recém-nascidos e adultos (Brekke et al., 2015). A ingestão de leite com alto teor lipídico favorece o uso de corpos cetônicos em oposição à glicose, principal substrato energético do encéfalo adulto (McKenna et al., 2015). No capítulo 1 demonstramos através do imageamento por [^{18}F]FDG microPET um aumento linear na captação de glicose pelo encéfalo, que dobra entre P4 e P14. Num período similar, entre P4 e P12 também observamos uma redução da oxidação de β-hidroxibutirato (Figura 4). Esses resultados traduzem justamente o amadurecimento do encéfalo através do aumento do consumo de glicose e da redução do consumo de corpos cetônicos.

O uso de diferentes substratos metabólicos influencia a severidade da lesão. Enquanto a hiperglicemia está associada a uma piora no prognóstico da lesão, tanto na clínica (Pinchefsky et al., 2019) quanto em modelos experimentais (Park et al., 2001), o aumento de corpos cetônicos parece possuir o efeito oposto. Ratos pré-tratados com dexametasona e submetidos ao modelo de HIP7 apresentaram uma grande redução de efeitos deletérios, essa proteção estava ligada a um aumento nos níveis plasmáticos de β-hidroxibutirato (Dardzinski et al., 2000). Além disso, nesse mesmo modelo de HI em ratos foi demonstrado que a administração de β-hidroxibutirato exógeno é capaz de reduzir o dano tecidual e a morte celular (Lee et al., 2018). Tratamentos baseados no aumento do uso de corpos cetônicos já são utilizados na clínica pediátrica para o tratamento da epilepsia refratária, sendo uma abordagem eficiente e segura (Cai et al., 2017; Neal et al., 2009). Portanto, os achados do presente estudo, somados a estudos prévios sugerem que o metabolismo de corpos cetônicos é um importante alvo terapêutico que deve ser melhor estudado.

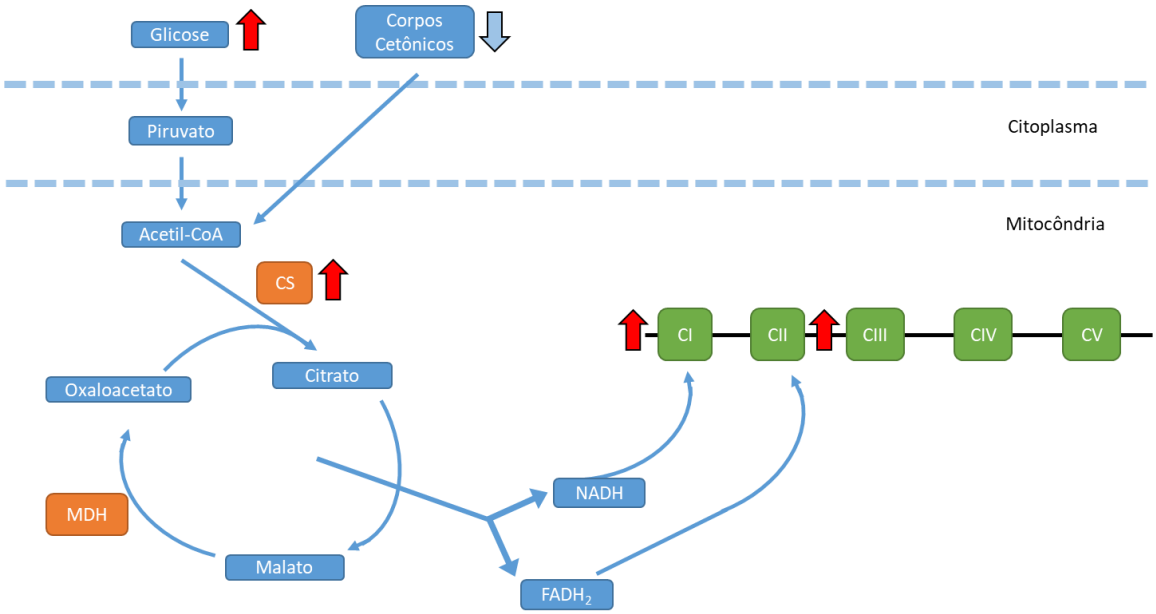

Figura 4. Alterações observadas no metabolismo encefálico durante o desenvolvimento. Ao compararmos os grupo ShP3 e ShP11 observamos grandes mudanças do metabolismo entre essas idades mesmo na ausência de lesão. A maior captação de glicose, bem como a menor oxidação de corpos cetônicos pelo encéfalo foi notável. Além disso observamos um aumento na atividade da CS, bem como aumento dos complexos respiratórios mitocondriais I e II-III. Siglas: CS: Citrato sintase; MDH: Malato desidrogenase.

As diferenças metabólicas observadas durante o desenvolvimento não se limitam ao substrato energético utilizado. No capítulo 2 investigamos a atividade do ciclo do TCA e da cadeia respiratória, sendo estudadas duas das enzimas chaves deste ciclo: a CS e a MDH. Apesar da MDH não ter apresentado alterações em sua atividade, a CS teve sua atividade triplicada entre P4 e P12. Esses resultados estão de acordo com estudos prévios que mostram aumento tanto na atividade da CS (Booth et al., 1980) quanto na do ciclo do TCA como um todo (Baquer et al., 1977) durante o desenvolvimento. O mesmo padrão foi seguido pelos complexos respiratórios mitocondriais, especialmente o complexo I, avaliado através da respirometria, e dos complexos II e III, que tiveram sua atividade aumentada. O aumento da atividade desses complexos e do ciclo do TCA sugere uma maior demanda metabólica do SNC com o desenvolvimento. Logicamente, um encéfalo que possui uma demanda metabólica maior sofrerá mais dano em lesões que imponham um desafio metabólico como é o caso da HI, tanto que o principal mecanismo protetor da

hipotermia terapêutica é a redução da atividade metabólica (Globus et al., 1995; Jacobs et al., 2013).

O combate ao estresse oxidativo é também uma parte importante do metabolismo. No capítulo 2 demonstramos aumento da peroxidação lipídica e redução da atividade das enzimas antioxidantes SOD e GPx com o desenvolvimento. O aumento da peroxidação lipídica pode ser atribuído ao processo de mielinização que ocorre durante o desenvolvimento, aumentando a quantidade de lipídeos e consequentemente sua peroxidação (Semple et al., 2013). Já a redução da atividade das enzimas antioxidantes foi surpreendente tendo em vista o aumento do consumo de oxigênio observado nesse mesmo período. Esses resultados, portanto, sugerem que com o desenvolvimento temos um encéfalo que ao mesmo tempo possui maior demanda metabólica, mas menos defesas antioxidantes.

5.2 A resposta à HI em encéfalos de diferentes estágios de desenvolvimento

A neuroproteção intrínseca do encéfalo imaturo não se limitou aos testes comportamentais e análises histológicas descritos no capítulo I. A HI em animais P3 não teve efeito sobre o uso de substratos energéticos, não apresentando alterações na captação de glicose (observada por [^{18}F]FDG microPET), nem na oxidação da mesma; de forma similar, a oxidação de β-hidroxibutirato manteve-se constante (Figura 5). A maior resiliência do encéfalo imaturo frente a situações de estresse metabólico já foi demonstrada em um modelo de hipoglicemia em ratos de diferentes idades (P7, P14, P28 e adultos), onde foi demonstrada menor lesão neuronal nos animais P7 quando comparado às demais idades (Ennis et al., 2008). A lesão nos animais P3 também não aumentou a morte celular por apoptose, nem provocou alterações no potencial de membrana mitocondrial. A atividade das enzimas do ciclo do TCA também se manteve

constante, bem como a atividade da cadeia respiratória. Os únicos resultados que foram capazes de detectar o efeito da HI nos animais P3 foram os de parâmetros de estresse oxidativo do capítulo II. Neles observamos um aumento da formação de EROs e de lipoperoxidação, apesar de não termos detectado redução na atividade mitocondrial.

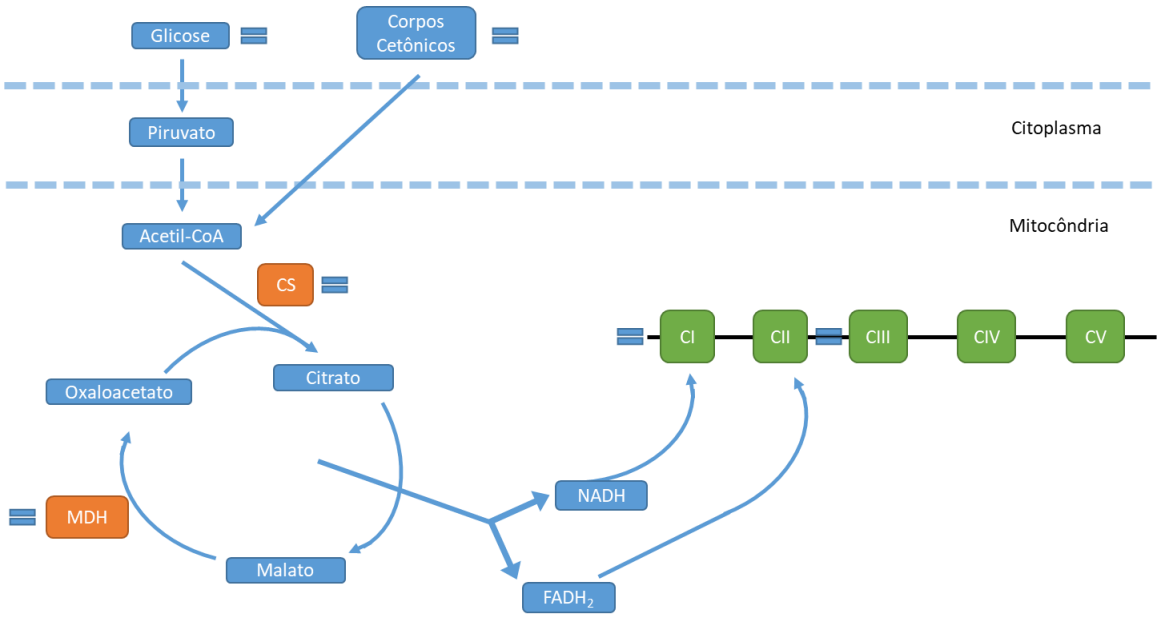

Figura 5. Efeitos da HI no metabolismo encefálico em animais P3. A HI não provocou muitas mudanças no metabolismo encefálico nos animais P3. As ausências de diferença na captação de glicose, oxidação de β-hidroxibutirato, nas atividades da CS, MDH, bem como dos complexos I, II e II-III são representadas pelo sinal de igual (=) em azul. Siglas: CS: Citrato sintase; MDH:Malato desidrogenase.

Em animais P11 os efeitos da HI foram claramente identificáveis. Apesar de não haver efeito da lesão na oxidação de β-hidroxibutirato, houve uma acentuada redução tanto na captação de glicose quanto na sua oxidação (Figura 6). Um aumento nos níveis de morte celular por apoptose foram observados, bem como um aumento do inchaço mitocondrial e a perda do potencial de membrana dessa organela. As enzimas do ciclo do TCA: CS e MDH também foram afetadas pela HI, tendo suas atividades reduzidas. O efeito da HI no metabolismo mitocondrial também foi claramente evidenciado na

atividade dos complexos II e III e no consumo de oxigênio avaliados através da respirometria nos complexos I e II. Parâmetros de estresse oxidativo também foram alterados pela HI, elevando a produção de EROs e peroxidação lipídica. Observamos um aumento da atividade das enzimas antioxidantes SOD e GPx, provavelmente para compensar o aumentos de EROs (Odorcyk et al., 2017).

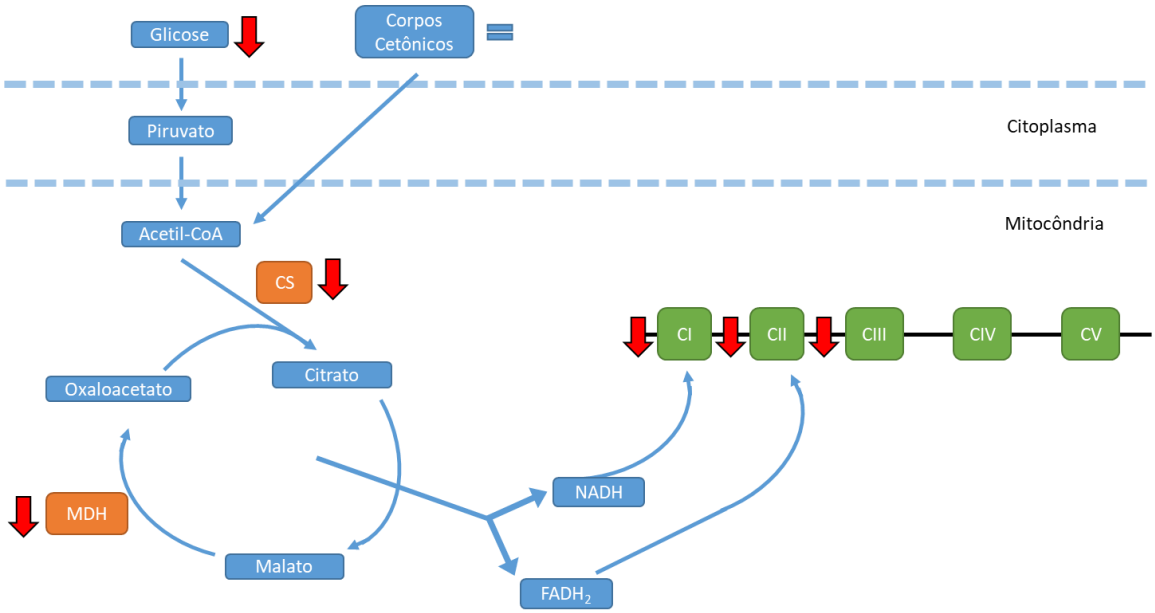

Figura 6. Efeitos da HI no metabolismo encefálico em animais P11. A HI induziu uma redução na captação de glicose no encéfalo desses animais, enquanto não alterou a oxidação de corpos cetônicos. Houve uma redução na atividade das enzimas do ciclo do TCA, CS e MDH, bem como dos complexos respiratórios mitocondriais I, II e II-III. Siglas: CS: Citrato sintase; MDH:Malato desidrogenase.

5.3 Estudos prévios já compararam lesões em diferentes idades

Embora a maior parte dos estudos concordem com a maior resiliência do encéfalo imaturo (Alexander et al., 2014; Casella et al., 2014; Ennis et al., 2008; Sanches et al., 2015), estudos em camundongos que foram submetidos à HI no período imaturo (P9) e juvenil (P21) revelaram perdas teciduais semelhantes nas regiões CA hipocampais, mas uma redução maior no giro denteado em animais P9 do que em animais P21 (Qiu et al., 2007). No entanto, o modelo utilizado produzia uma lesão menos severa e possuía tempos

de hipóxia diferentes para cada idade (10% de O_2 por 35 min em P9 e 30 min em P21). O achado de maior susceptibilidade à lesão em encéfalos imaturos não é incomum em modelos de lesão encefálica traumática, porém esses estudos, em geral, visam comparar uma lesão ocorrida nos primeiros dias pós-natais e no início da infância, não em diferentes idades gestacionais, como no presente estudo. Isso fica evidente quando observamos que estudos que comparam animais P7 com P17 e concluem que a lesão induzida em P17 causava alterações morfológicas de longo-prazo em neurônios hipocampais, enquanto os de animais com lesão em P7 não apresentavam tais mudanças (Casella et al., 2014). Outro estudo com um modelo similar mostrou que ratos lesados P11 possuem danos cognitivos e histológicos maiores do que lesados em P17 (Raghupathi and Huh, 2007). É interessante observar que embora a comparação de ambos estudos seja com P17, essa idade tem uma lesão mais severa quando comparada com P7 (Casella et al., 2014), mas menos quando comparada com P11 (Raghupathi and Huh, 2007), possivelmente essas diferenças devem-se em parte às diferenças metabólicas aqui evidenciadas. Embora estudos que comparem o efeito de lesões em diferentes fases do desenvolvimento na literatura, poucos deles, principalmente no contexto da HI, exploram os mecanismos que expliquem essas diferenças. Nesse sentido a presente tese apresenta o metabolismo encefálico como um dos principais fatores que explica tais diferenças.

5.4 Outros possíveis mecanismos que podem influenciar o prognóstico da lesão em diferentes idades

Além do metabolismo cerebral, foco do presente estudo, dois mecanismos se destacam como importantes para o diferente prognóstico da lesão induzida em diferentes fases do desenvolvimento que ainda não foram muito estudados: a proliferação celular e a maturação de neurônios GABAérgicos e glutamatérgicos. A proliferação celular no sistema nervoso é amplamente descrita e está mais ativa durante o desenvolvimento

(Bandeira et al., 2009; Gage, 2000; Vescovi et al., 2006). A proliferação celular ocorre diferentemente em cada tipo celular do SNC, em ratos o número de neurônios atinge seu ápice no P7, enquanto as células gliais têm sua proliferação aumentada nessa mesma idade, mas atingem seu número máximo somente no P21 (Bandeira et al., 2009; Semple et al., 2013). No hipocampo, por exemplo, a estrutura mais afetada pela HI, o número de neurônios é de 3,16 milhões no P3 representando 89,6% do total de células nessa estrutura. No P7 esse número chega a 6,8 milhões, sendo o dia que em que o número de neurônios atinge seu auge, e representa 88,7% das células. No P11, no entanto, esse número cai bruscamente para 3,04 milhões que representam apenas 52,2% das células na estrutura (Bandeira et al., 2009).

Após lesões no SNC ocorre proliferação a partir das células tronco neurais, esse processo é crucial para a fase de remodelamento tecidual e é um dos fatores que irá definir a severidade da lesão final (Burda & Sofroniew, 2014; Im et al., 2010). Já está bem demonstrado que após a HI há um aumento na proliferação celular em diversas estruturas, como a zona sub-ventricular (Iwai et al., 2006; Ong et al., 2005; Plane et al., 2004), no estriado (Ong et al., 2005) e giro denteado (Wei et al., 2015). Esse aumento da gênese celular induzida pela HI já tem sido usado como alvo terapêutico, sendo que tratamentos que aumentam a proliferação são capazes de reverter os déficits causados pela lesão: a administração de eritropoietina foi capaz de melhorar o fluxo sanguíneo e aumentar a proliferação celular, o que culminou numa lesão tecidual reduzida (Iwai et al., 2007); a oxigenação hiperbárica também foi capaz de aumentar a neurogênese hipocampal e reverter os déficits cognitivos causados pela HI; por fim, administração dos fatores neurotróficos aumentou a proliferação neuronal no estriado que reduziu os danos motores causados pela lesão (Im et al., 2010).

No entanto, é discutível se o simples fato de se estar em um período do desenvolvimento neural mais precoce, com maiores níveis de divisão celular, garante por si só que sua resposta à lesão também se dará em maior grau. Um estudo em que camundongos foram submetidos à HI no período imaturo (P9) e juvenil (P21) revelou que, embora os animais imaturos possuíssem maiores níveis de proliferação sem lesão, o aumento desse fator como resposta ao insulto foi muito maior nos animais juvenis (Qiu et al., 2007). Essa diferença de reação à HI foi atribuída ao fato de que a proliferação em animais imaturos estaria em níveis basais tão altos que não é possível aumentá-los, o que só seria possível nos animais juvenis (Qiu et al., 2007).

A diferença na maturação de neurônios GABAérgicos e glutamatérgicos também pode ser um fator determinante na severidade da lesão HI. No P7 ratos possuem apenas metade dos neurônios glutamatérgicos que possuirão na idade adulta, enquanto os níveis de neurônios GABAérgicos varia muito pouco (Brekke et al., 2015). Além disso, é de especial relevância o fato de que no encéfalo imaturo o GABA possui ações excitatórias e não inibitórias como na idade adulta (Ben-Ari, 2002). Isso ocorre, pois a proporção do transportador de cloreto NKCC1, que aumenta os níveis intracelulares desse íon, está elevada em relação ao transportador KCC2, que permite sua saída e reduz sua concentração no interior da célula (Ben-Ari, 2002). Tendo em vista que o principal receptor GABAérgico, o GABAa, é um receptor ionotrópico exclusivo do íon cloreto, quando a sua concentração intracelular é elevada, o gradiente eletroquímico faz com ele tenda a migrar para o meio extra-celular a causando a despolarização da célula; quando sua concentração extracelular é maior o oposto acontece. Durante o desenvolvimento, a proporção de transportadores NKCC1 é reduzida e a de KCC2 aumentada, fazendo com que o GABA tenha sua ação determinada pela presença desses transportadores (Ben-Ari, 2002).

A excitotoxicidade é um fenômeno de grande importância para a progressão da lesão HI. Em adultos esse processo é mediado principalmente pela ação do neurotransmissor glutamato, no entanto, apesar de possuírem menos neurônios glutamatérgicos, os neonatos são mais suscetíveis à excitotoxicidade (Azimi-Zonooz et al., 2006). Esse efeito deve-se ao efeito inibitório em adultos, que não está presente nos neonatos (Azimi-Zonooz et al., 2006). Ao contrário de seu efeito benéfico em adultos, em neonatos a ativação de receptores GABAérgicos possui efeitos deletérios (Nuñez and McCarthy, 2003; Tsuji et al., 2012), podendo inclusive causar despolarização da membrana que leva à ativação de receptores NMDA, principais mediadores da excitotoxicidade (Fukuda et al., 1998).

5.5 Redução da atividade metabólica e uso de corpos cetônicos como alvos terapêuticos

Os presentes resultados sugerem que as diferenças metabólicas que ocorrem durante o desenvolvimento estão entre os principais fatores que determinam a severidade da lesão. O maior uso de corpos cetônicos, a menor atividade basal do ciclo do TCA e da cadeia respiratória mitocondrial, bem como um sistema mais eficiente de combate ao estresse oxidativo aparentam ser os principais mecanismos que conferem a neuroproteção intrínseca do encéfalo imaturo. Esses fatores favoreceram a preservação da função mitocondrial, mantendo seu o potencial de membrana e a produção de ATP após a reperfusão, reduziram também o dano causado por estresse oxidativo e por consequência a morte celular. A redução da morte celular por apoptose preservou a integridade do tecido encefálico, bem como as conexões axonais e possibilitou a preservação da função cognitiva nos animais P3. A redução da atividade metabólica, bem como o maior uso de

corpos cetônicos no metabolismo encefálico devem ser mais estudados como alvos terapêuticos para a HI.

6. Conclusão

A presente tese demonstra a neuroproteção intrínseca do encéfalo imaturo (P3) à HI, apresentando menos déficits comportamentais e danos histológicos. Os presentes resultados sugerem que esse fenômeno se deve a uma maior capacidade de oxidação de corpos cetônicos. Também foi demonstrada a capacidade do imageamento com [^{18}F]FDG microPET, realizado nos primeiros dias pós-natais, de prever as consequências no aprendizado e dano tecidual observados na idade adulta. Além disso, a maior susceptibilidade mitocondrial dos animais P11 quando comparados aos P3 foi demonstrada pela redução da atividade do ciclo do TCA e complexos da cadeia respiratória mitocondrial, bem como pela perda do potencial mitocondrial, esses achados provavelmente se devem à maior demanda energética do encéfalo P11. Os resultados apresentados sugerem que a disfunção mitocondrial provocou um aumento na produção de EROs que associada a uma menor eficiência das defesas antioxidantes acabou induzindo processos apoptóticos. Portanto, a combinação do maior uso de corpos cetônicos, maior resiliência da função mitocondrial e menor demanda metabólica estão entre os fatores que conferem a neuroproteção intrínseca do encéfalo imaturo. Mais estudos são necessários para elucidar se esses mecanismos podem ser alvos terapêuticos para novos tratamentos da HI.

7. Perspectivas

Investigar a possível influência das diferenças no desenvolvimento dos sistemas GABAérgicos e glutamatérgicos, bem como os diferentes níveis de proliferação celular no prognóstico da lesão HI;

Avaliar se tratamentos que aumentem o metabolismo de corpos cetônicos, como a administração de β-hidroxibutirato têm propriedades neuroprotetoras frente à HI.

8.Referências

Abily-Donval, L., Pinto-Cardoso, G., Chadie, A., Guerrot, A.M., Torre, S., Rondeau, S., Marret, S., 2015. Comparison in outcomes at two-years of age of very preterm infants born in 2000, 2005 and 2010. PLoS One. https://doi.org/10.1371/journal.pone.0114567

Alexander, M., Garbus, H., Smith, A.L., Rosenkrantz, T.S., Fitch, R.H., 2014. Behavioral and histological outcomes following neonatal HI injury in a preterm (P3) and term (P7) rodent model. Behav. Brain Res. 259, 85–96. https://doi.org/10.1016/j.bbr.2013.10.038

Arnaiz, G.R. de L., Ordieres, M.G.L., 2014. Brain Na+, K+-ATPase activity in aging and disease. Int. J. Biomed. Sci. 10, 85–102.

Arteni, N.S., Pereira, L.O., Rodrigues, A.L., Lavinsky, D., Achaval, M.E., Netto, C.A., 2010. Lateralized and sex-dependent behavioral and morphological effects of unilateral neonatal cerebral hypoxia-ischemia in the rat. Behav. Brain Res. 210, 92–98. https://doi.org/10.1016/j.bbr.2010.02.015

Arteni, N.S., Salgueiro, J., Torres, I., Achaval, M., Netto, C.A., 2003. Neonatal cerebral hypoxia-ischemia causes lateralized memory impairments in the adult rat. Brain Res. 973, 171–178. https://doi.org/10.1016/S0006-8993(03)02436-3

Azimi-Zonooz, A., Shuttleworth, C.W., Connor, J. a, 2006. GABAergic protection of hippocampal pyramidal neurons against glutamate insult: deficit in young animals compared to adults. J. Neurophysiol. 96, 299–308. https://doi.org/10.1152/jn.01082.2005

Bandeira, F., Lent, R., Herculano-Houzel, S., 2009. Changing numbers of neuronal and non-neuronal cells underlie postnatal brain growth in the rat. Proc. Natl. Acad. Sci. U. S. A. 106, 14108–14113. https://doi.org/10.1073/pnas.0804650106

Baquer, N.Z., Hothersall, J.S., McLean, P., Greenbaum, A.L., 1977. Aspects of Carbohydrate Metabolism in Developing Brain. Dev. Med. Child Neurol. https://doi.org/10.1111/j.1469-8749.1977.tb08027.x

Bates, T.E., Almeida, A., Heales, S.J.R., Clark, J.B., 1994. Postanatal development of the complexes of the electron transport chain in isolated rat brain mitochondria. Dev. Neurosci.

https://doi.org/10.1159/000112126

Ben-Ari, Y., 2002. Excitatory actions of gaba during development: the nature of the nurture. Nat Rev Neurosci 3, 728–739. https://doi.org/10.1038/nrn920

Benjelloun, N., Joly, L.M., Palmier, B., Plotkine, M., Charriaut-Marlangue, C., 2003. Apoptotic mitochondrial pathway in neurones and astrocytes after neonatal hypoxia-ischaemia in the rat brain. Neuropathol. Appl. Neurobiol. 29, 350–360. https://doi.org/10.1046/j.1365-2990.2003.00467.x

Berger, R., Garnier, Y., 1999. Pathophysiology of perinatal brain damage. Brain Res. Brain Res. Rev. 30, 107–134. https://doi.org/10.1016/S0165-0173(99)00009-0

Booth, R.F.G., Patel, T.B., Clark, J.B., 1980. The Development of Enzymes of Energy Metabolism in the Brain of a Precocial (Guinea Pig) and Non-Precocial (Rat) Species. J. Neurochem. https://doi.org/10.1111/j.1471-4159.1980.tb04616.x

Brekke, E., Berger, H.R., Widerøe, M., Sonnewald, U., Morken, T.S., 2017. Glucose and Intermediary Metabolism and Astrocyte–Neuron Interactions Following Neonatal Hypoxia–Ischemia in Rat. Neurochem. Res. 42, 115–132. https://doi.org/10.1007/s11064-016-2149-9

Brekke, E., Morken, T.S., Sonnewald, U., 2015. Glucose metabolism and astrocyte-neuron interactions in the neonatal brain. Neurochem. Int. 82, 33–41. https://doi.org/10.1016/j.neuint.2015.02.002

Brekke, E.M.F., Morken, T.S., Wideroe, M., Haberg, A.K., Brubakk, A.-M., Sonnewald, U., 2014. The pentose phosphate pathway and pyruvate carboxylation after neonatal hypoxic-ischemic brain injury. J Cereb Blood Flow Metab 34, 724–734. https://doi.org/10.1038/jcbfm.2014.8

Browne, R.W., Armstrong, D., 1998. Reduced glutathione and glutathione disulfide. Methods Mol. Biol. https://doi.org/10.1385/0-89603-472-0:347

Burda, J.E., Sofroniew, M. V, 2014. Reactive gliosis and the multicellular response to CNS damage and disease. Neuron 81, 229–48. https://doi.org/10.1016/j.neuron.2013.12.034

Cai, Q.Y., Zhou, Z.J., Luo, R., Gan, J., Li, S.P., Mu, D.Z., Wan, C.M., 2017. Safety and tolerability of the ketogenic diet used for the treatment of refractory childhood epilepsy: a systematic review of

published prospective studies. World J. Pediatr. https://doi.org/10.1007/s12519-017-0053-2

Casella, E.M., Thomas, T.C., Vanino, D.L., Fellows-Mayle, W., Lifshitz, J., Card, J.P., Adelson, P.D., 2014. Traumatic brain injury alters long-term hippocampal neuron morphology in juvenile, but not immature, rats. Child's Nerv. Syst. https://doi.org/10.1007/s00381-014-2446-z

Cecatto, C., Godoy, K. dos S., da Silva, J.C., Amaral, A.U., Wajner, M., 2016. Disturbance of mitochondrial functions provoked by the major long-chain 3-hydroxylated fatty acids accumulating in MTP and LCHAD deficiencies in skeletal muscle. Toxicol. Vitr. 36, 1–9. https://doi.org/10.1016/j.tiv.2016.06.007

Clancy, B., Darlington, R.B., Finlay, B.L., 2001. Translating developmental time across mammalian species. Neuroscience. https://doi.org/10.1016/S0306-4522(01)00171-3

Dafre, A.L., Arteni, N.S., Siqueira, I.R., Netto, C.A., 2003. Perturbations in the thiol homeostasis following neonatal cerebral hypoxia-ischemia in rats. Neurosci. Lett. 345, 65–68. https://doi.org/10.1016/S0304-3940(03)00510-X

Dardzinski, B.J., Smith, S.L., Towfighi, J., Williams, G.D., Vannucci, R.C., Smith, M.B., 2000. Increased plasma beta-hydroxybutyrate, preserved cerebral energy metabolism, and amelioration of brain damage during neonatal hypoxia ischemia with dexamethasone pretreatment. Pediatr. Res. https://doi.org/10.1203/00006450-200008000-00021

Davidson, J.O., Wassink, G., van den Heuij, L.G., Bennet, L., Gunn, A.J., 2015a. Therapeutic hypothermia for neonatal hypoxic-ischemic encephalopathy - Where to from here? Front. Neurol. https://doi.org/10.3389/fneur.2015.00198

Davidson, J.O., Wassink, G., van den Heuij, L.G., Bennet, L., Gunn, A.J., 2015b. Therapeutic hypothermia for neonatal hypoxic-ischemic encephalopathy - Where to from here? Front. Neurol. 6. https://doi.org/10.3389/fneur.2015.00198

de-Souza-Ferreira, E., Rios-Neto, I.M., Martins, E.L., Galina, A., 2019. Mitochondria-coupled glucose phosphorylation develops after birth to modulate H2O2 release and calcium handling in rat brain. J. Neurochem. https://doi.org/10.1111/jnc.14705

Deng, W., 2010. Neurobiology of injury to the developing brain. Nat. Rev. Neurol. https://doi.org/10.1038/nrneurol.2010.53

Dobbing, J., Sands, J., 1979. Comparative aspects of the brain growth spurt. Early Hum. Dev. https://doi.org/10.1016/0378-3782(79)90022-7

Dranka, B.P., Hill, B.G., Darley-Usmar, V.M., 2010. Mitochondrial reserve capacity in endothelial cells: The impact of nitric oxide and reactive oxygen species. Free Radic. Biol. Med. https://doi.org/10.1016/j.freeradbiomed.2010.01.015

Durán-Carabali, L.E., Sanches, E.F., Marques, M.R., Aristimunha, D., Pagnussat, A., Netto, C.A., 2017. Longer hypoxia–ischemia periods to neonatal rats causes motor impairments and muscular changes. Neuroscience 340, 291–298. https://doi.org/10.1016/j.neuroscience.2016.10.068

Durán-Carabali, L.E., Sanches, E.F., Reichert, L., Netto, C.A., 2019. Enriched experience during pregnancy and lactation protects against motor impairments induced by neonatal hypoxia-ischemia. Behav. Brain Res. https://doi.org/10.1016/j.bbr.2019.03.048

Ennis, K., Tran, P. V., Seaquist, E.R., Rao, R., 2008. Postnatal age influences hypoglycemia-induced neuronal injury in the rat brain. Brain Res. https://doi.org/10.1016/j.brainres.2008.06.003

Erecińska, M., Silver, I.A., 1994. Ions and energy in mammalian brain. Prog. Neurobiol. 43, 37–71. https://doi.org/10.1016/0301-0082(94)90015-9

Fathali, N., Ostrowski, R.P., Hasegawa, Y., Lekic, T., Tang, J., Zhang, J.H., 2013. Splenic Immune Cells in Experimental Neonatal Hypoxia-Ischemia. Transl. Stroke Res. 4, 208–219. https://doi.org/10.1007/s12975-012-0239-9

Ferriero, D.M., 2001. Oxidant mechanisms in neonatal hypoxia-ischemia. Dev. Neurosci. 23, 198–202. https://doi.org/46143

Fischer, J.C., Ruitenbeek, W., Berden, J.A., Trijbels, J.M.F., Veerkamp, J.H., Stadhouders, A.M., Sengers, R.C.A., Janssen, A.J.M., 1985. Differential investigation of the capacity of succinate oxidation in human skeletal muscle. Clin. Chim. Acta. https://doi.org/10.1016/0009-8981(85)90135-4

Fukuda, A., Muramatsu, K., Okabe, A., Shimano, Y., Hida, H., 1998. Changes in Intracellular Ca 2 / Induced by GABA A Receptor Activation and Reduction in Cl 0 Gradient in Neonatal Rat Neocortex 439–446.

Gage, F.H., 2000. Mammalian neural stem cells. Science (80-.). 287, 1433–1438. https://doi.org/10.1126/science.287.5457.1433

Garcia, J.H., Lossinsky, A.S., Kauffman, F.C., Conger, K.A., 1978. Neuronal ischemic injury: Light microscopy, ultrastructure and biochemistry. Acta Neuropathol. https://doi.org/10.1007/BF00685002

Globus, M.Y.-., Alonso, O., Dietrich, W.D., Busto, R., Ginsberg, M.D., 1995. Glutamate Release and Free Radical Production Following Brain Injury: Effects of Posttraumatic Hypothermia. J. Neurochem. https://doi.org/10.1046/j.1471-4159.1995.65041704.x

Gnaiger, E., 2009. Capacity of oxidative phosphorylation in human skeletal muscle. New perspectives of mitochondrial physiology. Int. J. Biochem. Cell Biol. 41, 1837–1845. https://doi.org/10.1016/j.biocel.2009.03.013

Gregson, N.A., Williams, P.L., 1969. A COMPARATIVE STUDY OF BRAIN AND LIVER MITOCHONDRIA FROM NEW-BORN AND ADULT RATS. J. Neurochem. https://doi.org/10.1111/j.1471-4159.1969.tb06861.x

Hagberg, H., Carina, M., Catherine, R., Wang, X., 2009. Apoptotic Mechanisms in the Immature Brain: Inolvement of Mitochondria. Journal 24, 1141–1146. https://doi.org/10.1177/0883073809338212.Apoptotic

Hagberg, H., Mallard, C., Rousset, C.I., Thornton, C., 2014. Mitochondria: Hub of injury responses in the developing brain. Lancet Neurol. https://doi.org/10.1016/S1474-4422(13)70261-8

Hassell, K.J., Ezzati, M., Alonso-Alconada, D., Hausenloy, D.J., Robertson, N.J., 2015. New horizons for newborn brain protection: enhancing endogenous neuroprotection. Arch. Dis. Child. - Fetal Neonatal Ed. 100, F541–F552. https://doi.org/10.1136/archdischild-2014-306284

Herrera, T.I., Edwards, L., Malcolm, W.F., Smith, P.B., Fisher, K.A., Pizoli, C., Gustafson, K.E., Goldstein,

R.F., Cotten, C.M., Goldberg, R.N., Bidegain, M., 2018. Outcomes of preterm infants treated with hypothermia for hypoxic-ischemic encephalopathy. Early Hum. Dev. https://doi.org/10.1016/j.earlhumdev.2018.08.003

Huang, Z., Liu, J., Cheung, P.Y., Chen, C., 2009. Long-term cognitive impairment and myelination deficiency in a rat model of perinatal hypoxic-ischemic brain injury. Brain Res. 1301, 100–109. https://doi.org/10.1016/j.brainres.2009.09.006

Im, S.H., Yu, J.H., Park, E.S., Lee, J.E., Kim, H.O., Park, K.I., Kim, G.W., Park, C.I., Cho, S.R., 2010. Induction of striatal neurogenesis enhances functional recovery in an adult animal model of neonatal hypoxic-ischemic brain injury. Neuroscience 169, 259–268. https://doi.org/10.1016/j.neuroscience.2010.04.038

Iwai, M., Cao, G., Yin, W., Stetler, R.A., Liu, J., Chen, J., 2007. Erythropoietin promotes neuronal replacement through revascularization and neurogenesis after neonatal hypoxia/ischemia in rats. Stroke 38, 2795–2803. https://doi.org/10.1161/STROKEAHA.107.483008

Iwai, M., Ikeda, T., Hayashi, T., Sato, K., Nagata, T., Nagano, I., Shoji, M., Ikenoue, T., Abe, K., 2006. Temporal profile of neural stem cell proliferation in the subventricular zone after ischemia/hypoxia in the neonatal rat brain. Neurol. Res. 28, 461–468. https://doi.org/10.1179/016164105X49283

Iwata, O., Iwata, S., Thornton, J.S., De Vita, E., Bainbridge, A., Herbert, L., Scaravilli, F., Peebles, D., Wyatt, J.S., Cady, E.B., Robertson, N.J., 2007. “Therapeutic time window” duration decreases with increasing severity of cerebral hypoxia-ischaemia under normothermia and delayed hypothermia in newborn piglets. Brain Res. 1154, 173–180. https://doi.org/10.1016/j.brainres.2007.03.083

Jacobs, S.E., Berg, M., Hunt, R., Tarnow-Mordi, W.O., Inder, T.E., Davis, P.G., 2013. Cooling for newborns with hypoxic ischaemic encephalopathy. Cochrane Database Syst. Rev. https://doi.org/10.1002/14651858.CD003311.pub3

James, M.L., Gambhir, S.S., 2012. A Molecular Imaging Primer: Modalities, Imaging Agents, and Applications. Physiol. Rev. 92, 897–965. https://doi.org/10.1152/physrev.00049.2010

Jansen, E.M., Low, W.C., 1996. Long-term effects of neonatal ischemic-hypoxic brain injury on

sensorimotor and locomotor tasks in rats. Behav. Brain Res. 78, 189–194. https://doi.org/10.1016/0166-4328(95)00248-0

Jellema, R.K., Lima Passos, V., Zwanenburg, A., Ophelders, D.R.M.G., De Munter, S., Vanderlocht, J., Germeraad, W.T. V, Kuypers, E., Collins, J.J.P., Cleutjens, J.P.M., Jennekens, W., Gavilanes, A.W.D., Seehase, M., Vles, H.J., Steinbusch, H., Andriessen, P., Wolfs, T.G.A.M., Kramer, B.W., 2013. Cerebral inflammation and mobilization of the peripheral immune system following global hypoxia-ischemia in preterm sheep. J. Neuroinflammation 10, 13. https://doi.org/10.1186/1742-2094-10-13

Jin, Y., Silverman, A.J., Vannucci, S.J., 2009. Mast cells are early responders after hypoxia-ischemia in immature rat brain. Stroke. 40, 3107–3112. https://doi.org/10.1161/STROKEAHA.109.549691

Johnston, M. V, Trescher, W.H., Ishida, A., Nakajima, W., 2001. Neurobiology of hypoxic-ischemic injury in the developing brain. Pediatr. Res. 49, 735–41. https://doi.org/10.1203/00006450-200106000-00003

Khwaja, O., Volpe, J.J., 2008. Pathogenesis of cerebral white matter injury of prematurity. Arch. Dis. Child. - Fetal Neonatal Ed. 93, F153–F161. https://doi.org/10.1136/adc.2006.108837

Kitto, G., 1969. [19] Intra- and extramitochondrial malate dehydrogenases from chicken and tuna heart. Methods Enzymol. https://doi.org/10.1016/0076-6879(69)13023-2

Laptook, A.R., Shankaran, S., Tyson, J.E., Munoz, B., Bell, E.F., Goldberg, R.N., Parikh, N.A., Ambalavanan, N., Pedroza, C., Pappas, A., Das, A., Chaudhary, A.S., Ehrenkranz, R.A., Hensman, A.M., Van Meurs, K.P., Chalak, L.F., Hamrick, S.E.G., Sokol, G.M., Walsh, M.C., Poindexter, B.B., Faix, R.G., Watterberg, K.L., Frantz, I.D., Guillet, R., Devaskar, U., Truog, W.E., Chock, V.Y., Wyckoff, M.H., McGowan, E.C., Carlton, D.P., Harmon, H.M., Brumbaugh, J.E., Cotten, C.M., Sánchez, P.J., Hibbs, A.M., Higgins, R.D., 2017. Effect of therapeutic hypothermia initiated after 6 hours of age on death or disability among newborns with hypoxic-ischemic encephalopathy a randomized clinical trial. JAMA - J. Am. Med. Assoc. https://doi.org/10.1001/jama.2017.14972

LeBel, C.P., Bondy, S.C., 1990. Sensitive and rapid quantitation of oxygen reactive species formation in rat synaptosomes. Neurochem. Int. 17, 435–440. https://doi.org/10.1016/0197-0186(90)90025-O

Lee, B.S., Woo, D.C., Woo, C.W., Kim, K.S., 2018. Exogenous β-Hydroxybutyrate Treatment and Neuroprotection in a Suckling Rat Model of Hypoxic-Ischemic Encephalopathy. Dev. Neurosci. https://doi.org/10.1159/000486411

Leino, R.L., Gerhart, D.Z., Drewes, L.R., 1999. Monocarboxylate transporter (MCT1) abundance in brains of suckling and adult rats: A quantitative electron microscopic immunogold study. Dev. Brain Res. https://doi.org/10.1016/S0165-3806(98)00188-6

Li, J., Yu, W., Li, X.T., Qi, S.H., Li, B., 2014. The effects of propofol on mitochondrial dysfunction following focal cerebral ischemia-reperfusion in rats. Neuropharmacology. https://doi.org/10.1016/j.neuropharm.2013.08.029

Li, S., Liu, W., Zhang, Y., Zhao, D., Wang, T., Li, Y., 2014. The role of TNF-α, IL-6, IL-10, and GDNF in neuronal apoptosis in neonatal rat with hypoxic-ischemic encephalopathy. Eur. Rev. Med. Pharmacol. Sci. 18, 905–909.

Lima, K.G., Krause, G.C., da Silva, E.F.G., Xavier, L.L., Martins, L.A.M., Alice, L.M., da Luz, L.B., Gassen, R.B., Filippi-Chiela, E.C., Haute, G.V., Garcia, M.C.R., Funchal, G.A., Pedrazza, L., Reghelin, C.K., de Oliveira, J.R., 2018. Octyl gallate reduces ATP levels and Ki67 expression leading HepG2 cells to cell cycle arrest and mitochondria-mediated apoptosis. Toxicol. Vitr. https://doi.org/10.1016/j.tiv.2017.12.017

Liu, F., McCullough, L.D., 2013. Inflammatory responses in hypoxic ischemic encephalopathy. Acta Pharmacol. Sin. 34, 1121–30. https://doi.org/10.1038/aps.2013.89

Liu, W., Zhang, Y., 2014. in Neuronal Apoptosis in Neonatal Rat With Hypoxic-Ischemic Encephalopathy 905–909.

Lorek, A., Takei, Y., Cady, E.B., Wyatt, J.S., Penrice, J., Edwards, A.D., Peebles, D.M., Wylezinska, M., Owen-Rees, H., Kirkbride, V., Cooper, C., Aldridge, R.F., Roth, S.C., Brown, G., Delpy, D.T., Reynolds, E.O.R., 1994. Delayed ('secondary') cerebral energy failure following acute hypoxia-ischaemia in the newborn piglet: continuous 48-hour studies by 31P magnetic resonance spectroscopy. Pediatr. Res. 36, 699–706.

Lowry, O.H., Passonneau, J. V, Hasselberger, F.X., Schulz, D.W., 1964. EFFECT OF ISCHEMIA ON KNOWN SUBSTRATES AND COFACTORS OF THE GLYCOLYTIC PATHWAY IN BRAIN. J. Biol. Chem.

Lowry, O.H., Rosenbrough, N.J., Farr, A.L., Randall, R.J., 1951. Protein measurement with the folin. J. Biol. Chem. https://doi.org/10.1016/0304-3894(92)87011-4

Makrecka-Kuka, M., Krumschnabel, G., Gnaiger, E., 2015. High-resolution respirometry for simultaneous measurement of oxygen and hydrogen peroxide fluxes in permeabilized cells, tissue homogenate and isolated mitochondria. Biomolecules. https://doi.org/10.3390/biom5031319

Marik, J., Ogasawara, A., Martin-McNulty, B., Ross, J., Flores, J.E., Gill, H.S., Tinianow, J.N., Vanderbilt, A.N., Nishimura, M., Peale, F., Pastuskovas, C., Greve, J.M., van Bruggen, N., Williams, S.P., 2009. PET of Glial Metabolism Using 2-18F-Fluoroacetate. J. Nucl. Med. 50, 982–990. https://doi.org/10.2967/jnumed.108.057356

Marklund, S., Marklund, G., 1974. Involvement of the superoxide anion radical in the autoxidation of pyrogallol and a convenient assay for superoxide dismutase. Eur. J. Biochem. 47, 469–474. https://doi.org/10.1111/j.1432-1033.1974.tb03714.x

Mavelli, I., Rigo, A., Federico, R., Ciriolo, M.R., Rotilio, G., 1982. Superoxide dismutase, glutathione peroxidase and catalase in developing rat brain. Biochem. J. https://doi.org/10.1042/bj2040535

McKenna, M.C., Dienel, G.A., Sonnewald, U., Waagepetersen, H.S., Schousboe, A., 2012. Energy Metabolism of the Brain. Basic Neurochem. 200–231. https://doi.org/10.1016/B978-0-12-374947-5.00011-0

McKenna, M.C., Scafidi, S., Robertson, C.L., 2015. Metabolic alterations in developing brain after injury: knowns and unknowns. Neurochem. Res. 40, 2527–2543. https://doi.org/10.1007/s11064-015-1600-7

McLean, C., Ferriero, D., 2004. Mechanisms of hypoxic-ischemic injury in the term infant. Semin. Perinatol. https://doi.org/10.1053/j.semperi.2004.10.005

Mishra, O.P., Delivoria-Papadopoulos, M., 1999. Cellular mechanisms of hypoxic injury in the developing brain. Brain Res. Bull. https://doi.org/10.1016/S0361-9230(98)00170-1

Nannelli, G., Terzuoli, E., Giorgio, V., Donnini, S., Lupetti, P., Giachetti, A., Bernardi, P., Ziche, M., 2018. ALDH2 activity reduces mitochondrial oxygen reserve capacity in endothelial cells and induces senescence properties. Oxid. Med. Cell. Longev. https://doi.org/10.1155/2018/9765027

Neal, E.G., Chaffe, H., Schwartz, R.H., Lawson, M.S., Edwards, N., Fitzsimmons, G., Whitney, A., Cross, J.H., 2009. A randomized trial of classical and medium-chain triglyceride ketogenic diets in the treatment of childhood epilepsy. Epilepsia. https://doi.org/10.1111/j.1528-1167.2008.01870.x

Netto, C.A., Sanches, E., Odorcyk, F.K., Duran-Carabali, L.E., Weis, S.N., 2017. Sex-dependent consequences of neonatal brain hypoxia-ischemia in the rat. J. Neurosci. Res. https://doi.org/10.1002/jnr.23828

Nuñez, J.L., McCarthy, M.M., 2003. Estradiol exacerbates hippocampal damage in a model of preterm infant brain injury. Endocrinology 144, 2350–2359. https://doi.org/10.1210/en.2002-220840

Odorcyk, F.K., Duran-Carabali, L.E., Rocha, D.S., Sanches, E.F., Martini, A.P., Venturin, G.T., Greggio, S., da Costa, J.C., Kucharski, L.C., Zimmer, E.R., Netto, C.A., 2020. Differential glucose and beta-hydroxybutyrate metabolism confers an intrinsic neuroprotection to the immature brain in a rat model of neonatal hypoxia ischemia. Exp. Neurol. https://doi.org/10.1016/j.expneurol.2020.113317

Odorcyk, F.K., Kolling, J., Sanches, E.F., Wyse, A.T.S., Netto, C.A., 2017. Experimental neonatal hypoxia ischemia causes long lasting changes of oxidative stress parameters in the hippocampus and the spleen. J. Perinat. Med. 1–7. https://doi.org/10.1515/jpm-2017-0070

Ong, J., Plane, J.M., Parent, J.M., Silverstein, F.S., 2005. Hypoxic-ischemic injury stimulates subventricular zone proliferation and neurogenesis in the neonatal rat. Pediatr. Res. 58, 600–606. https://doi.org/10.1203/01.PDR.0000179381.86809.02

Park, W.S., Chang, Y.S., Lee, M., 2001. Effects of hyperglycemia or hypoglycemia on brain cell membrane function and energy metabolism during the immediate reoxygenation-reperfusion period after acute transient global hypoxia-ischemia in the newborn piglet. Brain Res. https://doi.org/10.1016/S0006-

8993(01)02295-8

Patel, S.D., Pierce, L., Ciardiello, A., Hutton, A., Paskewitz, S., Aronowitz, E., Voss, H.U., Moore, H., Vannucci, S.J., 2015. Therapeutic hypothermia and hypoxia-ischemia in the term-equivalent neonatal rat: characterization of a translational preclinical model. Pediatr. Res. 78, 264–71. https://doi.org/10.1038/pr.2015.100

Patel, S.D., Pierce, L., Ciardiello, A.J., Vannucci, S.J., 2014. Neonatal encephalopathy: pre-clinical studies in neuroprotection. Biochem. Soc. Trans. 42, 564–8. https://doi.org/10.1042/BST20130247

Pereira, L.O., Arteni, N.S., Petersen, R.C., da Rocha, A.P., Achaval, M., Netto, C.A., 2007. Effects of daily environmental enrichment on memory deficits and brain injury following neonatal hypoxia-ischemia in the rat. Neurobiol. Learn. Mem. 87, 101–108. https://doi.org/10.1016/j.nlm.2006.07.003

Pereira, L.O., Nabinger, P.M., Strapasson, A.C.P., Nardin, P., Gonçalves, C.A.S., Siqueira, I.R., Netto, C.A., 2009. Long-term effects of environmental stimulation following hypoxia-ischemia on the oxidative state and BDNF levels in rat hippocampus and frontal cortex. Brain Res. 1247, 188–195. https://doi.org/10.1016/j.brainres.2008.10.017

Pinchefsky, E.F., Hahn, C.D., Kamino, D., Chau, V., Brant, R., Moore, A.M., Tam, E.W.Y., 2019. Hyperglycemia and Glucose Variability Are Associated with Worse Brain Function and Seizures in Neonatal Encephalopathy: A Prospective Cohort Study. J. Pediatr. https://doi.org/10.1016/j.jpeds.2019.02.027

Plane, J.M., Liu, R., Wang, T.W., Silverstein, F.S., Parent, J.M., 2004. Neonatal hypoxic-ischemic injury increases forebrain subventricular zone neurogenesis in the mouse. Neurobiol. Dis. 16, 585–595. https://doi.org/10.1016/j.nbd.2004.04.003

Qiu, L., Zhu, C., Wang, X., Xu, F., Eriksson, P.S., Nilsson, M., Cooper-Kuhn, C.M., Kuhn, H.G., Blomgren, K., 2007. Less neurogenesis and inflammation in the immature than in the juvenile brain after cerebral hypoxia-ischemia. J. Cereb. Blood Flow Metab. 27, 785–794. https://doi.org/10.1038/sj.jcbfm.9600385

Raghupathi, R., Huh, J.W., 2007. Diffuse brain injury in the immature rat: Evidence for an age-at-injury

effect on cognitive function and histopathologic damage. J. Neurotrauma. https://doi.org/10.1089/neu.2007.3790

Rao, R., Trivedi, S., Vesoulis, Z., Liao, S.M., Smyser, C.D., Mathur, A.M., 2017. Safety and Short-Term Outcomes of Therapeutic Hypothermia in Preterm Neonates 34-35 Weeks Gestational Age with Hypoxic-Ischemic Encephalopathy. J. Pediatr. https://doi.org/10.1016/j.jpeds.2016.11.019

Ribeiro, R.T., Zanatta, Â., Amaral, A.U., Leipnitz, G., de Oliveira, F.H., Seminotti, B., Wajner, M., 2018. Experimental Evidence that In Vivo Intracerebral Administration of L-2-Hydroxyglutaric Acid to Neonatal Rats Provokes Disruption of Redox Status and Histopathological Abnormalities in the Brain. Neurotox. Res. https://doi.org/10.1007/s12640-018-9874-6

Rice, J.E., Vannucci, R.C., Brierley, J.B., 1981. The influence of immaturity on hypoxic-ischemic brain damage in the rat. Ann. Neurol. 9, 131–141. https://doi.org/10.1002/ana.410090206

Rustin, P., Chretien, D., Bourgeron, T., Gérard, B., Rötig, A., Saudubray, J.M., Munnich, A., 1994. Biochemical and molecular investigations in respiratory chain deficiencies. Clin. Chim. Acta. https://doi.org/10.1016/0009-8981(94)90055-8

Saito, A., Maier, C.M.., Purnima Narasimhan, Nishi, T., Song, Y.S., Yu, F., Liu, J., Lee, Y., Nito, C., Kamada, H., Dodd, R.L., Hsieh, L.B., Hassid, B., Kim, E.E., González, M., Chan, P.H., 2005. Oxidative Stress and Neuronal Death / Survival Signaling in Cerebral Ischemia. Mol. Neurobiol. 31, 105–116.

Sanches, E.F., Arteni, N., Nicola, F., Aristimunha, D., Netto, C.A., 2015. Sexual dimorphism and brain lateralization impact behavioral and histological outcomes following hypoxia-ischemia in P3 and P7 rats. Neuroscience 290, 581–593. https://doi.org/10.1016/j.neuroscience.2014.12.074

Sanderson, T.H., Reynolds, C.A., Kumar, R., Przyklenk, K., Hüttemann, M., 2013. Molecular mechanisms of ischemia-reperfusion injury in brain: Pivotal role of the mitochondrial membrane potential in reactive oxygen species generation. Mol. Neurobiol. https://doi.org/10.1007/s12035-012-8344-z

Semple, B.D., Blomgren, K., Gimlin, K., Ferriero, D.M., Noble-Haeusslein, L.J., 2013. Brain development in rodents and humans: Identifying benchmarks of maturation and vulnerability to injury across

species. Prog. Neurobiol. 106–107, 1–16. https://doi.org/10.1016/j.pneurobio.2013.04.001

Shevell, M.I., Majnemer, A., Rosenbaum, P., Abrahamowicz, M., 2001. Etiologic determination of childhood developmental delay. Brain Dev. 23, 228–235. https://doi.org/10.1016/S0387-7604(01)00212-1

Shi, Y., Zhao, J.N., Liu, L., Hu, Z.X., Tang, S.F., Chen, L., Jin, R. Bin, 2012. Changes of positron emission tomography in newborn infants at different gestational ages, and neonatal hypoxic-ischemic encephalopathy. Pediatr. Neurol. https://doi.org/10.1016/j.pediatrneurol.2011.11.005

Silbereis, J.C., Huang, E.J., Back, S. a, Rowitch, D.H., 2010. Towards improved animal models of neonatal white matter injury associated with cerebral palsy. Dis. Model. Mech. 3, 678–688. https://doi.org/10.1242/dmm.002915

Sizonenko, S. V., Kiss, J.Z., Inder, T., Gluckman, P.D., Williams, C.E., 2005. Distinctive neuropathologic alterations in the deep layers of the parietal cortex after moderate ischemic-hypoxic injury in the P3 immature rat brain. Pediatr. Res. 57, 865–872. https://doi.org/10.1203/01.PDR.0000157673.36848.67

Srere, P.A., 1969. [1] Citrate synthase. [EC 4.1.3.7. Citrate oxaloacetate-lyase (CoA-acetylating)]. Methods Enzymol. 13, 3–11. https://doi.org/10.1016/0076-6879(69)13005-0

Thorngren-jerneck, K., Ohlsson, T., Sandell, A., Erlandsson, K., Strand, S., Ryding, E., Svenningsen, N.W., 2001. Cerebral Glucose Metabolism Measured by Positron Emission Tomography in Term Newborn Infants with Hypoxic Ischemic Encephalopathy 49, 495–501.

Thurston, J.H., McDougal, D.B., 1969. Effect of ischemia on metabolism of the brain of the newborn mouse. Am. J. Physiol. https://doi.org/10.1152/ajplegacy.1969.216.2.348

Tsuji, M., Taguchi, A., Ohshima, M., Kasahara, Y., Ikeda, T., 2012. Progesterone and allopregnanolone exacerbate hypoxic-ischemic brain injury in immature rats. Exp. Neurol. 233, 214–220. https://doi.org/10.1016/j.expneurol.2011.10.004

Vannucci, S.J., 2004. Hypoxia-ischemia in the immature brain. J. Exp. Biol. 207, 3149–3154.

https://doi.org/10.1242/jeb.01064

Vannucci, S.J., Reinhart, R., Maher, F., Bondy, C. a, Lee, W.H., Vannucci, R.C., Simpson, I. a, 1998. Alterations in GLUT1 and GLUT3 glucose transporter gene expression following unilateral hypoxia-ischemia in the immature rat brain. Brain Res. Dev. Brain Res. 107, 255–64.

Vannucci, S.J., Seaman, L.B., Brucklacher, R.M., Vannucci, R.C., 1994. Glucose transport in developing rat brain: Glucose transporter proteins, rate constants and cerebral glucose utilization. Mol. Cell. Biochem. https://doi.org/10.1007/BF00926756

Verklan, T.., 2009. The chilling details: Hypoxic-ischemic encephalopathy. J. Perinat. Neonatal Nurs. 23, 59–68. https://doi.org/10.1097/01.JPN.0000346222.25331.e8

Vescovi, A.L., Galli, R., Reynolds, B. a, 2006. Brain tumour stem cells. Nat. Rev. Cancer 6, 425–36. https://doi.org/10.1038/nrc1889

Volpe, J.J., 2009. Brain injury in premature infants: a complex amalgam of destructive and developmental disturbances. Lancet Neurol. https://doi.org/10.1016/S1474-4422(08)70294-1

Wei, L., Wang, Jinshen, Cao, Y., Ren, Q., Zhao, L., Li, X., Wang, Jiwen, 2015. Hyperbaric oxygenation promotes neural stem cell proliferation and protects the learning and memory ability in neonatal hypoxic-ischemic brain damage 8, 1752–1759.

Weis, S.N., Schunck, R.V.A., Pettenuzzo, L.F., Krolow, R., Matté, C., Manfredini, V., do Carmo R Peralba, M., Vargas, C.R., Dalmaz, C., Wyse, A.T.S., Netto, C.A., 2011. Early biochemical effects after unilateral hypoxia-ischemia in the immature rat brain. Int. J. Dev. Neurosci. 29, 115–20. https://doi.org/10.1016/j.ijdevneu.2010.12.005

Wendel, A., 1981. Glutathione Peroxidase. Methods Enzymol. https://doi.org/10.1016/S0076-6879(81)77046-0

Wilson-Costello, D., Friedman, H., Minich, N., Siner, B., Taylor, G., Schluchter, M., Hack, M., 2007. Improved neurodevelopmental outcomes for extremely low birth weight infants in 2000-2002. Pediatrics. https://doi.org/10.1542/peds.2006-1416

Yagi, K., 1998. Simple procedure for specific assay of lipid hydroperoxides in serum or plasma. Methods Mol. Biol. https://doi.org/10.1385/0-89603-472-0:107

Zhao, J., Chen, Y., Xu, Y., Pi, G., 2013. Effect of intrauterine infection on brain development and injury. Int. J. Dev. Neurosci. https://doi.org/10.1016/j.ijdevneu.2013.06.008